8-2022

Assessing Intra-urban Particulate Matter (PM2.5) Concentrations at the Lower Rio Grande Valley (RGV), South Texas, USA, Using Low-Cost Sensors

Esmeralda Mendez
The University of Texas Rio Grande Valley

ASSESSING INTRA-URBAN PARTICULATE MATTER ($PM_{2.5}$) CONCENTRATIONS AT THE LOWER RIO GRANDE VALLEY (RGV), SOUTH TEXAS, USA, USING LOW-COST SENSORS

A Thesis

by

ESMERALDA MENDEZ

Submitted in Partial Fulfillment of the

Requirements for the Degree of

MASTER OF SCIENCE

Major Subject: Agricultural, Environmental, and Sustainability Sciences

The University of Texas Rio Grande Valley

August 2022

ASSESSING INTRA-URBAN PARTICULATE MATTER ($PM_{2.5}$) CONCENTRATIONS AT THE LOWER RIO GRANDE VALLEY (RGV), SOUTH TEXAS, USA, USING LOW-COST SENSORS

A Thesis
by
ESMERALDA MENDEZ

COMMITTEE MEMBERS

Amit U. Raysoni, Ph.D., M.P.H
Committee Chair

Owen Temby, Ph.D.
Committee Member

Katarzyna Sepielak, Ph.D.
Committee Member

Dawid Wladyka, Ph.D.
Committee Member

August 2022

ABSTRACT

Mendez, Esmeralda, Assessing Intra-Urban Particulate Matter ($PM_{2.5}$) Concentrations at the Lower Rio Grande Valley (RGV), South Texas, USA, Using Low-Cost Sensors. Master of Science (MS), August, 2022, 95 pp., 16 tables, 56 figures, references, 143 titles.

Rapid technological developments of novel low-cost air quality sensors enable long-term ambient monitoring in neighborhood areas. In this study, spatial and temporal trends are analyzed by localized level monitoring with low-cost sensors (TSI BlueSky Air Quality Monitor). Eleven low-cost sensors were deployed across the Lower Rio Grande Valley, South Texas region: Brownsville, Edinburg, Weslaco, and Port Isabel. 24-hour $PM_{2.5}$ concentrations are

correlated with $PM_{2.5}$ from existing Texas Commission on Environmental Quality (TCEQ) Continuous Ambient Monitoring Stations (CAMSs) to express temporal and spatial heterogeneity from March 01, 2021, to March 31, 2022. Results indicated the deployed low-cost sensors as a better representation of accurate exposure patterns at the intra-urban level, rather than at the CAMSs. Conclusions from this study will shed light on the concerns and issues with $PM_{2.5}$ pollutant exposure by assessing real-time exposures in intra-and-inter-urban communities.

DEDICATION

This thesis is dedicated to all my friends and family who motivated me to continue my education. This is for my grandparents-- Janie Mendez, Luis Adame, and late grandmother, Alicia Adame. Likewise, this is for my siblings who have been patient and understanding. Moreover, I would like to give a special dedication to my caring parents-- Sandra and David Mendez, for their unconditional love, guidance, and prayers. In addition, I am honored to represent the Latin X community and inspire others to continue their education. I am forever grateful for the encouragement and support these individuals faithfully provided.

ACKNOWLEDGMENTS

First and foremost, I would like to sincerely express my deepest gratitude to Amit U. Raysoni Ph.D., M.P.H for his mentorship and advice during my master's studies. Similarly, my thesis committee members provided invaluable input and ensured the quality of my work, thereby I would like to extend my appreciation-- thank you Owen Temby Ph.D., Katarzyna Sepielak Ph.D., and Dawid Wladyka Ph.D. I would also like to recognize my father, David Mendez, and brother, Jonathan D. Mendez, for their assistance with the fieldwork. This is for all of those who allowed us to use their residences as part of our study, thank you. Your support allowed for this to be possible, and I truly appreciate it.

Finally, thank you to the UTRGV College of Sciences for my research assistantship and the School of Earth, Environmental, and Marine Sciences at the University of Texas Rio Grande Valley for the funds and aid to make this study possible.

TABLE OF CONTENTS

Page

LIST OF TABLES

Page

LIST OF FIGURES

Page

CHAPTER I

INTRODUCTION

Nearly eight million people are estimated to die annually on a global scale due to air pollution exposure (e.g., fine particulate matter $PM_{2.5}$) (Zamora et al., 2020; Anderson et al., 2012; Organization, 2018). Continuous monitoring of various air pollutant species is not only prevalent in academic research, but also among the common citizen, businesses, and governments (Pang et al., 2021; Lewis & Edwards, 2016). For non-expert users, access to air pollutant data is rare and challenging (Pang et al., 2021). In recent years, the use of low-cost air quality monitors has caught the attention of scholars and individuals alike, because of their easy-access properties and locally relevant data (Pang et al., 2021; deSouza et al., 2017; Morawska et al., 2018; Sun et al., 2016; Weissert et al., 2017). Apart from aerial measurements and personal exposure monitoring, additional features of such sensors include economic costs, low energy consumption, convenient size, and lightweight properties (Pang et al., 2021; Pikridas et al., 2019; Rüdiger et al., 2018). Moreover, an increase in air quality studies around low-cost sensors gains traction due to accessible flexibility (Feenstra, 2020; Pang et al., 2021). Low-cost sensors are manufactured for ambient monitoring in local areas while providing high-resolution spatial and temporal networks or near-to-real-time data (Liu et al., 2020; Wang, 2020; Feenstra, 2020; Lee et al., 2019; Gao et al., 2015; Mukherjee et al., 2017). The improved availability of local ambient monitoring will enhance pollution awareness in neighborhood environments surrounded by growing industrialization (Zamora et al., 2020).

1.1 Particulate Matter Classification

Particulate pollution or particulate matter (PM) is classified as either primary or secondary aerosols (Burton, 2017). The primary aerosols are released into the atmosphere while secondary aerosols originate from the reaction of gases in the atmosphere (Burton, 2017). Airborne PM varies in different aerodynamic diameters and chemical compositions in space and time, generally consisting of a heterogeneous mixture of liquid and solid particles (Raysoni, 2011; Brook et al., 2004; Kim et al., 2015; Organization, 2013).

The United States Environmental Protection Agency regulates two size categories for particles, generally $PM_{2.5}$ and PM_{10} particulates (Kim et al., 2015; Esworthy, 2013; *Particulate Matter (PM) Pollution,* 2021). Coarse particulates (PM_{10}) indicate a diameter range of less than 10μm with a travel distance of 1 to 10 kilometers (Burton, 2017; Kim et al., 2015; Dausman, 2017; Srimuruganandam & Shiva Nagendra, 2012; Raysoni, 2011). $PM_{2.5}$ fine inhalable particles have a diameter of less than 2.5μm and a travel distance of 100 to 1000 kilometers (*Particulate Matter (PM) Pollution,* 2021; Kim et al., 2015; Srimuruganandam & Shiva Nagendra, 2012). The lifespan of $PM_{2.5}$ may exist from days to weeks while PM_{10} can last from minutes to hours (Kim et al., 2015; Cheung et al., 2011). For comparison, in Figure 1.1, the size of $PM_{2.5}$ and PM_{10} was scaled to human hair (50-70μm) and fine beach sand (90μm), resulting in the hair being roughly thirty times larger than $PM_{2.5}$ (*Particulate Matter (PM) Pollution,* 2021).

Markedly, the chemical composition of $PM_{2.5}$ consists of sulfate, nitrate, ammonium, elemental carbon, organic compounds, hydrogen ions, biogenic organics, and particle-bound water (Kim et al., 2015; Cheung et al., 2011). PM_{10} constituents are composed of resuspended dust, coal and oil fly ash, mold spores, plant parts, and metal oxides (Kim et al., 2015; Cheung et al., 2011). Organic and elemental carbon, metals, and particle-bound water expand the inorganic

ions that comprise PM chemical constituents (Kim et al., 2015; Cheung et al., 2011). PM chemical compositions are diverse enough to comprise biological or organic compounds, and metals (Kim et al., 2015).

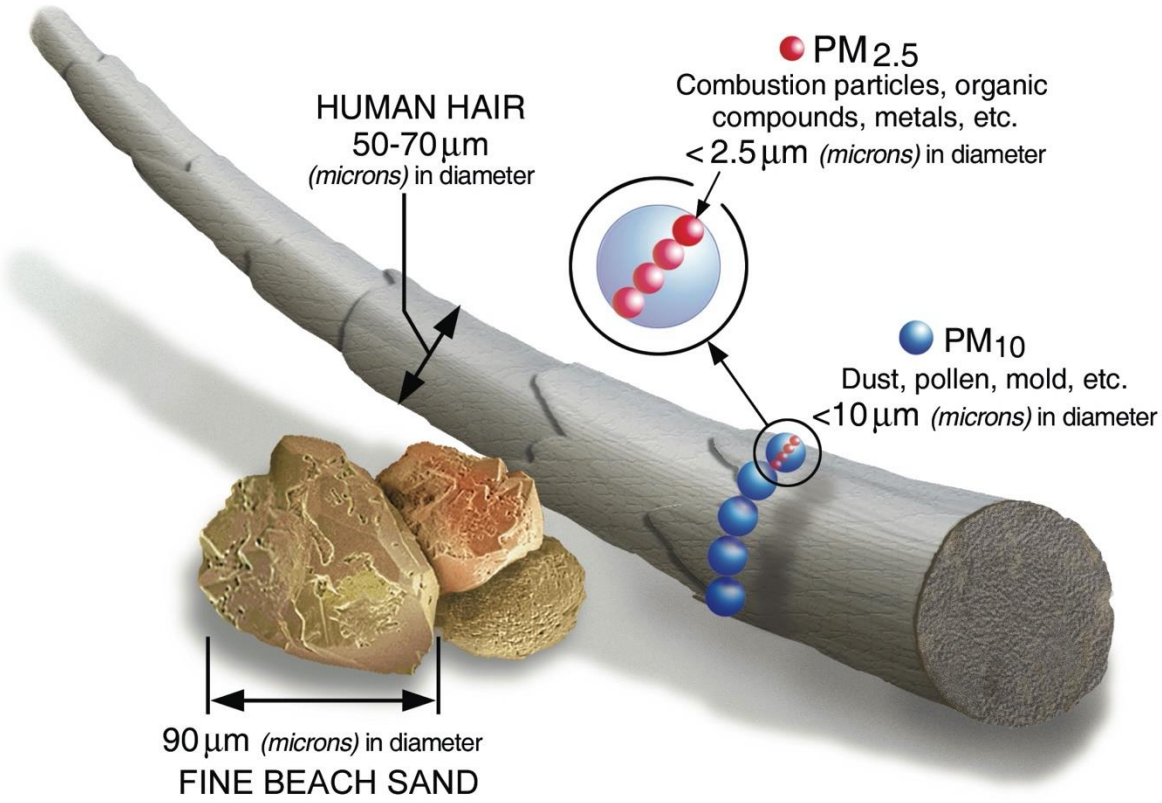

Figure 1.1: Size scale comparison of $PM_{2.5}$ and PM_{10} to the diameter(µm) of human hair and fine beach sand (Source: *Particulate Matter (PM) Pollution*, 2021).

1.2 Sources of Particulate Matter

PM species are built from gaseous precursor conversions (i.e. non-methane organic compounds) and/or direct emissions from anthropogenic or natural sources (Kim et al., 2015; Atkinson et al., 2010). Anthropogenic sources are human-associated and highly variable, for instance, industrial activities, biomass burning, and solid-fuel combustion (Kim et al., 2015; Srimuruganandam & Shiva Nagendra, 2012). On the contrary, natural sources of particulate matter originate from dust storms, volcanoes, and forest fires (Kim et al., 2015; Burton, 2017;

Misra et al., 2001). PM exposures pose a greater risk to human health than other common air pollutants like ground-level ozone (Kim et al., 2015). $PM_{2.5}$ sources include the combustion of coal, gasoline, oil, and high-temperature processes like smelters and steel mills (Kim et al., 2015). PM_{10} originates from the suspension of disturbed soils, ocean spray, construction, coal, and oil combustions (Kim et al., 2015).

The majority of PM pollution is directly connected to traffic originating from motor vehicular-related emissions (Raysoni, 2011; Kim et al., 2015; de Kok et al., 2006). Additional PM sources range from construction sites, road dust, mining operations, oil combustion, agriculture dust, riverbeds, and crustal sources (Kim et al., 2015; Juda-Rezler et al., 2011; Bozlaker et al., 2013; Bozlaker et al., 2014; Kulkarni et al., 2006; Kulkarni et al., 2007; Williamson et al., 2021; Rayonsi, 2011). Construction areas increase PM levels by encompassing large machinery that emits exhaust while upturning dust and dirt into the air (*BlueSky Air Quality Monitor*). Considering these various sources, traffic aerosol exposure is a significant concern in intra-and-inter-urban environments. An increase of studies suggests residential areas in the same vicinity of major highways result in higher $PM_{2.5}$ exposure patterns (Askariyeh et al., 2020; Kioumourtzoglou et al., 2016; Girguis et al., 2016; Weinstock et al., 2013; Vallamsundar et al., 2016). Vehicles idling at crowded intersections and parking lots result in elevated PM levels due to the high concentration of vehicle exhaust, poor ventilation near buildings, and brake pad dust (Kim et al., 2015; Raysoni, 2011).

Poor ventilation in buildings is proven to increase the concentration of indoor PM (Kim et al., 2015). Raysoni et al. (2013) studied four schools in the El Paso region near construction sites, intersections, and main roads to have a mean (standard deviation) of indoor $PM_{2.5}$ ranging from 8.2 (3.1) and 8.7 (2.4) $\mu g\ m^{-3}$. Indoor activities such as cooking and the use of household

products (e.g., printers and candles) may act as indoor PM sources (Kim et al., 2015; Madureira et al., 2012). Wang (2020) indicated acute exposure to $PM_{2.5}$ concentration (194 $\mu g/m^3$) during residential cooking, whereas Draggan (2011) reported the burning of an individual candle with 100 to 1700 $\mu g\ hr^{-1}$ (Kim et al., 2015).

1.3 Health Effects of Particulate Matter Exposure

Urban areas experience increased hospital admissions with human health effects involving respiratory symptoms, premature mortality, decreased lung function, exacerbation of chronic respiratory and cardiovascular diseases (Kim et al., 2015; Guaita et al., 2011; Halonen et al., 2009; Perez et al., 2012; Samoli et al., 2008; Burton, 2017). Children exposed to high PM levels are at risk of developing asthma, respiratory symptoms, and reduced lung function (Kim et al., 2015; Burton, 2017; Wang, 2020). An estimation of 11-19% of the U.S. populace resides within a couple of meters of major roads, resulting in about forty million citizens being affected by high levels of $PM_{2.5}$ (Askariyeh et al., 2020; Weinstock et al., 2013; Brugge et al., 2007; Rowangould, 2013).

Aerodynamic diameter is one of the main factors to determine PM transportation in the atmosphere and/or the inhalation in the respiratory system (Kim et al., 2015; Esworthy, 2013). Thus, PM diameter correlates with certain types of health issues in humans (Kim et al., 2015; Brown et al., 2013). $PM_{2.5}$ particles are fine enough to transport and penetrate themselves deep into the respiratory tract passage (Kim et al., 2015; Brunekreef & Forsberg, 2005; *Ambient (outdoor) air pollution*, 2021). PM_{10} particles enter through nasal breathing, with mucus and cilia effectively acting as a filter (Kim et al., 2015; Atkinson et al., 2010). The natural human body counters such invaders with sneezes and coughs (Kim et al., 2015; Cadelis et al., 2014). The remaining coarse particles settle into the trachea and/or the bronchi (Kim et al., 2015; Burton,

2017; Wang, 2020). Respiratory health effects occur after acute or chronic exposures. Acute exposures result in premature mortality, heart attacks, respiratory symptoms, respiratory diseases, and lung inflammation, whereas, chronic exposures lead to asthma, stunt lung growth, and overall lung damage, and function (Kim et al., 2015; Atkinson et al., 2010; Cadelis et al., 2014; Correia et al., 2013; Fang et al., 2013; Meister et al., 2012).

1.4 Air Quality Guidelines for Particulate Matter

The United States Environmental Protection Agency (USEPA) regulates fine and coarse particulate matter as "criteria" air pollutants harmful to human health (Askariyeh et al., 2020; Protection, 2022). National Ambient Air Quality Standards (NAAQS) are mandated under the Clean Air Act of 1990 (Protection, 2022). The NAAQS includes primary standards focusing on the protection of the public's health including the health of sensitive populations (i.e. children, asthmatics, and the elderly). Secondary standards aim to protect public welfare including damaged vegetation, crops, animals, and buildings (Protection, 2022). The latest NAAQS (2012) declares the annual mean (averaged over a three-year period) of $PM_{2.5}$ concentrations at 12 $\mu g/m^3$ as the primary standard and 15 $\mu g/m^3$ as the secondary standard (Table 1.1). The daily mean (98^{th} percentile averages over three years) of $PM_{2.5}$ concentration is 15 $\mu g/m^3$ for both primary and secondary standards (Protection, 2022).

Additionally, the Worlds Health Organization's (WHO) global air quality guidelines (GAQG) (updated in 2021) have provided thresholds for harmful pollution levels. In 2019, 99% of the world's population was residing in locations where the GAQG levels were not met. In 2016, a worldwide estimation of 4.2 million premature deaths (cancers and cardiovascular and respiratory disease) in urban and rural areas were caused by exposure to fine particulate matter. In Table 1.2, the $PM_{2.5}$ daily concentration averaged threshold is 15 $\mu g/m^3$ and the annual mean

is 5 μg/m³ (*Ambient (outdoor) air pollution*, 2021). The GAQG interim goals are aimed to shift PM concentrations lower and achieve significant reductions in health-associated effects.

Table 1.1: NAAQS reported standards as of 2012.

PM	Standard	Time	Level
$PM_{2.5}$	Primary	1 year	12.0 μg/m³
	Secondary	1 year	15.0 μg/m³
	Primary & Secondary	24 hours	35 μg/m³
PM_{10}	Primary & Secondary	24 hours	150 μg/m³

Table 1.2: WHO global air quality guidelines for 2021.

Particle pollution (PM)	Annual	Daily
$PM_{2.5}$	5 μg/m³	15 μg/m³
PM_{10}	15 μg/m³	45 μg/m³

1.5 Air Quality in the Rio Grande Valley

The United States (U.S.) and Mexico border region expands about 2000 miles throughout four U.S. states (Texas, New Mexico, Arizona, and California) and six Mexican states (Tamaulipas, Nuevo Leon, Coahuila, Chihuahua, Sonora, and Baja California) (Raysoni, 2011). Population across the region estimates to be twelve million, with the expectation to double by the year 2030 (Raysoni, 2011; Peach & Williams, 2004).

The Rio Grande Valley, South Texas, is located along the international U.S. -Mexico border with a total population of 1,402,340 persons as of 2022 (*Population Data for Region: Rio Grande Valley*). Given the proximity to the border, the RGV encounters cross-border trade with Mexico (Akland et al., 1997). In 1994, the North American Free Trade Agreement (NAFTA) formed a free trade zone for qualifying goods between Canada, Mexico, and United States. Developments of U.S. -Mexico bilateral commercial trade in goods and services continued to grow with Mexico ranking as the third-largest trading partner and second-largest exporter for the U.S. (since 2018) (*North American Free Trade Agreement (NAFTA)*). As a result, vehicular

transportation, industrialization, and population have increased in the U.S. -Mexico border regions (Raysoni, 2011). For instance, the study by Raysoni (2011) confirmed the Paso del Norte region (the border area between Texas and Chihuahua) experienced high automobile emissions from the accelerated border crossings.

Markedly, residents in the U.S. -Mexican border region shared their concerns about environmental contaminants in the immediate air and water (Akland et al., 1997). Contaminants ranged from transboundary pollution, traffic, refuse burning, local sources, and pesticides throughout the agricultural areas (Akland et al., 1997). These environmental contamination scenarios elicited interest in the local population to understand the actual exposure patterns. In 1983, the La Paz Agreement acknowledged the importance to improve and protect the environment in the U.S. -Mexican border region (*U.S.-Mexico border buffer polygon (la paz 1983), u.s. and mexico, 2019, u.s. environmental protection agency region 6*, 2019; Raysoni, 2011). This framework established the border region to be within a sixty-two-mile range from either side of the border (*U.S.-Mexico border buffer polygon (la paz 1983), u.s. and mexico, 2019, u.s. environmental protection agency region 6*, 2019). Most recently, The Border 2025 program stemmed from the La Paz Agreement to emphasize communities and local stakeholder involvement (*U.S.-Mexico Border Program*, 2022). The goals for the Border 2025 program include reducing air pollution, expanding access to clean water, promoting sustainable management of materials and waste, improving joint emergency preparedness, and enhancing emergency response to harmful environmental disasters (*U.S.-Mexico Border Program*, 2022). The findings from this current study will add to the evolving body of air quality literature in the U.S. -Mexican border region.

1.6 Local Conditions in the Rio Grande Valley

Exposure effectiveness of PM is influenced by conditions locally such as weather, topography, seasons, sources of particles, microenvironments, and concentration of the emissions (Kim et al., 2015; Casati et al., 2007). The RGV is a floodplain terrain that experiences hurricanes from the Gulf of Mexico's warm waters. Hurricane season typically begins June 1st to November 30th with a higher chance of rain between August and September months. The RGV region has a history of hurricanes occurring in the past two decades, from Hurricane Katrina in 2005 (category 5) to Hurricane Harvey in 2017 (category 4) to the most recent Hurricane Hanna in 2020 (category 1), affecting the Texas coast (Mendez et al., 2022; *The Official South Texas Hurricane Guide,* 2021). Moreover, every year usually from June to September, tons of dust is transported roughly 5,000 miles across the Atlantic Ocean originating from the Saharan desert in Africa (Danner, 2022; Spivey et al., 2022). The Saharan air layer (SAL) of dust brings dry air containing very fine particulates of minerals forming an orange-brownish haze that may affect those with respiratory issues. The tropical development is kept at a minimum when the SAL dry air overlaps the humidity (Danner, 2022; Spivey et al., 2022). Lastly, in April 2022 RGV Hidalgo County Commissioner Court ruled a local state of disaster and an emergency burn ban due to wildfires in the county region. Dry weather conditions and outdoor burning had prompted wildfires to burn over 800 acres in the county (*Hidalgo County declares local state of disaster due to wildfires*, 2022; *Outdoor burning*, 2022). It is important to note the recent local conditions in the RGV as it effectively influences PM exposure.

1.7 Thesis Goals and Hypothesis

The main objective of this research study is neighborhood-level monitoring of particulate matter with low-cost air quality monitors. The findings of this research will help elucidate

particulate matter temporal and spatial trends. The conclusions emanating from this research work will help characterize the accurate exposure burdens of communities in the Lower Rio Grande Valley while complementing the existing Texas Commission on Environmental Quality (TCEQ) Continuous Ambient Monitoring Stations (CAMSs). The Lower Rio Grande Valley region consists of five active CAMSs i.e., CAMS 43, CAMS 80, CAMS 323, CAMS 1023, and CAMS 1046 with only three stations monitoring $PM_{2.5}$ i.e., CAMS 80, CAMS 43, and CAMS 323. Therefore, how can the limited amount of active CAMSs accurately access the exposure burden for the populace of the RGV at over one million people? Given there is only three CAMSs recording PM in local conditions, the PM exposure patterns will be a general estimation. The average distance between the PM CAMSs is estimated to be fifty-one miles away from each other in separate cities. Placing low-cost sensors in intra-and-inter-urban locations will provide better access to PM ambient data at a personal exposure level. Significantly, this study is the first to characterize PM exposures in the Lower Rio Grande Valley region using low-cost sensors.

This research was constructed on the following hypothesis that $PM_{2.5}$ will vary spatially and temporally in the various cities (Brownsville, Edinburg, Weslaco, and Port Isabel) in the Lower Rio Grande Valley region. The resulting, statistical data analysis will demonstrate PM concentrations from the TCEQ CAMSs (CAMS 43, CAMS 80, and CAMS 323) may not be an accurate representation of the actual exposure patterns at an intra-urban level.

In order to proceed with this hypothesis, ambient monitoring of $PM_{2.5}$ was collected for over a year and correlated with Texas Commission on Environmental Quality (TCEQ) Continuous Ambient Central Monitoring Stations (CAMSs). Site-specific temporal and spatial relationships between low-cost sensors and CAMSs were examined with correlation analytics.

CHAPTER II

LITERATURE REVIEW

A literature review of low-cost sensors (LCSs) was performed to understand different methods of ambient measuring of particulate matter. These indoor/outdoor consumer-grade sensors emanate high-resolution data while providing near or real-time aerosol local ambient air quality levels (Khreis et al., 2022; Wu et al., 2022; Gómez-Suárez et al., 2022; Pawar & Sinha, 2022; He et al., 2022; Huang et al., 2022; Lu et al., 2021). Thus, the LCS ambient monitoring networks are rapidly expanding temporally and spatially (Feenstra, 2020; Wang, 2020; Lee et al., 2019). LCSs abilities range from measuring ambient, personal, or mobile exposures depending on the manufactured purpose (Feenstra, 2020; Gómez-Suárez et al., 2022). The reviewed LCSs varied with pre-set calibrations and metrics. In order to achieve quality assurance, it is recommended to sample reference-grade instruments Federal Reference Methods (FRM) and Federal Equivalent Method (FEM) near the LCSs to verify the sensors' accuracy and dependability (Lee et al., 2019; Lu et al., 2021; Feenstra, 2020; Lung et al., 2022). Additional collocation samples with the same LCSs are suggested to further confirm the accuracy and precision of the sensors (Feenstra, 2020; Lung et al., 2022).

Literature works focused on assessing PM species (PM_1, $PM_{2.5}$, PM_4, and PM_{10}) were incorporated into the review. Typically, PM LCSs operate with optical scattering sensors that detect IR refracted by PM when particles pass through the optical chamber (Mykhaylova, 2018).

These optical sensors are warned to be wary of temperature, relative humidity, and pressure obscuring the PM sensor, therefore, PM sensors are often built with independent sensors for relative humidity and temperature (Mykhaylova, 2018; Oluwadairo et al., 2022; Khreis et al., 2022; Gómez-Suárez et al., 2022). Quality control warrants the use of correction formulas for the resultant PM data and/or calibration methods for the LCSs (Lu et al., 2021). The Air Quality Sensor Performance Evaluation Center (AQ-SPEC) also provides thorough field testing evaluations of available commercial LCSs to the public (*TSI - BlueSky*).

The review only considered literature after the publication date of January 2000 to the current year 2022, with most of the literature published after 2015. Two literature review articles were found in which Karagulian et al. (2019) reviewed LCSs with reference monitors and Lung et al. (2022) conducted a review of LCSs used in the Southeast Asian region. A total of fifty-one studies underwent review. The studies performed LCS monitoring in different site settings, with some samples collected at multiple settings. As a result, the fifty-one studies included ten indoor samples, thirty-eight urban/semi-urban sites, six rural/semi-rural locations, and six suburban sites. All countries were included in the review, comprising of fourteen countries including the U.S.A., Australia, Canada, China, Greece, India, Japan, Norway, Oman, Portugal, South Korea, Spain, Taiwan, and the United Kingdom. Given that each research strove for different objectives and goals, the duration of the study varied. Out of the fifty-one studies, 41% were long-term studies (duration greater than or equal to six months), and 59% were short-term (less than six months) studies.

Emission sources from the literature review varied with about 84% of the selected studies determining the most common emissions for urban and suburban areas are vehicle and traffic exhaust-related (Liu et al., 2020; Castell et al., 2017; Pang et al., 2021; Ardon-Dryer et al., 2020;

Kelly et al., 2017; Chen, 2020; Zhang, 2019; Munir et al., 2019; Sayahi et al., 2019; Borrego et al., 2016; Carvlin et al., 2017; Gupta et al., 2018; Jayaratne et al.; Stavroulas et al., 2020; Steinle et al., 2015; Austin et al., 2015; Arvind et al., 2016; Wendt et al., 2019; Feenstra et al., 2019; Jiao et al., 2016; Feenstra, 2020; Zheng et al., 2018; Marto, 2018; Hartin, 2015; Wang, 2020; Dausman, 2017; Mykhaylova, 2018; Al Hanai, 2019; Williams & Duvall, 2018; Datta et al., 2020; Wallace et al., 2021; Lee et al., 2019; Zamora et al., 2020; Tsou et al., 2021; Malings et al., 2019; Magi et al., 2019; Wu et al., 2022; Khreis et al., 2022; Gómez-Suárez et al., 2022; Tian et al., 2022; Lu et al., 2021). Indoor samples detected human activity emitting PM sources such as cooking (Levy Zamora et al., 2019; Zervaki, 2018; Zhang, 2019; He et al., 2022; Steinle et al., 2015), air conditioning for cooling and heating (Steinle et al., 2015), and using office equipment (Huang et al., 2022), incense burning (Levy Zamora et al., 2019; Burton, 2017), cigarettes (Burton, 2017; Steinle et al., 2015) and wood smoke (Wells, 2020).

In 78% of the studies, reference instruments were included in the sampling to determine the LCSs accuracy. The other 22% of studies were nonapplicable with limited resources to access reference instruments. Twenty-nine of the studies calibrated their LCSs with FRM or FEM instruments (Liu et al., 2020; Castell et al., 2017; Ardon-Dryer et al., 2020; Kelly et al., 2017; Chen, 2020; Sayahi et al., 2019; Borrego et al., 2016; Carvlin et al., 2017; Gupta et al., 2018; Jayaratne et al.; Stavroulas et al., 2020; Wells, 2020; Steinle et al., 2015; Austin et al., 2015; Wendt et al., 2019; Feenstra et al., 2019; Jiao et al., 2016; Feenstra, 2020; Zheng et al., 2018; Marto, 2018; Wang, 2020; Al Hanai, 2019; Orlando, 2019; Levy Zamora et al., 2019; Williams & Duvall, 2018; Datta et al., 2020; Wallace et al., 2021; Tsou et al., 2021; Magi et al., 2019). Respective studies calibrated their LCS with the reference monitors GRIMM **(**Grimm Aerosol Technik GmbH & Co. KG, Airing, Germany) (Oluwadairo et al., 2022; Huang et al.,

2022; Gómez-Suárez et al., 2022; Williams & Duvall, 2018; Chen, 2020) and DustTrak DRX (TSI Inc., Minnesota, USA) (Huang et al., 2022). Most recently in Dallas, Tx urban region, Khreis et al. (2022) co-located twelve commercial grade LCSs to a reference site operated by the Texas Commission on Environmental Quality (TCEQ) with R^2 ranging from 0.20 to 0.39.

The objective of this review was to summarize various studies determining LCSs performance to assess ambient PM concentrations. As a result, these global studies confirm FRM/FEM samples and other collocation samples to calibrate LCSs accuracy and precision pre- and post-study. The results from the review will aid in this study's performance with the selected LCSs.

CHAPTER III

STUDY DESIGN AND METHODS

3.1 Rio Grande Valley Demographics

The Rio Grande Valley (RGV) region of South TX, includes Starr, Hidalgo, Cameron, and Willacy counties (represented in Figure 3.1). Our study focuses on the lower region of the RGV (Hidalgo and Cameron counties). According to the U.S. Census Bureau, as of July 1st, 2021, the Hidalgo County estimated population recorded 880,356 people, while Cameron County registered 423,029 persons. Given the proximity of the RGV to the U.S. -Mexican border, these county populations are predominantly of Hispanic or Latino ethnicity consisting of 92.5% of the total population in Hidalgo county and 90% of Cameron county. The percent living in poverty in the Hidalgo region was 23.9% while Cameron county was 24.4% of the population (*QuickFacts Hidalgo County, Texas; Cameron County, Texas*).

As of 2022, the total population in the RGV consist of 1,402,340 people with Hispanics/Latinos comprising about 94% of those persons (*Population Data for Region: Rio Grande Valley*). The percentage of families living below poverty in the region accounts for 25% of the population. The median household income in the RGV ranks $45,599 with Hispanic/Latino households making a median of $44,001 (*Population Data for Region: Rio Grande Valley*).

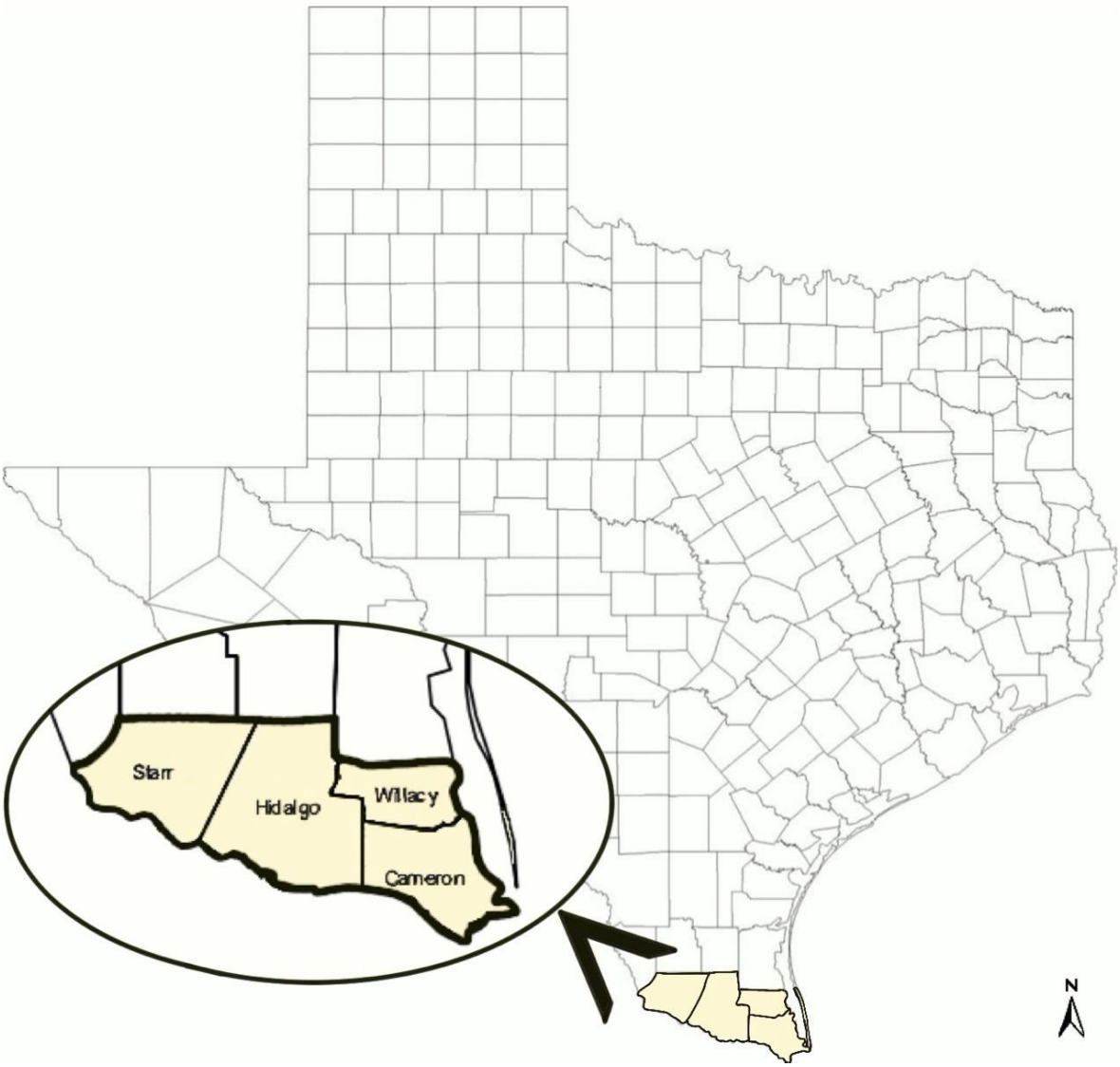

Figure 3.1: Texas outlined county map with the Rio Grande Valley region highlighted.

3.2 Site Selection

Five low-cost sensors (LCSs) were deployed in the city of Brownsville, three in Edinburg, two in Weslaco, and one at Port Isabel. The labeling of LCSs was based on the deployed city and numbered chronologically i.e., Brownsville locations (B1, B2, B3, B4, B5), Edinburg (E1, E2, E3), Weslaco (W1, W2), and Port Isabel (PI). Figure 3.2 illustrates the study area, in the Lower RGV, with color-coordinated location pinpoints to represent the location of the deployed LCSs, followed by a U.S. map with a red marker denoting the Lower RGV. The

Brownsville locations are marked with a deep blue pin. Edinburg sites are noted with gold pins. LCS sites in Weslaco are symbolized with green pins. The Port Isabel site is signified by the purple pin. Lastly, the TCEQ CAMSs are indicated with black triangle markers. The monitors were strategically placed in neighborhoods, university centers, and police departments to represent areas of low, medium, and high traffic density.

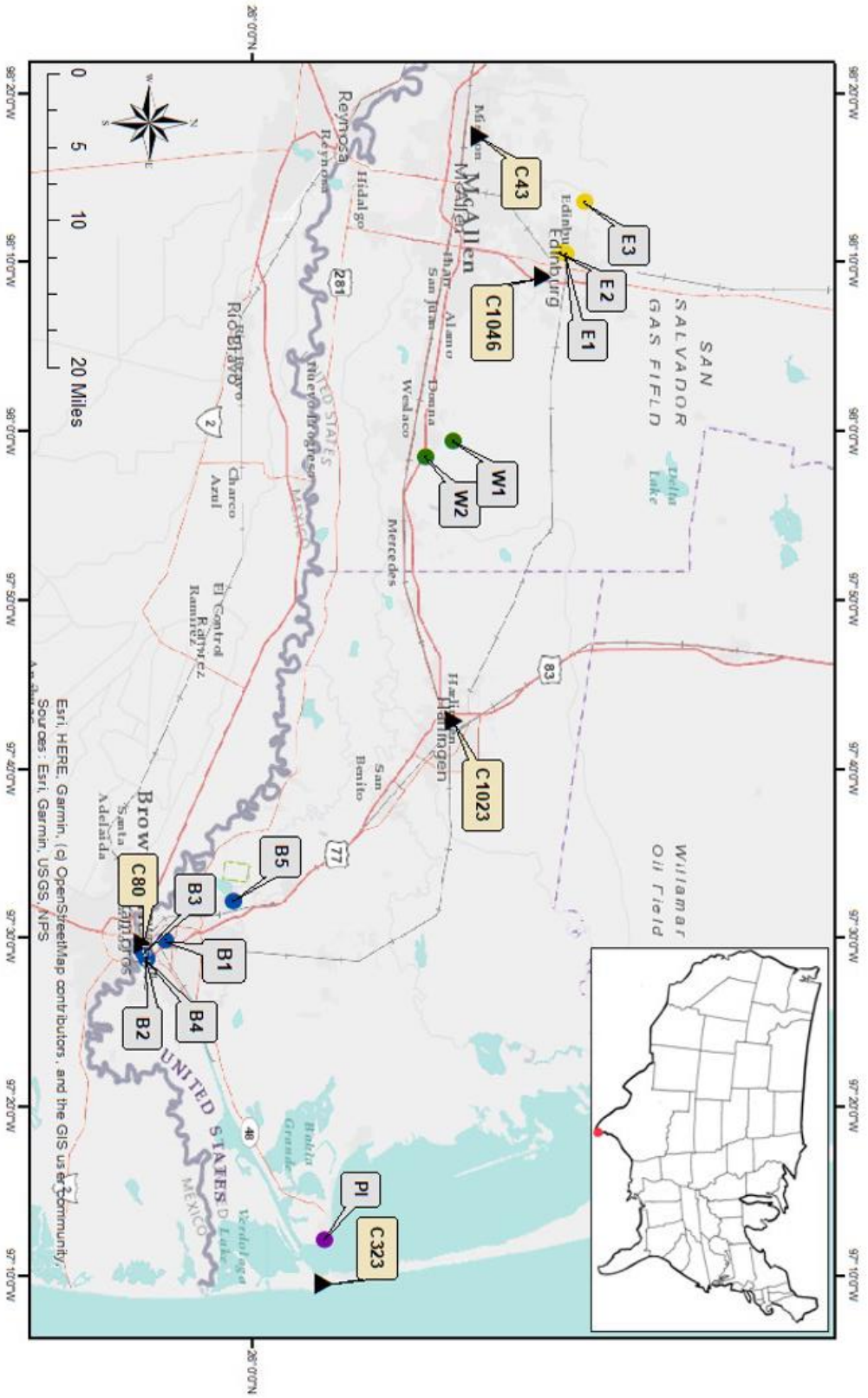

Figure 3.2: Map of the study area identifying LCSs and TCEQ CAMSs across the Lower Rio Grande Valley of South Texas.

The study duration was from March 1st, 2021, to March 31st, 2022 (396 days) to assess a little more than a complete year of ambient PM monitoring by LCSs. General site specifications for each of the LCSs are summarized in Table 3.1.

Table 3.1: Summarized site specifications of LCS sites in the Lower RGV.

LCS	City	County	Site specifications
B1	Brownsville	Cameron	Right across from Dean Porter Park and adjacent to the Gladys Porter Zoo in a semi-residential area.
B2	Brownsville	Cameron	University of Texas Rio Grande Valley (UTRGV) Brownsville Campus police department, near the campus student dormitories 'Casa Bella'.
B3	Brownsville	Cameron	Music and Science Learning Center on University Boulevard at the UTRGV campus.
B4	Brownsville	Cameron	Adjacent to Texas State Highway 69E and is only 0.04 miles away from the U.S. -Mexico International Port of Entry.
B5	Brownsville	Cameron	Neighborhood surrounded by Resaca del Rancho Viejo (Resacas are ox-bow lakes unique to Rio Grande River (natural U.S -Mexico boundary)
E1	Edinburg	Hidalgo	UTRGV Edinburg campus facing commonly used road: Schunior St.
E2	Edinburg	Hidalgo	UTRGV Edinburg campus facing commonly used road: 107 Texas
E3	Edinburg	Hidalgo	Closed gated residential community
W1	Weslaco	Hidalgo	Further from the city in a residence right off of Farm to Market Road 88 (FM88).
W2	Weslaco	Hidalgo	One of the buildings of the Weslaco Police department on the frontage of Texas State Expressway 83
PI	Port Isabel	Cameron	UTRGV Coastal labs between two neighborhoods near the tourist place of South Padre Island

Site B1 was in a semi-residential area adjacent to Brownsville's Gladys Porter Zoo (300m or 0.2 miles), the Town Resaca, and Dean Porter Park (Figure 3.3). The home is situated on a road trailing off to a major Texas State Highway (69E) approximately 600m (0.4 miles) east. On the University of Texas Rio Grande Valley (UTRGV) Brownsville campus, B2 was established outside the campus police department building near the Casa Bella residential campus apartments (Figure 3.4). This location is about 280m (0.2 miles) away from Texas State Highway 69E. The B3 sensor was deployed in the Music and Science Learning Center 22.7m

(0.01 miles) from the University Blvd at the UTRGV Brownsville campus (Figure 3.5). Furthermore, the university's music center stands in the middle of the Lozano Banco Resaca and a frequently used parking lot. B4 resided at the edge of the UTRGV campus on the Vaquero Plaza building, about 60m (0.04 miles) from a major intersection where University Blvd. and Texas State Highway 69E connect (Figure 3.6). Further south, Highway 69E leads to the customs and border U.S. -Mexico International Port of Entry. Markedly, the entire UTRGV Brownsville Campus is located on the main state highway 69E on the U.S. -Mexico border. Thus, traffic and vehicular-related exposures are of great concern in this region. Lastly in Brownsville, B5 was deployed in a neighborhood surrounded by the Resaca del Rancho Viejo. The residential household itself is on the cusp of the curved neighborhood (Figure 3.7). Resacas are unique features in the city of Brownsville representing the distributary channels of the Rio Grande River, a natural international boundary between the U.S. and Mexico.

Outside the School of Medicine at the UTRGV Edinburg campus, site E1 directly faced traffic and was surrounded by campus parking lots (Figure 3.8). The School of Medicine building is 9.8m (0.01 miles) beside the commonly used W Schunior St. Station E2 was deployed on the Student Academic Center of the Edinburg UTRGV campus (Figure 3.9). The Center is 70.3m (0.04 miles) off the main road 107 Texas near the intersection with Sugar Rd. E3 was enclosed in a gated residential community with a resaca in the center (Figure 3.10).

Moreover, the first Weslaco location, W1, was located further from the city at a household 164m (0.1 miles) near the crossroads of Farm to Market Road 88 (FM88) (Figure 3.11). Whereas W2 was deployed 63m (0.04 miles) on the frontage of Texas State Expressway 83 at the Weslaco police department (Figure 3.12). Site W2 was also adjacent to Weslaco's Border Patrol and approximately 600m (0.37 miles) from Mid Valley Airport. Lastly for this

study, the PI sensor was deployed at the UTRGV Port Isabel: Coastal Studies building (Figure 3.13). These labs are located between two neighborhoods on the coast of the Laguna Madre near the draw bridge towards Long Island. Port Isabel is the neighboring city to the popular tourist destination, South Padre Island.

Overall, these LCSs deployed locations were deliberately chosen in order to present an accurate representation of the daily $PM_{2.5}$ neighborhood exposure patterns. As a result, these studied locations will capture spatial resolution in all the selected cities in the Lower RGV region. Figures 3.3 -3.13 demonstrates the eleven LCSs installations and an aerial snapshot of their adjourning environments.

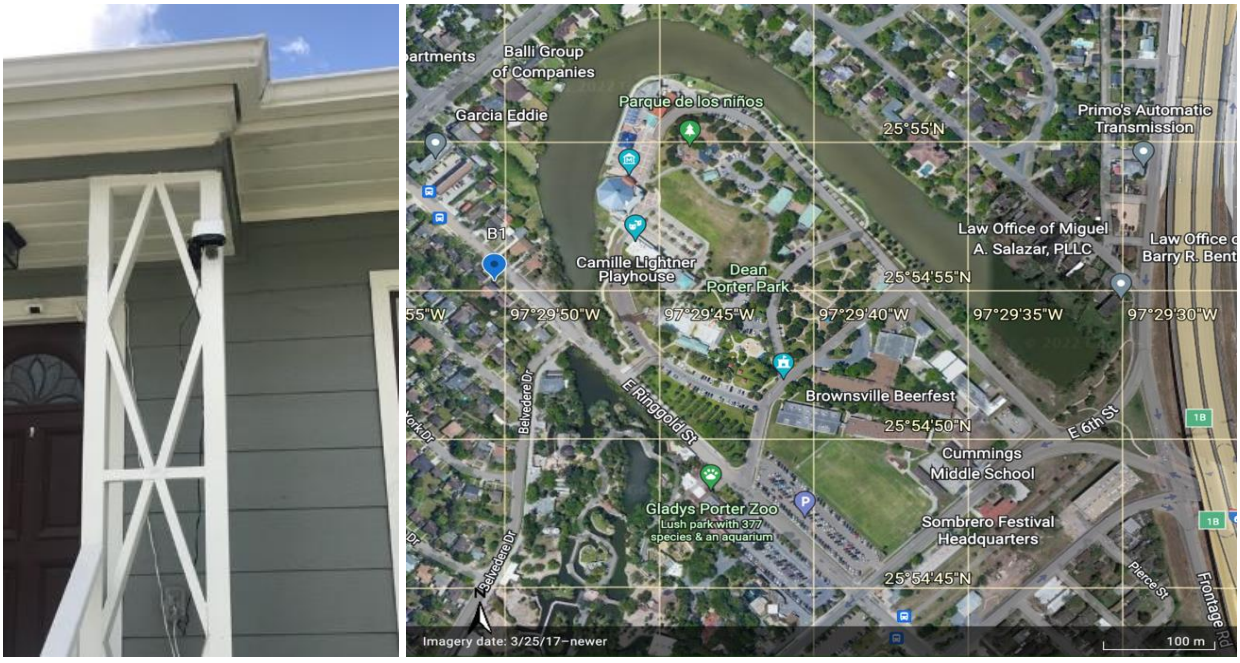

Figure 3.3: B1 installation photo with a satellite aerial view of the adjoining environment (Source: Google Earth).

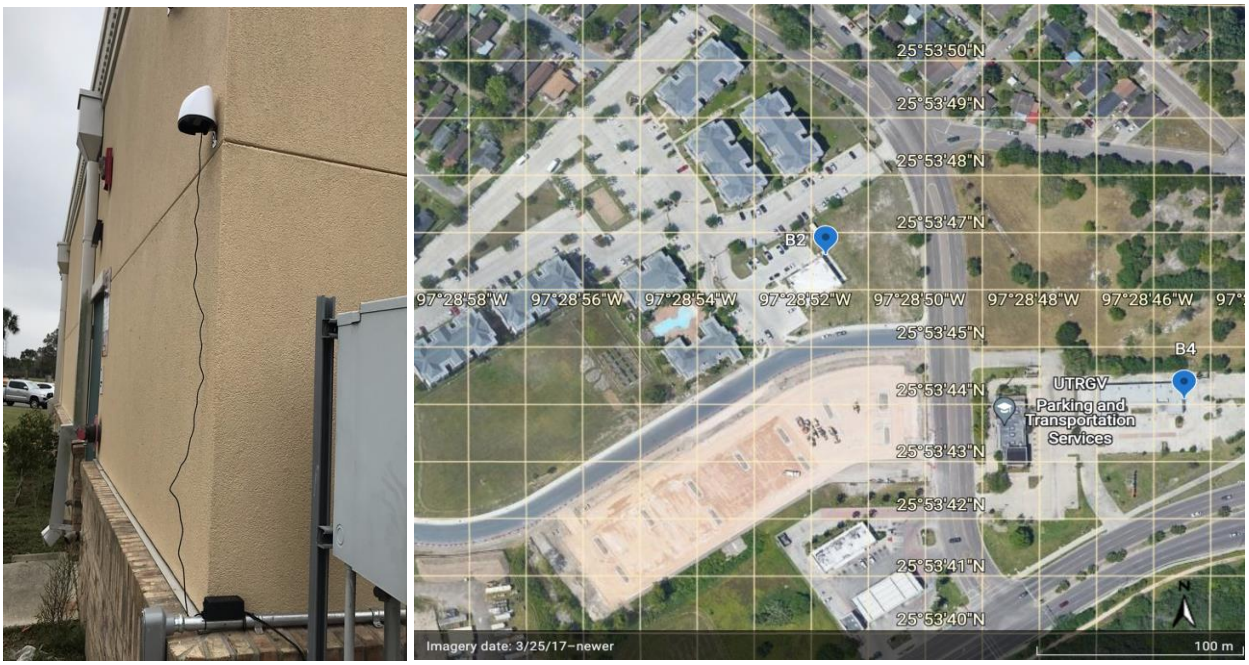

Figure 3.4: B2 installation photo with a satellite aerial view of the adjoining environment (Source: Google Earth).

Figure 3.5: B3 installation photo with a satellite aerial view of the adjoining environment (Source: Google Earth).

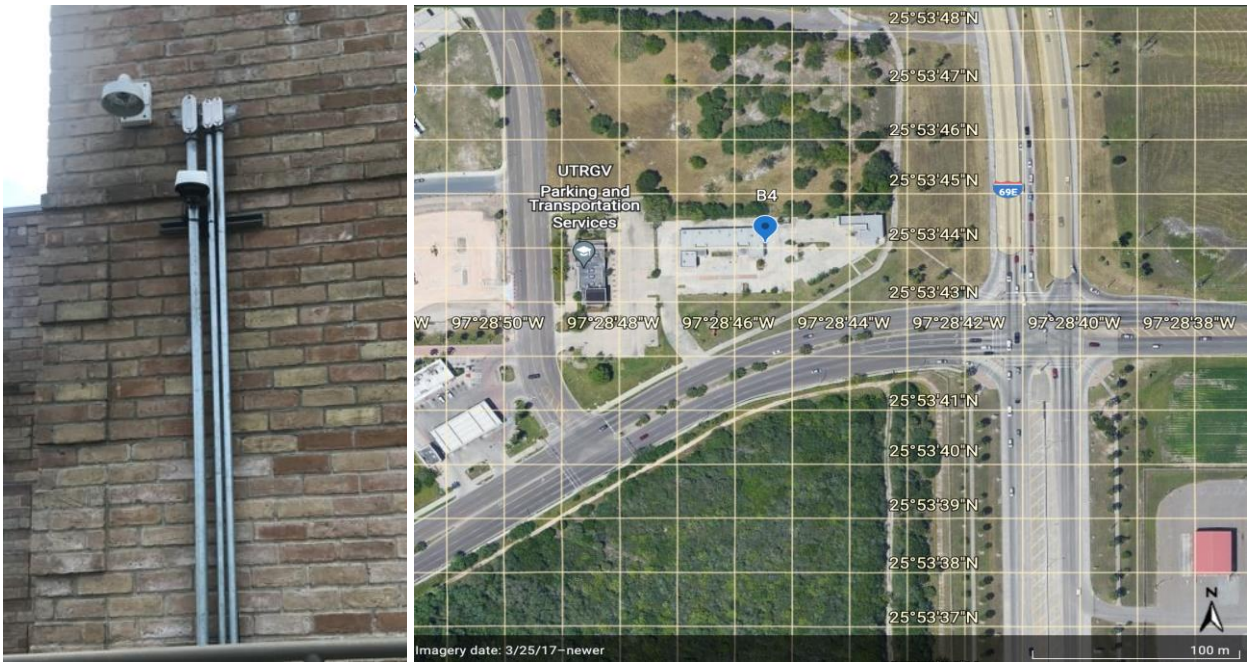

Figure 3.6: B4 installation photo with a satellite aerial view of the adjoining environment (Source: Google Earth).

Figure 3.7: B5 installation photo with a satellite aerial view of the adjoining environment (Source: Google Earth).

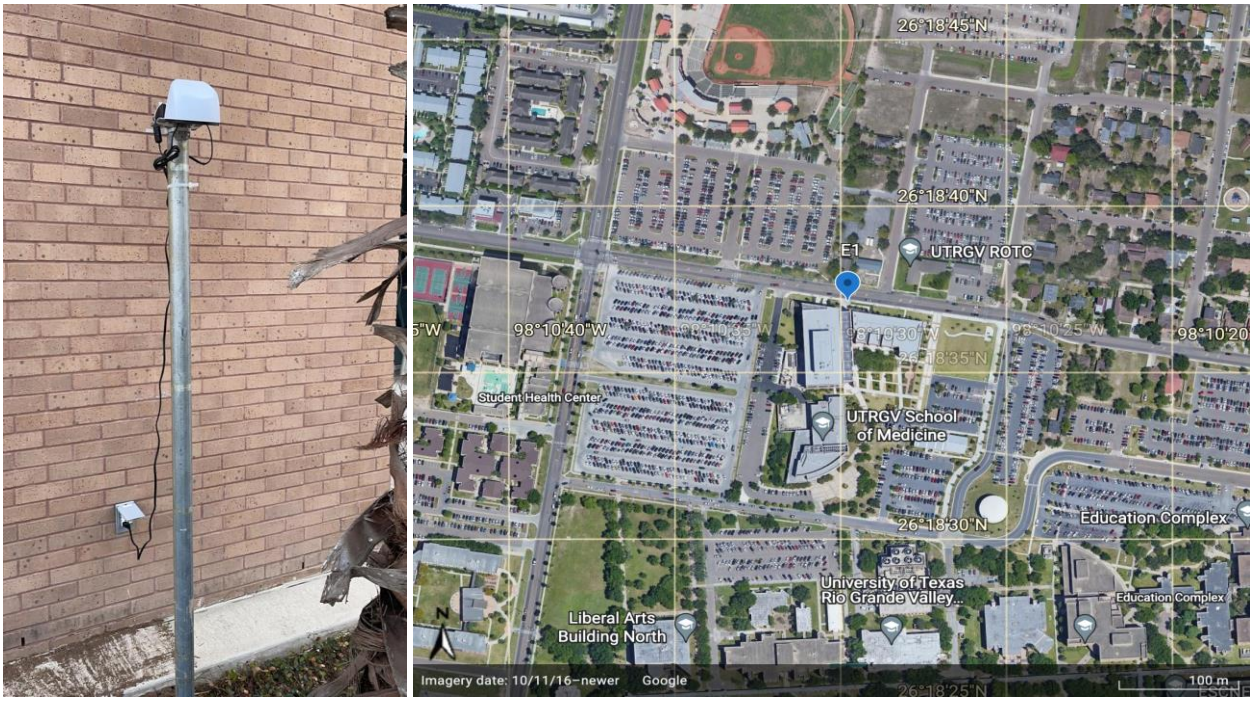

Figure 3.8: E1 installation photo with a satellite aerial view of the adjoining environment (Source: Google Earth).

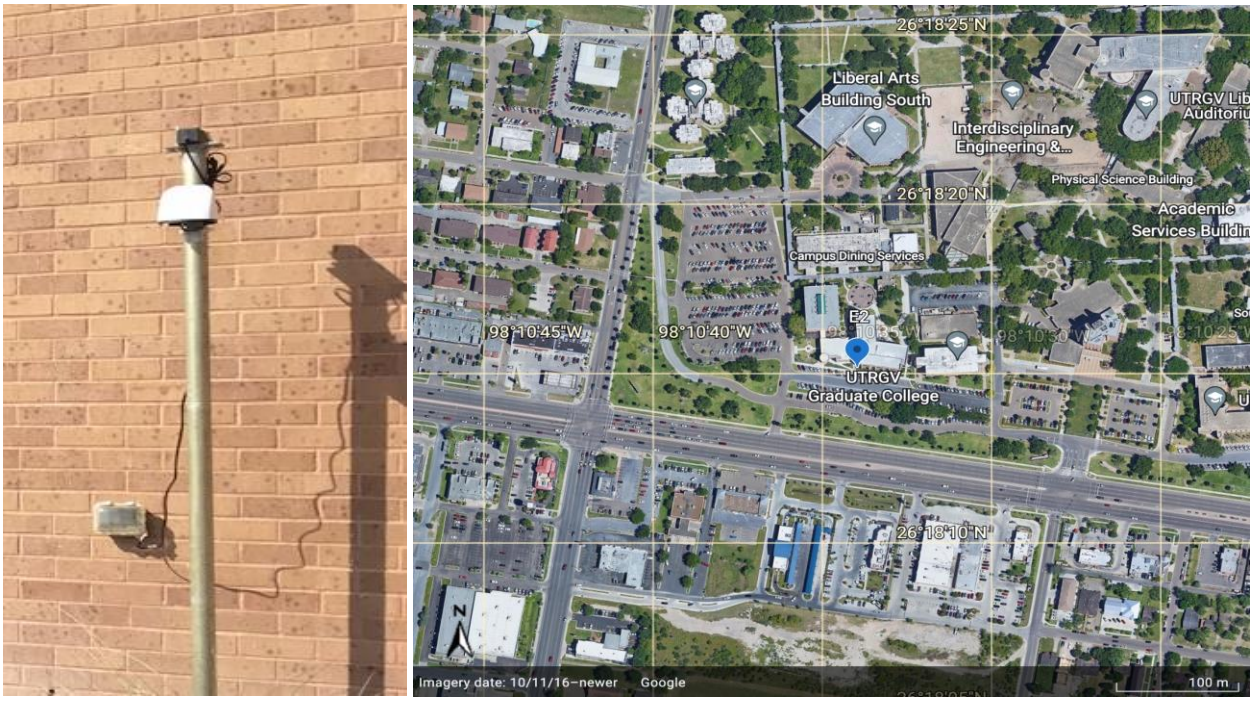

Figure 3.9: E2 installation photo with a satellite aerial view of the adjoining environment (Source: Google Earth).

Figure 3.10: E3 installation photo with a satellite aerial view of the adjoining environment (Source: Google Earth).

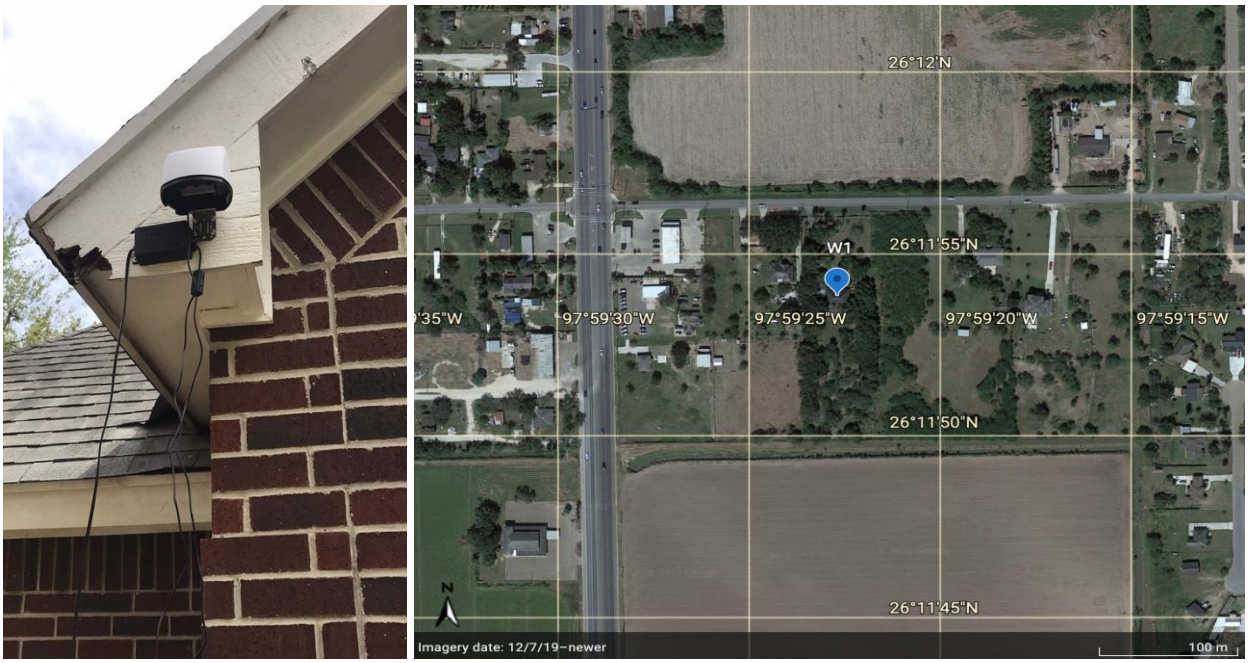

Figure 3.11: W1 installation photo with a satellite aerial view of the adjoining environment (Source: Google Earth).

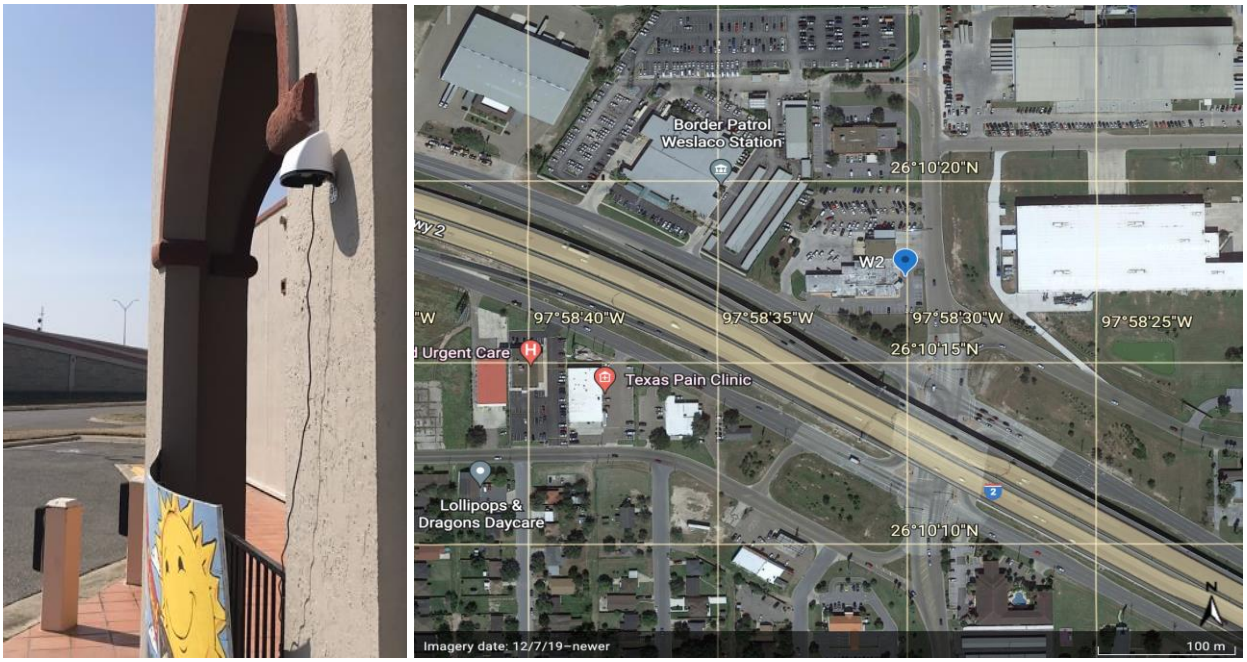

Figure 3.12: W2 installation photo with a satellite aerial view of the adjoining environment (Source: Google Earth).

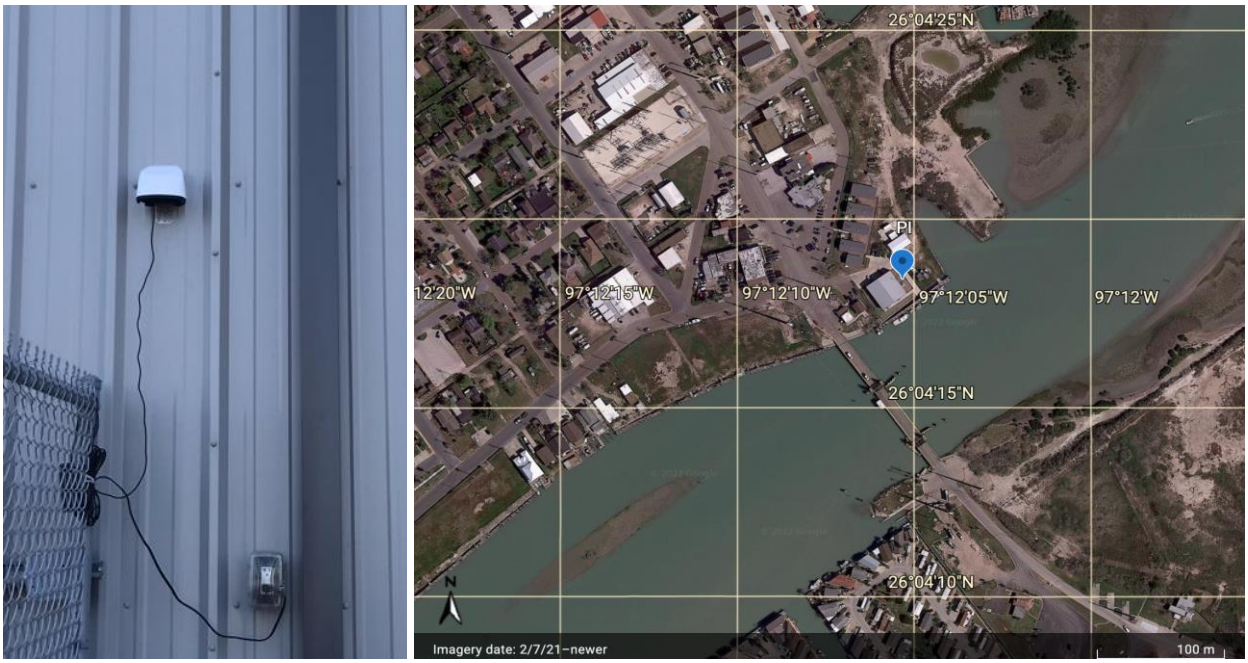

Figure 3.13: PI installation photo with a satellite aerial view of the adjoining environment (Source: Google Earth).

3.3 Topography and Meteorology of the Lower Rio Grande Valley

The Lower Rio Grande Valley is a semi-tropical floodplain with humid summers located on the border of Mexico near the Gulf Coast shores (Mendez et al., 2022; *The Official South*

Texas Hurricane Guide, 2021; *Rio Grande Valley, Texas Travel Guide*). The proximity to the Gulf of Mexico effectively incites a hurricane season from June 1st to November 30th, with the possibility of a hurricane occurring each month (Mendez et al., 2022; *The Official South Texas Hurricane Guide,* 2021).

Prevailing wind patterns throughout the duration of this study (March 1st, 2021, to March 31st, 2022) are provided by the RGV active TCEQ CAMSs mandated by the USEPA. Meteorological parameters influence the quality of air when hurricanes are present (Mendez et al., 2022). Averaged wind direction is illustrated by the wind roses in Figures 3.14 -3.18 with winds blowing from the southeast. Averaged wind speed for the continuous monitoring sites for C43 at 2.82m/s, C80 blew at 3.01m/s, C323 at 3.37m/s, C1023 at 3.55m/s, and C1046 at 2.73m/s.

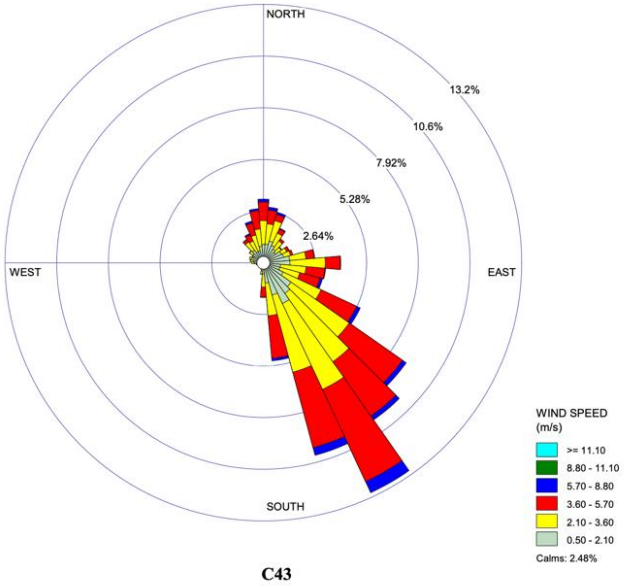

Figure 3.14: Wind rose diagram for CAMS C43 (March 1st, 2021, to March 31st, 2022).

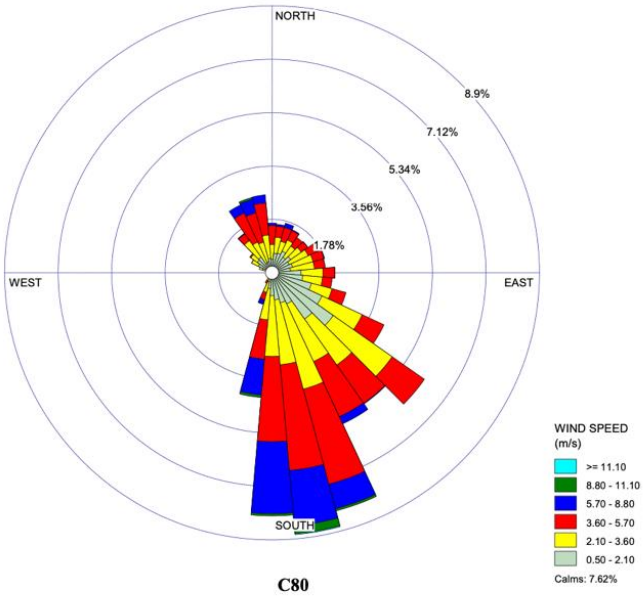

Figure 3.15: Wind rose diagram for CAMS C80 (March 1st, 2021, to March 31st, 2022).

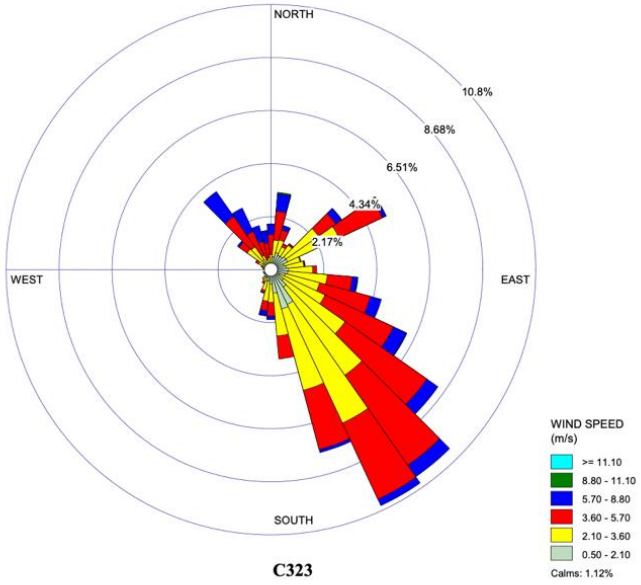

Figure 3.16: Wind rose diagram for CAMS C323 (March 1st, 2021, to March 31st, 2022).

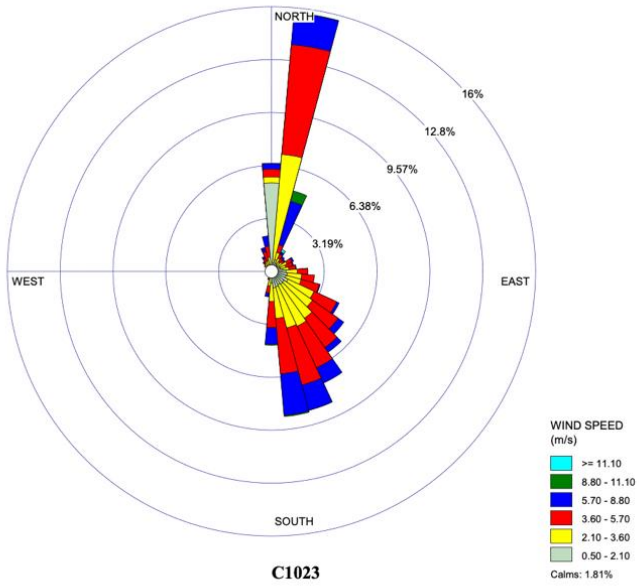

Figure 3.17: Wind rose diagram for CAMS C1023 (March 1st, 2021, to March 31st, 2022).

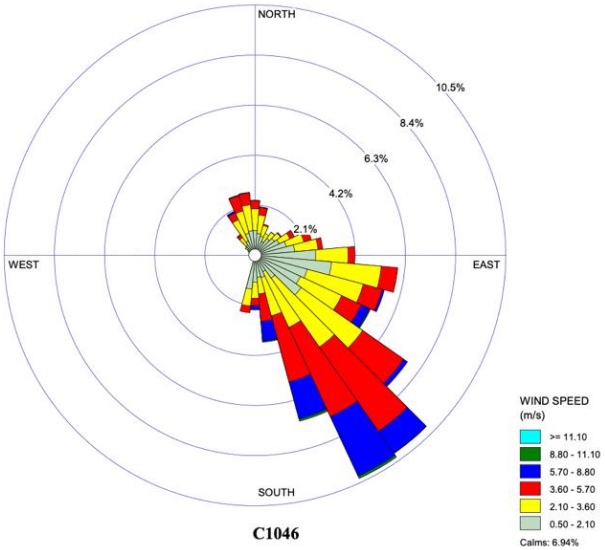

Figure 3.18: Wind rose diagram for CAMS C1046 (March 1st, 2021, to March 31st, 2022).

3.4 Instrumentation

The LCSs used for this study - BlueSky Air Quality Monitor (Model: 8143) are manufactured by TSI Incorporated, Minnesota, U.S. Currently these LCS were priced at $400

and is practical enough to be installed in neighborhoods and related locations. The small device weighs 0.35 lbs. with a power consumption to be less than 5W (5 VDC @ 1 Amp). The dimensions of the monitor are 6-inch x 5.5 inches x 4.5 inches (*BlueSky Air Quality Monitor*, 2020). The LCS is a 6-channel particulate counter measuring PM mass concentrations, temperature, and relative humidity. The sensor parameters of PM, temperature, and humidity are listed in *f*Table 3.2. The temperature sensor range is from -40ºC to 125 ºC, the humidity sensor ranges between 0 to 100% RH, and lastly, the aerosol mass concentration varies between 0 to 1000 μg/m^3 (*BlueSky Air Quality Monitor*, 2020). The PM sensor is pre-calibrated in the factory to adhere to the same standards as those from high-quality monitors such as AM520 (TSI Incorporated, Minnesota, U.S.) and DustTrak™ models (TSI Incorporated, Minnesota, U.S). The self-diagnostic ability allows the monitor to run with more than 95% up-time to obtain high-quality data (*BlueSky Air Quality Monitor*, 2020). TSI has measured the accuracy of the low-cost PM sensor against the TSI DustTrak DRX PM sensor in a month-long study comparing $PM_{2.5}$ readings in 2019 (*Measure and Record your Air Quality Data*). As a result, the accuracy of the PM sensor is ±10% @ 100 to 1000 μg/m^3 when compared to the DustTrak sensor (*BlueSky Air Quality Monitor Operation and Maintenance Manual*, 2021).

Table 3.2: LCS specifications.

Sensor	Range	Accuracy	Measurement Resolution	Response Time
PM	0 to 1000 μg/m^3	±10 % @ 100 to 1000 μg/m^3	1 μg/m^3	1 second
Temperature	-40 ºC to 125 ºC	±0.2ºC	0.04ºC (12 BIT A/D)	5 to 30 seconds
Humidity	0 to 100% RH	±1.8% RH	0.04 RH (12 BIT A/D)	8 seconds

3.4.1 Theory of Operation

LCS units use an optical particle counter (OPC) to identify PM species (inside mechanics are shown in Figures 3.19- 3.21). Typically, instruments containing optical PM sensors are either

scattering-based or camera-based optical sensors (Molaie & Lino, 2021). In this case, these LCSs are constructed to use the laser scattering single particle counter (Sensirion SPS30) principle to sense particulate matter in real-time data (*BlueSky Air Quality Monitor*, 2020; *TSI - BlueSky*). The particulate matter sensor is exhibited in Figure 3.22. Scattered-based OPC measures scattered light from particles with a single-particle photodetector. The scattered intensity is proportional to any particle individual size, thus reading in a range between low and high concentrations (Molaie & Lino, 2021). This laser-based measurement converts particles to mass concentrations through the appropriate algorithms (*TSI - BlueSky*).

Figure 3.19: Photo of the installed PM sensor.

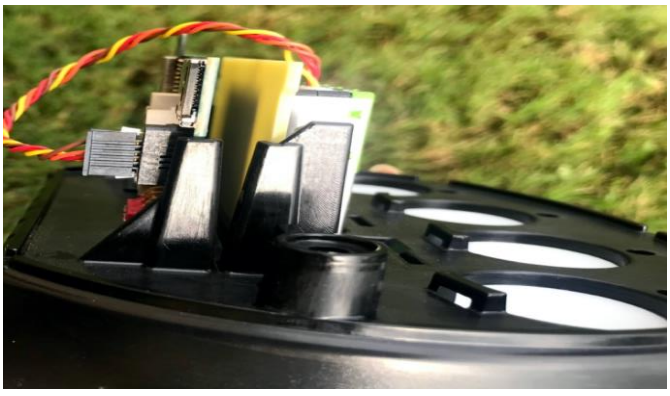

Figure 3.20: Side profile of the installed PM sensor.

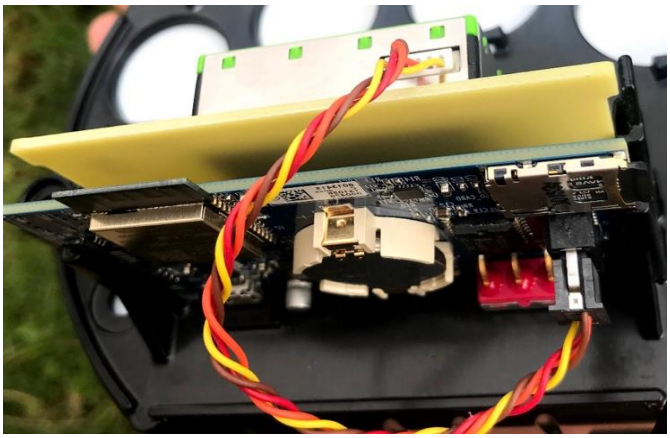

Figure 3.21: Top profile of the installed PM sensor.

Figure 3.22: Uninstalled PM sensor.

The light measured is commonly IR-refracted with PM transitory in the optical chamber (Figure 3.23). Light scattering is disadvantaged by the inability to detect ultrafine particulate matter (less than 0.1μm) nor is it a direct mass measurement (Mykhaylova, 2018).

OPC is one of the main common gas sensors to operate the monitoring of ambient air pollutants and one of the least expensive technologies (Mykhaylova, 2018). The gas sensor creates an indicator when the target gas is contacted (Pang et al., 2021). The signal created generally presents a linear relationship between the targeted gas concentration and the sensor output (Pang et al., 2021). Interference may occur with environmental factors, such as co-pollutants (CO, CO_2, NO, NO_2, SO_2, and O_3), temperature, and relative humidity (Pang et al., 2021, 2018). Consequently, the machine learning method, sensor clustering technique, and/or

correcting linear calculations are methods suggested to correct interference and accuracy in complex aerosol systems (Pang et al., 2021; Mykhaylova, 2018).

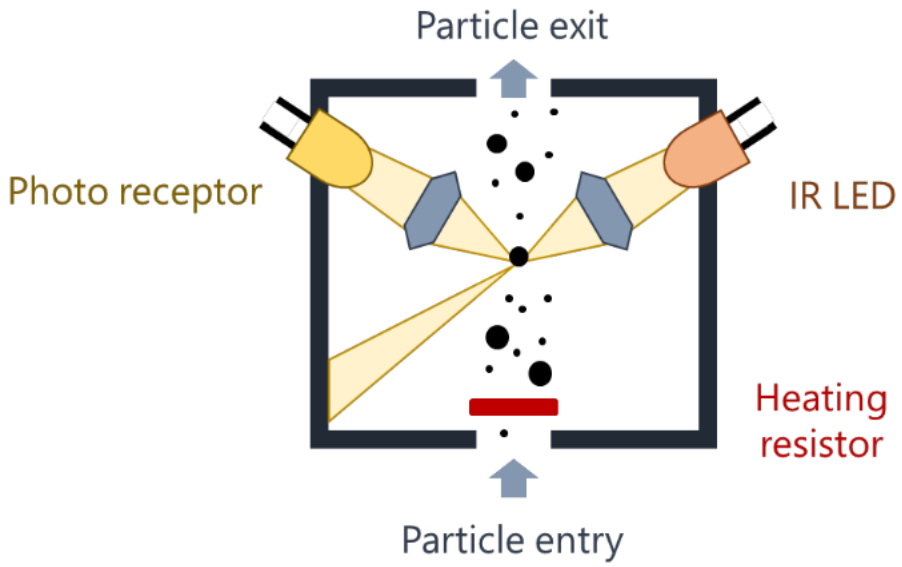

Figure 3.23: Diagram of optical light scattering sensor used for monitoring PM (Source: Mykhaylova, 2018).

3.4.2 Low-Cost Sensor Database

Deployment of these LCSs can be utilized either outdoors or indoors with a setup duration of fewer than 10 minutes. The sensors were installed at least six feet above the ground to represent the human breathing zone. The sensors are normally used outdoors with 24/7 operation under the condition to maintain a constant power supply. When the database is continuously connected to the internet network, data is transmitted through the cloud via online TSIlink.com (*BlueSky Air Quality Monitor Operation and Maintenance Manual*, 2021). A web browser and internet connection are required in order to access the LCSs' real-time data. $PM_{2.5}$, PM_{10}, relative humidity, and temperature data are automatically uploaded to the cloud and ready to be downloaded. Sensors are recommended to be in constant connection to the internet, in order to foresee device and/or sensor error alerts. Simultaneously, aerosol mass concentration

measurements of $PM_{1,}$ $PM_{2.5,}$ PM_{4}, and PM_{10} are stored in the built-in microSD card as duplicate storage. The units of concentration of the PM species are $\mu g/m^3$.

Logging intervals have the option of 1, 5, 10, 15, 30, and 60-minute averages. Each monitor has the option to run an internal cleaning every day or week, depending on the location of the monitor. Dusty areas may interfere with the PM sensors, as well as the quality of the data. In this study, the logging intervals for the eleven LCSs are five minutes averaged with daily cleaning intervals to receive the most accurate data. Data is collected every other week by extracting the microSD card from the internal setup and downloading the .csv files. Fine particulate matter $PM_{2.5}$, temperature, and relative humidity were the chosen parameters for this study.

3.4.3 TCEQ CAMS Database

The LCSs' resultant ambient data were compared to available continuous data from the Texas Commission on Environmental Quality (TCEQ) Continuous Ambient Monitoring Stations (CAMSs) from the RGV region. Table 3.3 provides the status of all the Lower RGV stations and Figures 3.24- 3.28 reveal the aerial satellite view of each location.

Table 3.3: General location, site specifications, status, and logged PM at TCEQ CAMSs.

CAMS	EPA site	City	County	Status	PM	Latitude	Longitude
C80	480610006	Brownsville	Cameron	Active	$PM_{2.5}$	25.8925176	-97.4938295
C43	482150043	Mission	Hidalgo	Active	$PM_{2.5}$	26.2262097	-98.2910690
C323	480612004	South Padre	Cameron	Active	$PM_{2.5}$	26.0711000	-97.1577000
C1046	482151046	Edinburg	Hidalgo	Active	N/A	26.2886220	-98.1520660
C1023	480611023	Harlingen	Cameron	Active	N/A	26.2003347	-97.7126837

CAMS-43 (C43) is located outside of John H. Shary Elementary school behind a pediatric clinic and urgent care center in Mission (Figure 3.24). The nearest road is N. Glasscock Rd about 65m (0.04 miles) from the CAMS. CAMS-80 (C80) is located at the UTRGV Brownsville campus 280m (.17 miles) from the U.S. -Mexican border (Figure 3.25). CAMS-323

(C323) is deployed at the South Padre Island UTRGV Coastal labs near a trailer park community (Figure 3.26). South Padre Island is a barrier island along the Gulf of Mexico connected to the city of Port Isabel via the Queen Isabella Causeway located over the Laguna Madre. CAMS-1046 (C1046) is located on the frontage about 126m (0.08 miles) from Texas State Highway 69C outside of the UTRGV CESS building (Figure 3.27). The adjourning surroundings include an Edinburg middle school, park, and doctor's office. Lastly, CAMS-1023 (C1023) lies on the outskirt of a neighborhood on the field in a high school Freshman Academy HCISD (Figure 3.28). The TCEQ CAMSs were labeled with their given CAMS number from the USEPA i.e., C43, C80, C323, C1046, and C1023. A limited number of CAMSs are distributed across the Lower RGV region with only one station in each city (i.e. Mission (C43), Brownsville (C80), South Padre Island (C323), Edinburg (C1046), and Harlingen (C1023)).

CAMSs that qualify for this study must be actively recording particulate matter during the years 2021-2022 in the RGV region. As a result, there are three qualifying stations C43, C80, and C323. This study will assess how these three CAMSs accurately access the exposure burden for over one million people in the RGV region. A yearly summary report was downloaded for the two years 2021 and 2022 from tceq.texas.gov (accessed March 2022) from all CAMSs to evaluate all relevant parameters from March 1st, 2021, to March 31st, 2022. CAMSs measure hourly particulate matter concentrations in local conditions in $\mu g/m^3$.

Figure 3.24: CAMS C43 satellite aerial view and adjoining environment (Source: Google Earth).

Figure 3.25: CAMS C80 satellite aerial view and adjoining environment (Source: Google Earth).

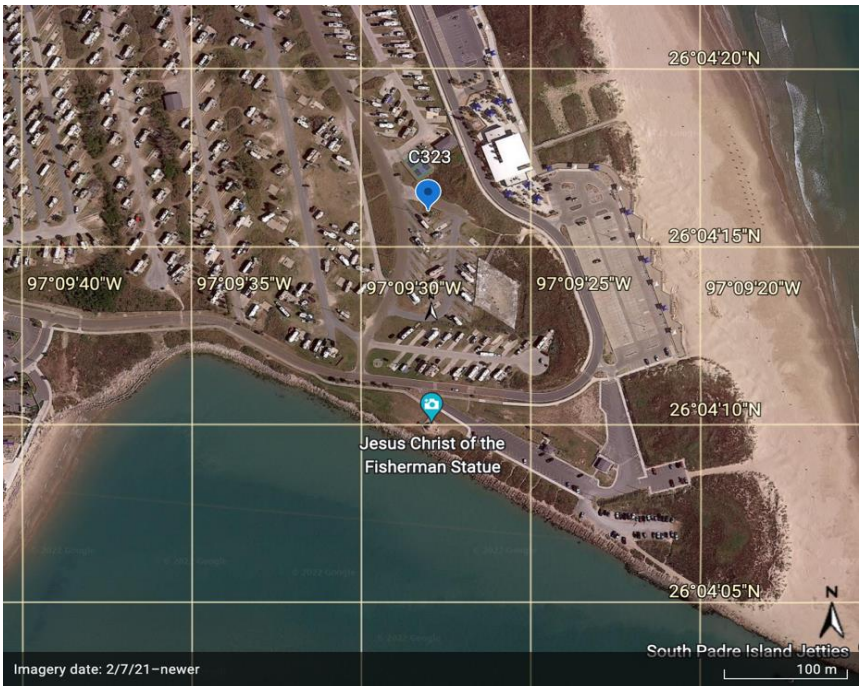

Figure 3.26: CAMS C323 satellite aerial view and adjoining environment (Source: Google Earth).

Figure 3.27: CAMS C1046 satellite aerial view and adjoining environment (Source: Google Earth).

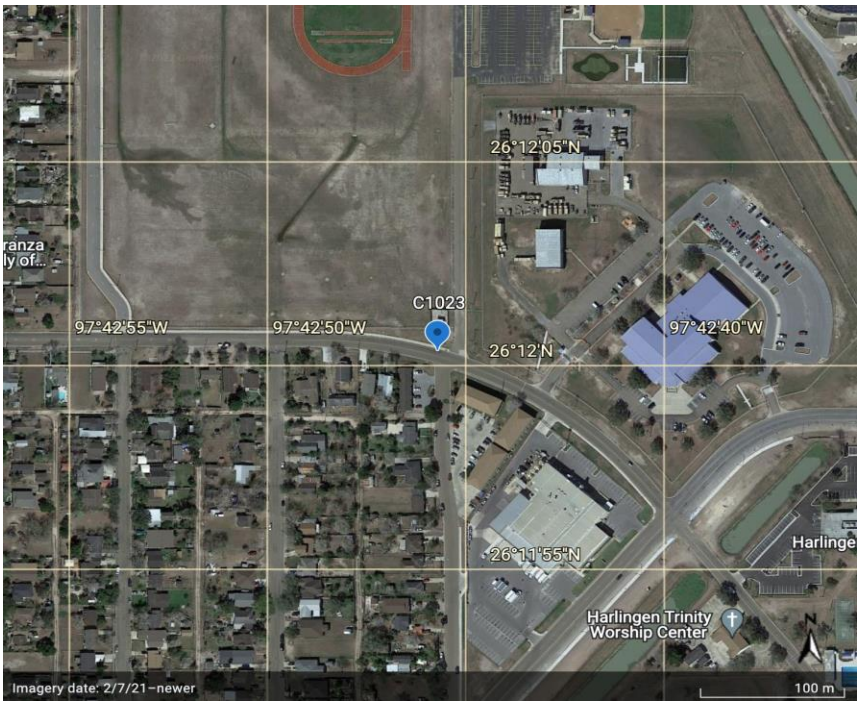

Figure 3.28: CAMS C1023 satellite aerial view and adjoining environment (Source: Google Earth).

CHAPTER IV

STATISTICAL METHODS AND DESIGN

4.1 Quality Assurance and Quality Control (QA/QC) of $PM_{2.5}$ Data

For this study, standard data quality assurance procedures from the USEPA (Protection, 2001) were implemented and demonstrated in Table 4.1. Completeness was computed by dividing the observed sample by the targeted amount sampled (Raysoni et al., 2013). All samples collected were recorded in five-minute intervals and converted to hourly $PM_{2.5}$ ($\mu g/m^3$) concentrations. The total number of hours sampled and percent completion for each sample are recorded in Table 4.1. Before the main study, a collocated sample was collected for four weeks (with 600 sampled hours) in the city of Weslaco to sample the LCS W1. The resulting R^2 is 0.98 with the scatter plot and installation photo shown in Figure 4.1 and Figure 4.2. Once the main study was over, four additional duplicate collocation samples were collected for the duration of approximately one week (165 to 169 sampled hours) to sample at locations B4, B3, W2, and E3 (Figures 4.3 -4.10 respectively). All the hourly post-study tests proved the LCS' accuracy with moderate to strong $0.95< R^2 >0.99$ correlations.

Furthermore, samples alongside Federal Equivalent Method (FEM) instruments such as FEM TSI DustTrak Environmental Monitor and FEM DustTrak™ DRX Aerosol Monitor 8534 by TSI Incorporated, Minnesota, U.S. were calibrated to assure performance in the field (shown in Figures 4.11 -4.13). As a result, the LCSs established good performance and evaluation with

a strong $0.92 < R^2 > 0.98$ correlation to federal reference-grade instruments and a 100% completion.

Table 4.1: Hourly $PM_{2.5}$ concentrations from collocated samples.

Sampled Test	Duplicate	Sampler	Start (0 to 23 hr.)	End (0 to 23 hr.)	Sampled Hours	Completeness	R^2
Pre-study	B5	W1	2/12/21 0:00	3/9/21 23:00	600	600/624 (96.2)	0.98
Post-study	W1	B4	4/15/22 11:00	4/22/22 12:00	169	169/169 (100%)	0.98
	W1	B3	4/22/22 13:10	4/29/22 14:00	169	169/169 (100%)	0.95
	W1	W2	4/29/22 17:00	5/6/22 14:00	165	165/165 (100%)	0.99
	E1	E3	5/13/22 11:00	5/20/22 10:00	167	167/167 (100%)	0.99
FEM	FEM[1]	E2	5/16/22 16:00	5/20/22 16:00	97	97/97 (100%)	0.98
	FEM[2]	E2	5/16/22 16:00	5/20/22 16:00	97	97/97 (100%)	0.92

FEM[1] TSI DustTrak Environmental, FEM[2] DustTrak™ DRX Aerosol Monitor 8534

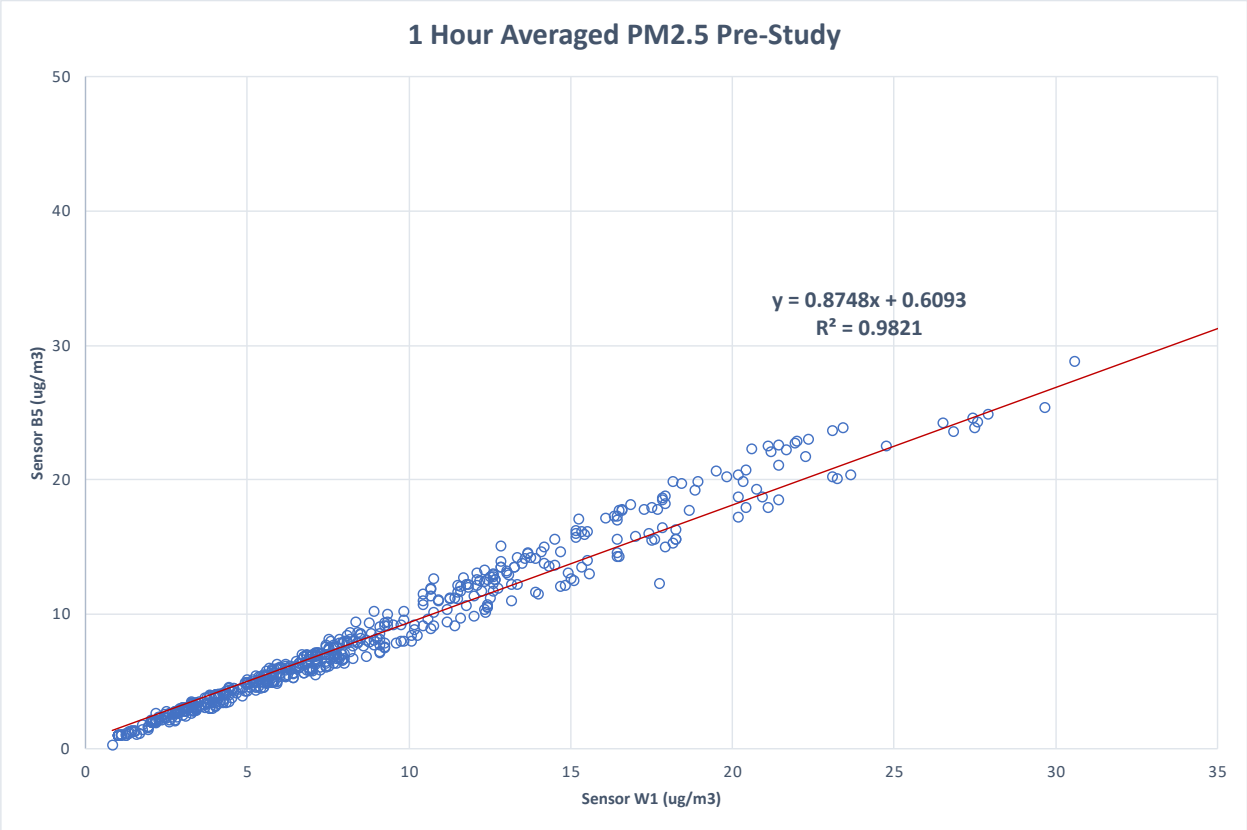

Figure 4.1: Scatter-line plot of the pre-study sample in site W1.

Figure 4.2: Installation photo of the pre-study sample in site W1.

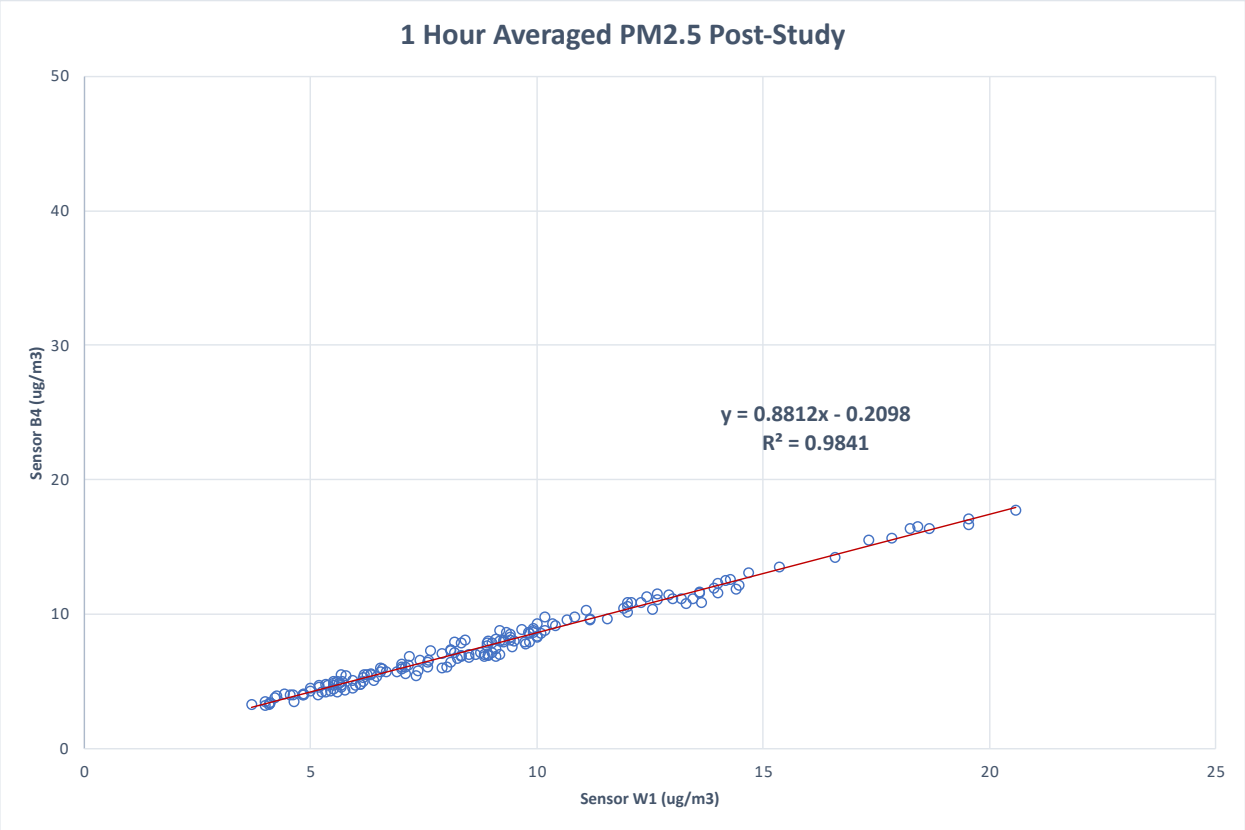

Figure 4.3: Scatter-line plot of the post-study sample in site B4.

Figure 4.4: Installation photo of the post-study sample in site B4.

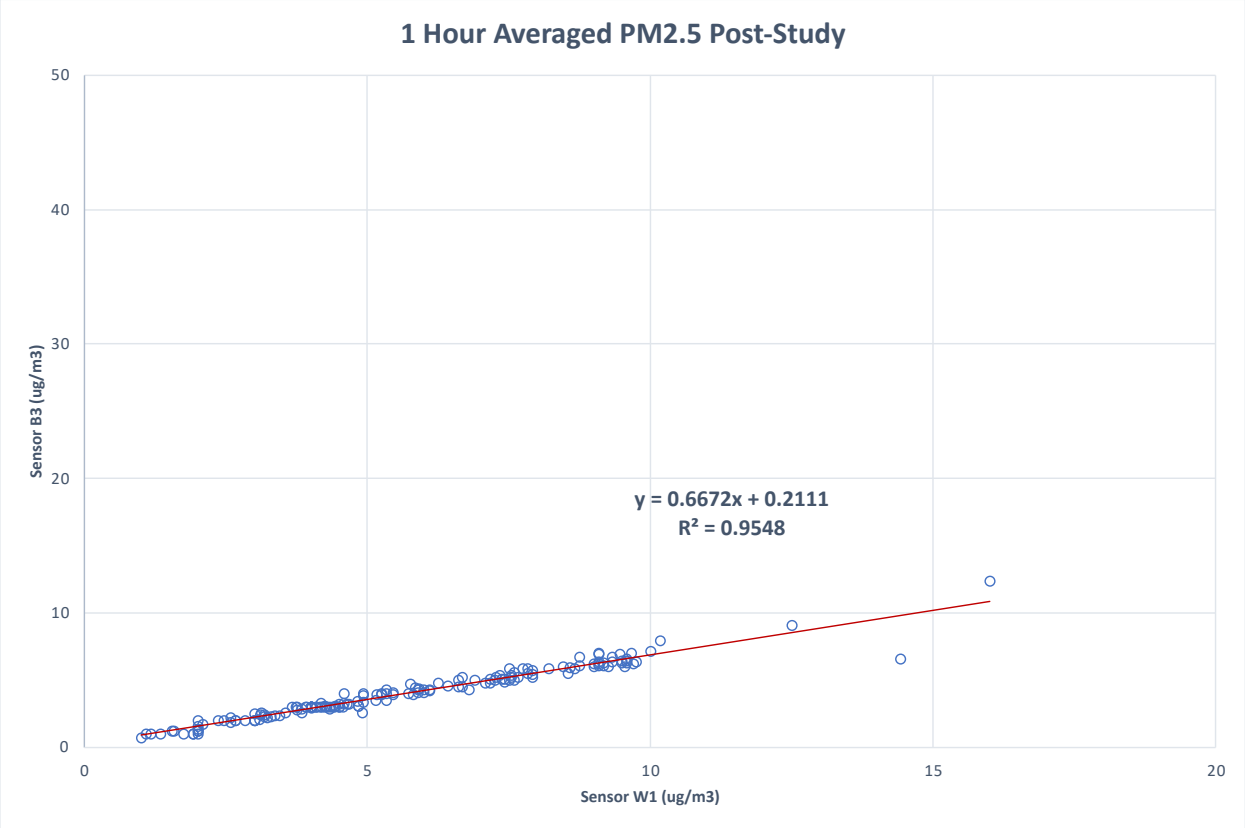

Figure 4.5: Scatter-line plot of the post-study sample in site B3.

Figure 4.6: Installation photo of the post-study sample in site B3.

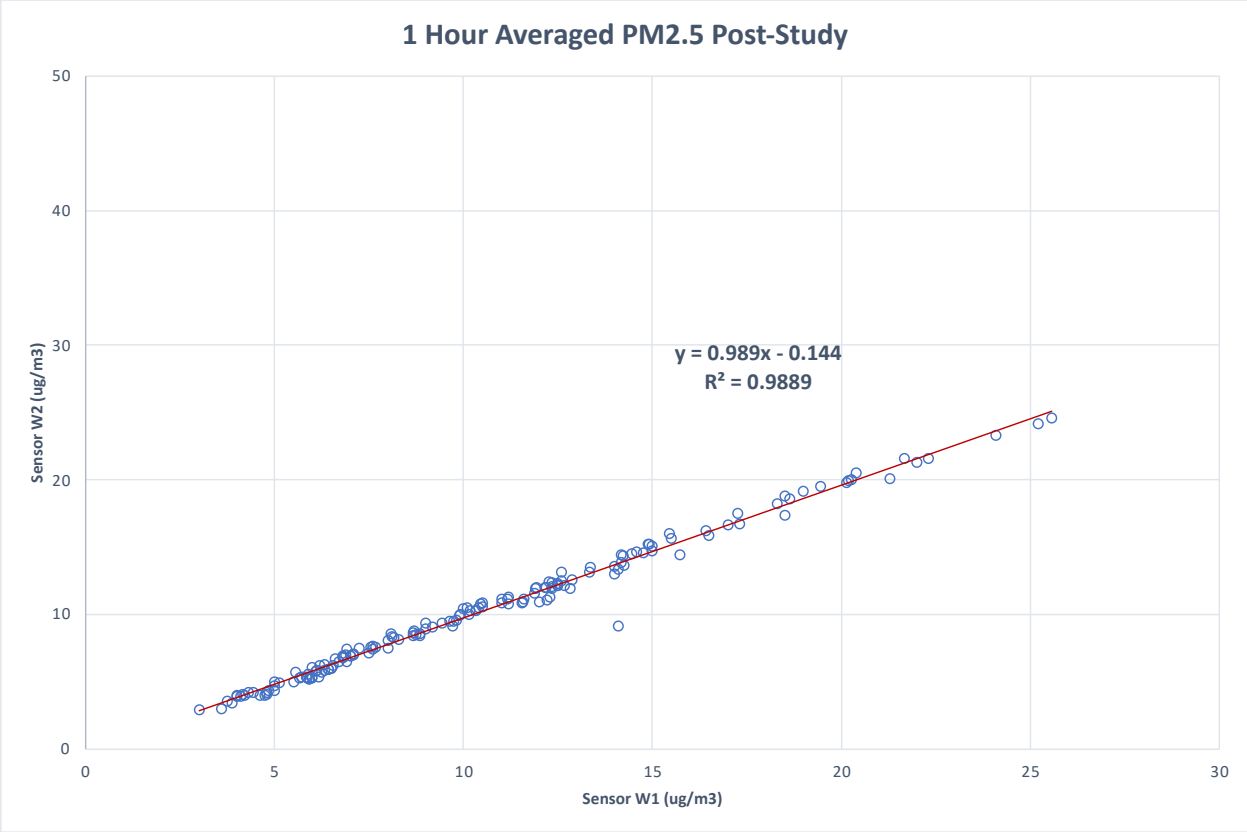

Figure 4.7: Scatter-line plot of the post-study sample in site W2.

Figure 4.8: Installation photo of the post-study sample in site W2.

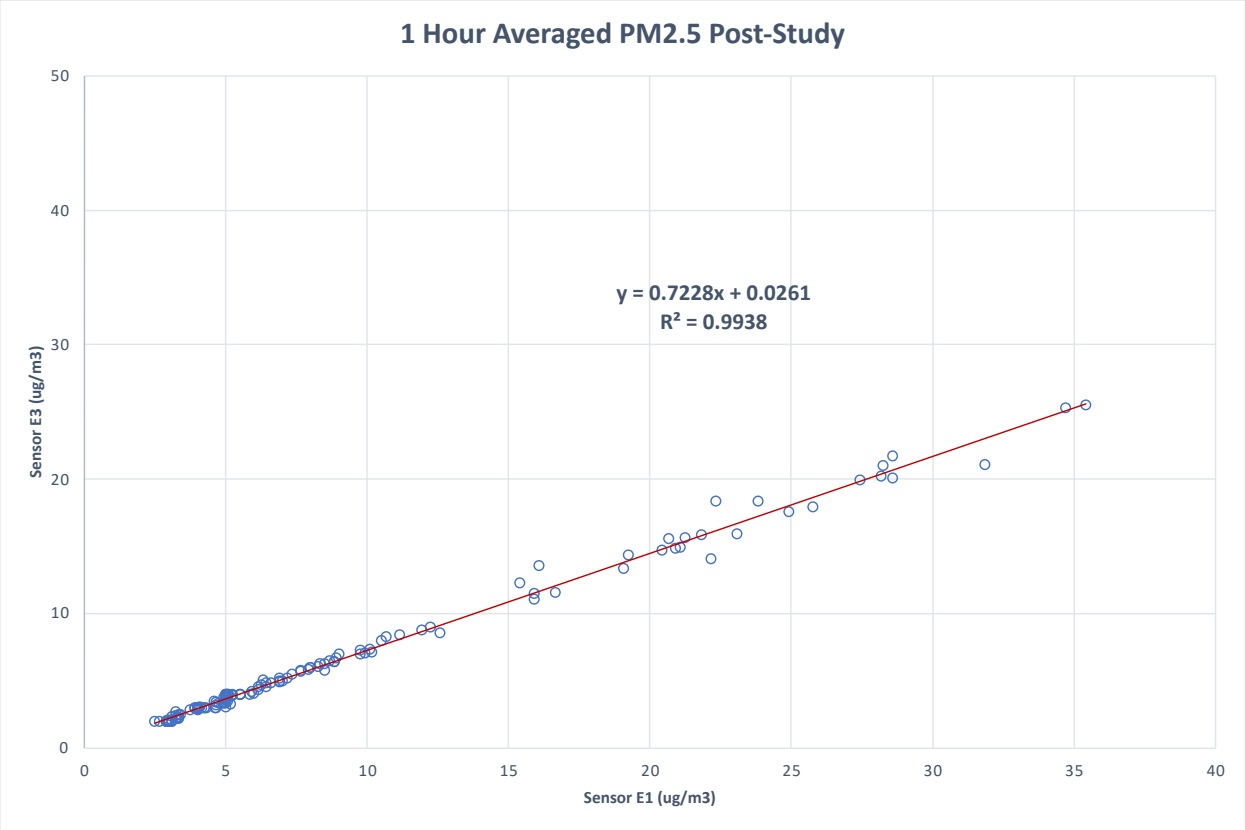

Figure 4.9: Scatter-line plot of the post-study sample in site E3.

Figure 4.10: Installation photo of the post-study sample in site E3.

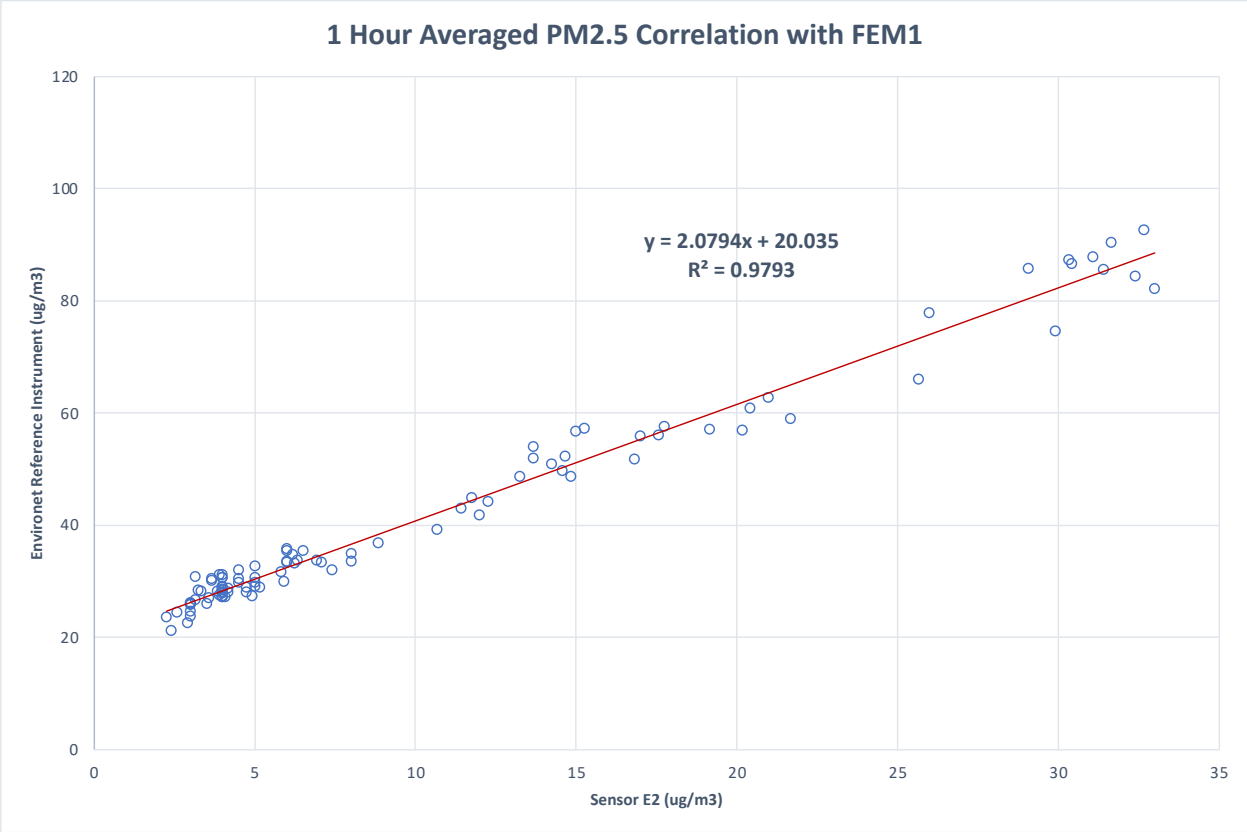

Figure 4.11: Scatter-line plot of the post-study sample with the FEM1 DustTrak Environmental Monitor.

Figure 4.12: Installation photo of FEM1 DustTrak Environmental Monitor with FEM2 DRX Aerosol Monitor.

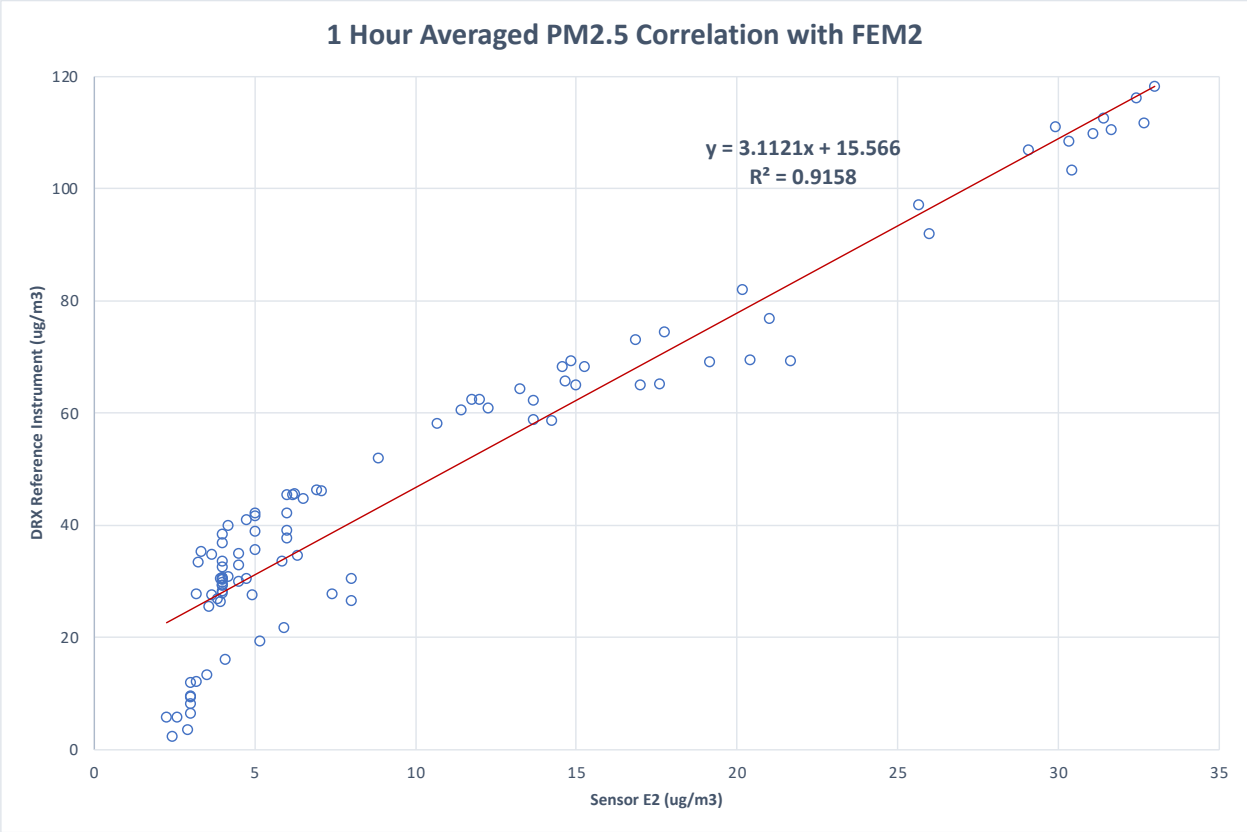

Figure 4.13: Scatter-line plot of the post-study sample with the FEM2 DRX Aerosol Monitor.

Hourly $PM_{2.5}$ (µg/m³) concentrations were calculated to 24-hour (µg/m³) concentrations to estimate precision for the pre- and post-study samples (Table 4.2). $PM_{2.5}$ was estimated as the root mean square difference amongst the collocated samplers and divided by the square root of 2 (Raysoni et al., 2013; Protection, 2001). The precision percentage was evaluated by group, so the four post-study samples were calculated together with 0.18% precision. The pre-study sample estimated a 0.08% precision.

Table 4.2: 24-hour $PM_{2.5}$ estimates of precision.

$PM_{2.5}$ Sample	Relative precision %
Pre-study	0.08
Post-study	0.18

According to a study in 2022 that evaluated long-term outdoor LCS' completeness, the main reason for missing data was the instability or loss of wireless connection (Connolly et al., 2022). Therefore, in this study, the PM data was collected via microSD card to limit the loss of data. Measurements were logged in the microSD card despite having a wireless connection. The completeness values for the LCSs during the entire study duration were calculated in Table 4.3.

Data loss is due to many reasons, such as power outages or errors/malfunctions with the PM sensors. In the LCS manual, the manufacturer TSI suggests replacing the PM sensor once a year. The study period was from March 1st, 2021, to March 31st, 2022, with a total duration of 396 days. At certain points in the study, three sites B3, E1, and E2 required a PM sensor replaced on the specified dates listed in Table 4.4. Shortly after replacing the PM sensor in B3, a device error message ensued, resulting in a device (a new LCS) replacement on May 19th, 2021. Toward the end of the study on March 21st, 2022, the PM sensor in site B1 malfunctioned. Thus, site B1 ended PM monitoring ten days prior to the study end date.

Despite the study difficulties with the sensor malfunctioning errors, the completeness values from the Brownsville (B1-B5), Edinburg (E1-E3), Weslaco (W1 and W2), and Port Isabel (PI) sites were > 89.4%. Comparably, the completeness of the TCEQ CAMS were C43(99.2%), C80 (99.0%), and C323 (88.9%). The CAMSs were down when they underwent either preventative maintenance or quality control auditing. If these CAMSs had delays and breakdowns in the data communications or the data failed the automatic criteria, PM data was not logged.

Table 4.3: $PM_{2.5}$ 24-hour samples calculated for completion.

Site	Completeness
B1	384 /396 (97.0%)
B2	354 /396 (89.4%)
B3	379 /396 (95.7%)
B4	373 /396 (94.2%)
B5	385 /396 (97.2%)
E1	390 /396 (98.5%)
E2	396 /396 (100.0%)
E3	394 /396 (99.5%)
W1	383 /396 (96.7%)
W2	396 /396 (100.0%)
PI	396 /396 (100.0%)
C43	393 /396 (99.2%)
C80	392 /396 (99.0%)
C323	352 /396 (88.9%)

Table 4.4: Sensor replacement dates for the appropriate sites.

Site	Date of replacement	
B3	4/27/2021	5/19/2021
E1	7/8/2021	
E2	7/8/2021	

4.2 Statistical Data Analyses

The resulting PM, temperature, and relative humidity data from the entire study duration of March 1st, 2021, to March 31st, 2022, was downloaded from the microSD card from the eleven LCSs and respective TCEQ CAMS to be processed for spatial and temporal analyses. Descriptive statistics were prepared with Microsoft Excel (v.16.06 2022), SPSS for MacOS (SPSS, Inc., Chicago, IL), and R programming software (RStudio, Inc., Boston, MA). Raw data directly from the sensors were cleaned and processed in Microsoft Excel using a conditional (TRUE and FALSE) IF statement to flag any inconsistencies with the time interval settings of 5 minutes. These missing data points were all accounted for by the addition of blank rows in the data sets. Subsequently, the cleaned data was converted into hourly and 24-hour data sets in Microsoft Excel. $PM_{2.5}$ variability from both LCSs and TCEQ CAMSs is demonstrated with box

and whisker plots and time series. Spearman's Rho Correlations were assessed, with a significance level of 0.01, to determine $PM_{2.5}$ site-specific temporal relationships between the studied sites. Spatial heterogeneity between the various LCS locations and CAMSs were examined from the following Coefficient of Divergence (COD) formula:

$$COD_{jk} = \sqrt{\frac{1}{p}\sum_{i-1}^{p}\left[\frac{x_{ij} - x_{ik}}{x_{ij} + x_{ik}}\right]^2}$$

where X_{ij} represents the i^{th} concentration measured in site *j* over the 24-hour study duration, the number of observations is *p*, while the two sampled sites are *j* and *k* (Raysoni, 2011; Raysoni et al., 2013; Krudysz et al., 2008; Pinto et al., 2004; Raysoni et al., 2011; Raysoni et al., 2022; Mendez et al., 2022). COD estimates will underline a degree of uniformity between simultaneously sampled study areas (Raysoni, 2011; Raysoni et al., 2013; Krudysz et al., 2008; Pinto et al., 2004; Raysoni et al., 2011; Raysoni et al., 2022; Mendez et al., 2022). COD values greater than 0.20 suggests a significant difference in the concentrations and thus spatial heterogeneity between the selected sites. A low COD value of less than or equal to 0.20 specifies similarities and refers to spatial homogeneity.

GIS ArcMap was used to prepare exposure patterns for $PM_{2.5}$ in the Lower RGV region. Hot-Spot Analysis (Getis-Ord Gi) in the region was performed using GIS spatial and mapping techniques. Additionally, the spatial tools were used to conduct Cluster and Outlier Analysis Anselin Local Moran's Index (Raysoni, 2018).

CHAPTER V

RESULTS AND DISCUSSION

5.1. $PM_{2.5}$ 24-hour Concentration Analyses

Boxplot visual analyses were devised from $PM_{2.5}$ 24-hour concentrations ($\mu g/m^3$) with the applicable CAMSs and LCS sites for the entire study (Figures 5.1). The interquartile ranges (75^{th} & 25^{th}) are demonstrated as the box while the whiskers show the minimum and maximum values. $PM_{2.5}$ outliers are shown as an asterisk. In the box, the median is shown as a line and the diamond signifies the mean. Figures 5.1 displays the boxplot for $PM_{2.5}$ with the Lower RGV sites labeled by color to symbolize the situated city. The color coordination catalogs B1, B2, B3, B4, and B5 (deep blue) for the sites in Brownsville and E1, E2, and E3 (gold) in the city of Edinburg. Sites W1 and W2 (green) are in Weslaco, and lastly, PI (purple) is in Port Isabel. The CAMSs are colored black and identified as follows: CAMS43 (C43) in Mission, CAMS80 (C80) in Brownsville, and CAMS232 (C323) in South Padre. Evident outliers are clear when performing a boxplot. The $PM_{2.5}$ averages for all sites can be recognized as less than 15 $\mu g/m^3$ with outliers less than 45 $\mu g/m^3$.

Apart from the major identified outliers, CAMSs C43, C80, and C323 notably recorded fewer outliers than those from the LCSs. Brownsville LCSs in the UTRGV (B2, B3, B4) all demonstrated lower 24-hour averaged results when compared to the UTRGV C80 located

0.17 miles from the U.S. -Mexican border. In the Brownsville residential sites B1 and B5, averaged values were slighter greater than those reported at the university Brownsville campus. Correspondingly, the UTRGV Edinburg campus sites (E1 and E2) had marginally higher $PM_{2.5}$ average concentrations than the sensor in the gated residential community (E3). W1 deployed site right off of Farm to Market Road 88 (FM88) exhibited greater averaged concentrations than the other Weslaco location W2 off Texas State Highway 69. The Port Isabel (PI) averaged values are noticeably lower than the famous touristed city of South Padre Island (C323), both sites located outside the URTGV coastal labs.

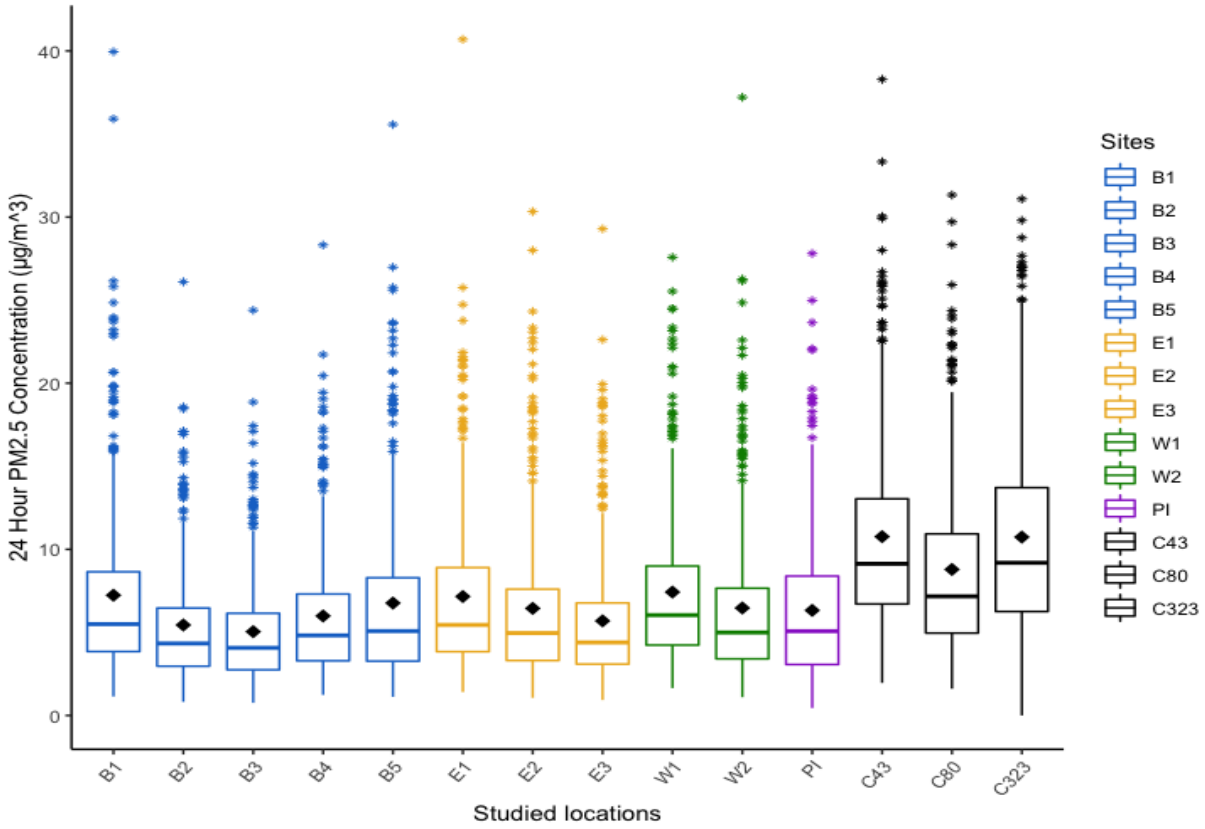

Figure 5.1: Boxplot of 24-hour $PM_{2.5}$ concentrations (µg/m^3) from the LCSs and TCEQ CAMSs. Asterisks correspond to outliers and diamond corresponds to the mean.

The LCSs deployed locations were intentionally selected in intra-and-inter-urban areas to demonstrate accurate representations of daily $PM_{2.5}$ exposures at the neighborhood level. With resultant daily averaged $PM_{2.5}$ concentrations, spatial resolution can be assessed in the selected

cities and compared with the logged $PM_{2.5}$ from CAMSs. Descriptive statistics (mean, standard deviation, median, maximum, minimum, and count) of 24-hr ambient $PM_{2.5}$ concentrations ($\mu g/m^3$) at each LCS site and the three CAMSs (C43, C80, C323) are presented in Table 5.1.

Notably, greater $PM_{2.5}$ concentrations in Brownsville varied with the mean and standard deviation in C80 at 8.79 ± 5.39 μg/m³ to B1 of 7.24 ± 5.39 μg/m³. The university Brownsville campus averaged lower concentrations in B3 of 5.05 ± 3.35 μg/m³ and in B4 5.99 ± 4.01 μg/m³ than the residential areas B1 and B5. In the city of Edinburg, concentrations ranged from 5.69 ± 4.08 μg/m³ in E3 (gated community) to 7.16 ± 4.97 μg/m³ in E1 (university medical building facing W Schunior St). C43 deployed outside of an elementary school recorded the overall highest $PM_{2.5}$ average concentration of 10.76 ± 5.81 μg/m³ in local conditions for the entire study duration. Site C323 coastal labs and a nearby trailer park in South Padre Island (a famed tourist area) recorded the second-greatest daily $PM_{2.5}$ average of 10.74 ± 6.00 μg/m³. Given South Padre Island acts as a barrier island to the Gulf of Mexico, it is expected to encounter the southeastern winds bringing humid air from the Gulf Coast and/or dust from SAL. The greatest $PM_{2.5}$ averaged concentrations from all the LCSs was recorded in site W2 (7.43 ± 4.68 μg/m³) residential household near the crossroads of FM88.

Maximum daily $PM_{2.5}$ concentrations from the LCSs ranged from 24.4 μg/m³ in site B3 and 40.7 μg/m³ in E1. The maximum $PM_{2.5}$ values from the CAMSs ranged from C323 (31.1 μg/m³) and C43 (38.3 μg/m³).

According to the NAAQS 2012 standards and the WHO global air quality guidelines of 2021, the average $PM_{2.5}$ concentrations from the research findings did not exceed the 24-hour mean threshold of 15 μg/m³. These studied sites are just within these designated standards as well throughout the study duration. Thresholds for harmful particulate matter levels are

significant for the protection of the public's health and welfare. Greater $PM_{2.5}$ exposure levels in urban areas would affect the health of sensitive populations and cause premature deaths.

The selected LCS locations are in the proximity of major Texas highways, commonly used roads, and minor roads to measure low, medium, and high traffic density. C43 is deployed approximately 0.04 miles from N. Glasscock Rd measuring a $PM_{2.5}$ average concentration of 10.76 ± 5.81 μg/m³. LCS B4 was deployed 0.04 miles from the major Texas State Highway 69E recording (5.99 ± 4.01 μg/m³) $PM_{2.5}$ daily average with standard deviation. Similarly, W2 (6.47 ± 4.79 μg/m³) site was deployed 0.04 miles from the Texas State Expressway 83. Site B1 had a higher averaged $PM_{2.5}$ of 7.24 ± 5.39 μg/m³ which may be because it is located on the same street as the Lower RGV's central attraction site Gladys Porter Zoo. School buses transporting children to and from the zoo for school field trips are very common during the school year (August to May). Site B2 (5.45 ± 3.62 μg/m³) and B3 (5.05 ± 3.35 μg/m³) are located within the UTRGV and exposed to Brownsville campus traffic with B2 only 0.2 miles away from Texas State Highway 69E.

UTRGV Edinburg campus traffic is demonstrated with site E1 (7.16 ± 4.97 μg/m³) situated 0.01 miles from the commonly used W Schunior St. and E2 (6.45 ± 4.78 μg/m³) 0.04 miles from 107 Texas and intersection with Sugar Rd. The residential site of W1 (7.43 ± 4.68 μg/m³) resided 0.1 miles near the crossroads of Farm to Market Road 88, and expresses traffic exposures away from the city center but off frequently used roads. Deployed sites B5 (6.77 ± 5.17 μg/m³) and E3 (5.69 ± 4.08 μg/m³) represent exposures with less traffic density with one being surrounded by the Resaca del Rancho Viejo and the other residing in an enclosed gated community (respectively).

Table 5.1: Descriptive statistics for 24-hour $PM_{2.5}$ concentrations ($\mu g/m^3$) in the studied sites.

Site	Mean	StDev	Median	Max	Min
B1	7.24	5.39	5.50	39.95	1.14
B2	5.45	3.62	4.33	26.10	0.82
B3	5.05	3.35	4.07	24.39	0.76
B4	5.99	4.01	4.82	28.32	1.24
B5	6.77	5.17	5.08	35.57	1.12
E1	7.16	4.97	5.45	40.70	1.41
E2	6.45	4.78	4.96	30.33	1.06
E3	5.69	4.08	4.40	29.29	0.93
W1	7.43	4.68	6.04	27.58	1.65
W2	6.47	4.79	5.00	37.21	1.10
PI	6.33	4.54	5.08	27.81	0.45
C43	10.76	5.81	9.13	38.29	1.96
C80	8.79	5.39	7.17	31.33	1.61
C323	10.74	6.00	9.19	31.09	0.00

StDev = standard deviation, N = 352 to 396 for all sites

The Time series plotted in Figure 5.2 conveys the temporal variations in $PM_{2.5}$ 24-hour concentrations during the study period. Markedly, the series aids in the visual representation of daily concentrations to compare the sites amongst each other and identify daily patterns. Figure 5.2 reveals that the daily concentrations across the sites, evidently, follow similar fluctuation patterns. Given the proximity of the LCSs in repeated cities i.e., Brownsville, Edinburg, and Weslaco, similar $PM_{2.5}$ levels are to be expected, apart from the occasional outliers. For instance, during the time period of December 23rd, 2021, to January 3rd, 2022, $PM_{2.5}$ levels peaked at all the sites. This temporal pattern may be a result of traditional U.S. celebrations such as Christmas and 4th of July Independence Day. These events are typically celebrated with outdoor cookouts and firework displays, causing a collective increase in $PM_{2.5}$ concentrations. Even though the total daily $PM_{2.5}$ averages did not pass the NAAQS standard of 15 $\mu g/m^3$, short-term $PM_{2.5}$ levels throughout the study duration were still high enough to result in respiratory health issues.

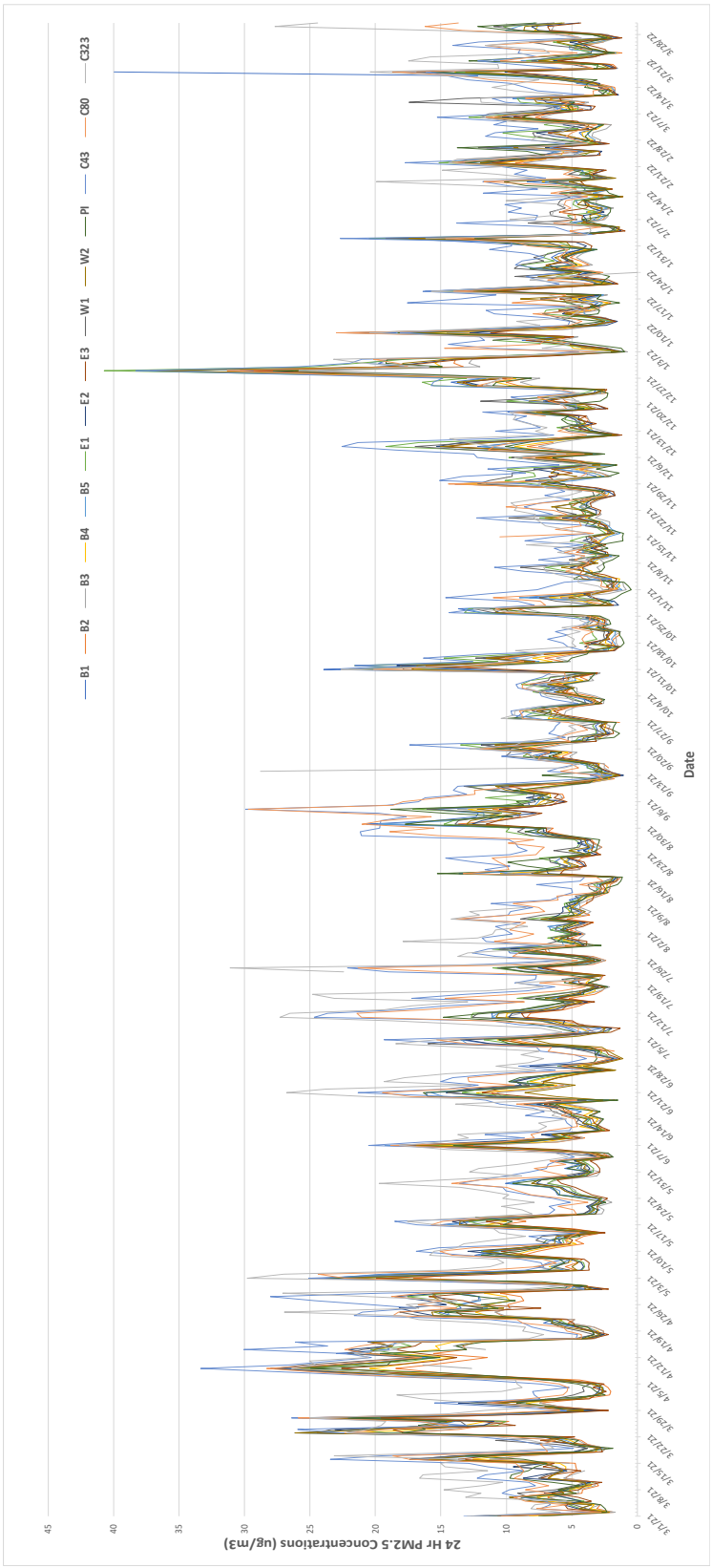

Figure 5.2: Time series of 24-hour $PM_{2.5}$ concentrations (µg/m^3) from the LCSs and TCEQ CAMSs.

5.2 Coefficient of Divergence Analyses

Ambient exposure of 24-hour $PM_{2.5}$ concentrations across the LCSs and CAMSs were calculated into the COD matrix composed in Table 5.2. COD values greater than 0.20 are in bold italics conveying spatial heterogeneity between selected locations. Selected CAMSs (C43, C80, and C323) recording $PM_{2.5}$ in local conditions suggest spatial non-uniformity with the LCS COD values ranging from C80-W2 (0.25) and C323-B2 (0.58). In CAMS C323, spatial variation was more pronounced with the LCSs pairings C323-B2 (0.58), C323-B3 (0.54), C232-B4 (0.5), and C323-E3 (0.5). The Brownsville site B2 expressed the highest coefficients amongst the three CAMSs with C43-B2 (0.49), C80-B2 (0.43), and C232-B2 (0.58), in thereof suggests site B2 and the CAMSs were spatially heterogenetic. In the city of Edinburg, site E3 insinuated spatial non-uniformity with CAMSs C43-E3 (0.38), C80-E3 (0.31), and C323-E3 (0.5). COD values between the city of Weslaco (W1 and W2) and CAMSs were greater than 0.25, implying spatial heterogeneity. Similarly, spatial non-homogeneity was exhibited in the values between the Port Isabel site (PI) and CAMSs. These resulting COD values may insinuate an inaccurate representation of neighborhood-level $PM_{2.5}$ exposures with the Central Ambient Monitoring Stations.

Spatial homogeneity was observed in the city of Edinburg location with COD values less than 0.20 in E2-E1 (0.16) and E3-E2 (0.11) and equal to 0.20 in E3-E1. Homogeneity between the LCS locations demonstrates the daily averages of $PM_{2.5}$ concentrations to be spatially similar. Equally, uniformity was also recognized in the following pairings: W2-E1 (0.17), W2-E2 (0.10), W2-E3 (0.14), and PI-W2 (0.19) sites. Slight heterogeneity may be determined with values proximate to 0.20 from pairings E2-B1 (0.23), E2-B5 (0.22), W2-B1 (0.21), W2-B5 (0.20), W2-W1 (0.22), P1-B5 (0.22), P1-E2 (0.21), PI-E3 (0.23), and C80-C43 (0.23). The resultant COD

statistics highlight the significance of ambient intra-and-inter-urban air monitoring of fine particulate matter; with the majority of values pertaining to spatial heterogeneity.

Table 5.2: COD values from LCSs and TCEQ CAMSs with spatial heterogeneity identified in bold italics.

$PM_{2.5}$	B2	B3	B4	B5	E1	E2	E3	W1	W2	PI	C43	C80	C323
B1	***0.37***	***0.31***	***0.31***	***0.25***	***0.26***	***0.23***	***0.26***	***0.28***	***0.21***	***0.24***	***0.33***	***0.27***	***0.47***
B2		***0.39***	***0.32***	***0.39***	***0.40***	***0.36***	***0.36***	***0.43***	***0.36***	***0.37***	***0.49***	***0.43***	***0.58***
B3			***0.33***	***0.30***	***0.31***	***0.27***	***0.27***	***0.35***	***0.26***	***0.26***	***0.45***	***0.36***	***0.54***
B4				***0.31***	***0.31***	***0.28***	***0.29***	***0.34***	***0.27***	***0.29***	***0.42***	***0.34***	***0.50***
B5					***0.25***	***0.22***	***0.24***	***0.29***	0.20	***0.22***	***0.37***	***0.29***	***0.48***
E1						0.16	0.20	***0.24***	0.17	***0.26***	***0.30***	***0.26***	***0.46***
E2							0.11	***0.24***	0.10	***0.21***	***0.33***	***0.27***	***0.47***
E3								***0.27***	0.14	***0.23***	***0.38***	***0.31***	***0.50***
W1									***0.22***	***0.29***	***0.31***	***0.28***	***0.46***
W2										0.19	***0.33***	***0.25***	***0.46***
PI											***0.37***	***0.28***	***0.47***
C43												***0.23***	***0.39***
C80													***0.40***

5.3 Spearman's Correlation Analyses

Spearman's rho correlation coefficients were processed to evaluate temporal relationships between LCSs and TCEQ CAMSs indicated in Table 5.3. Correlational coefficients are all statistically significant at the 0.01 level in a two-tailed test (represented by **). Resultant coefficients range from ± 1 to determine the association between the two variables, in this case sites. Stronger relationships will indicate values nearing +1, whereas coefficients nearing 0 imply a weaker correlation. The site pairings all validated positive correlations with statistical significance. The LCSs demonstrated moderate to strong correlations $0.76 > r < 0.99$ amongst the other LCSs. Similarly, the CAMSs had moderate correlations $0.62 > r < 0.89$ with the LCSs.

Within the city of Brownsville, the five LCSs and C80 were all moderately correlated with $r > 0.96$. Relatedly, Edinburg LCSs were also strongly correlated amongst each other with $r > 0.96$ as well as site W1 and W2 ($r = 0.95$). The sensor at the Port Isabel site indicated moderate

to strong correlations with the other sites and a moderate association with C43(r =0.68). Additionally, C80 (located in Brownsville) demonstrated a moderate correlation (r >0.85) with the five LCSs in Brownsville (B1-B5). Overall, the coefficients from Spearman's analyses determined the varied correlations of $PM_{2.5}$ concentrations in the Lower RGV region.

Furthermore, Figure 5.3 illustrates spearman's correlation-colored matrix. This diagram provides a visual aid for identifying coefficient relationships with a color scale. Therefore, as the value is nearing +1 the color is displayed as a darker shade of blue. The Brownsville sites illustrate darker shades of blue, conveying the stronger relationships between the sites. Coefficients nearing 0 are represented as the lighter shades of blue, which is seen in the CAMSs (C43, C80, C323). Although the resulting diagram consists of varying shades of blue, there are no indications of a weak negative correlation between ranks (red shade).

Consequently, a spearman's correlation plot is procured with appropriate histograms, density functions, and smoothed regression analysis is exhibited in Figure 5.4. The correlating coefficients are statistically significant with (***) corresponding to a 1% (0.01) level. Results are equivalent to Table 5.3 and Figure 5.3, with histogram curves and regression analyses confirming the positive correlational relationship between the LCSs and CAMSs.

Table 5.3: Spearman's rho correlation coefficients of $PM_{2.5}$ concentrations between the varied sites.

	B1	B2	B3	B4	B5	E1	E2	E3	W1	W2	PI	C43	C80	C323
B1	1													
B2	.976**	1												
B3	.975**	.957**	1											
B4	.983**	.978**	.973**	1										
B5	.986**	.960**	.961**	.973**	1									
E1	.881**	.877**	.853**	.881**	.881**	1								
E2	.888**	.868**	.865**	.883**	.893**	.963**	1							
E3	.873**	.857**	.850**	.874**	.877**	.967**	.972**	1						
W1	.889**	.879**	.860**	.889**	.879**	.933**	.915**	.927**	1					
W2	.934**	.915**	.910**	.927**	.927**	.944**	.941**	.934**	.945**	1				
PI	.903**	.877**	.898**	.895**	.905**	.770**	.786**	.764**	.763**	.824**	1			
C43	.764**	.762**	.768**	.778**	.756**	.862**	.833**	.846**	.817**	.816**	.678**	1		
C80	.861**	.857**	.894**	.880**	.851**	.785**	.791**	.776**	.780**	.829**	.809**	.838**	1	
C323	.706**	.697**	.734**	.720**	.715**	.615**	.676**	.638**	.619**	.672**	.826**	.672**	.790**	1

Correlation is significant at the 0.01 level (2-tailed), N = 352 to 396 for all pairs.

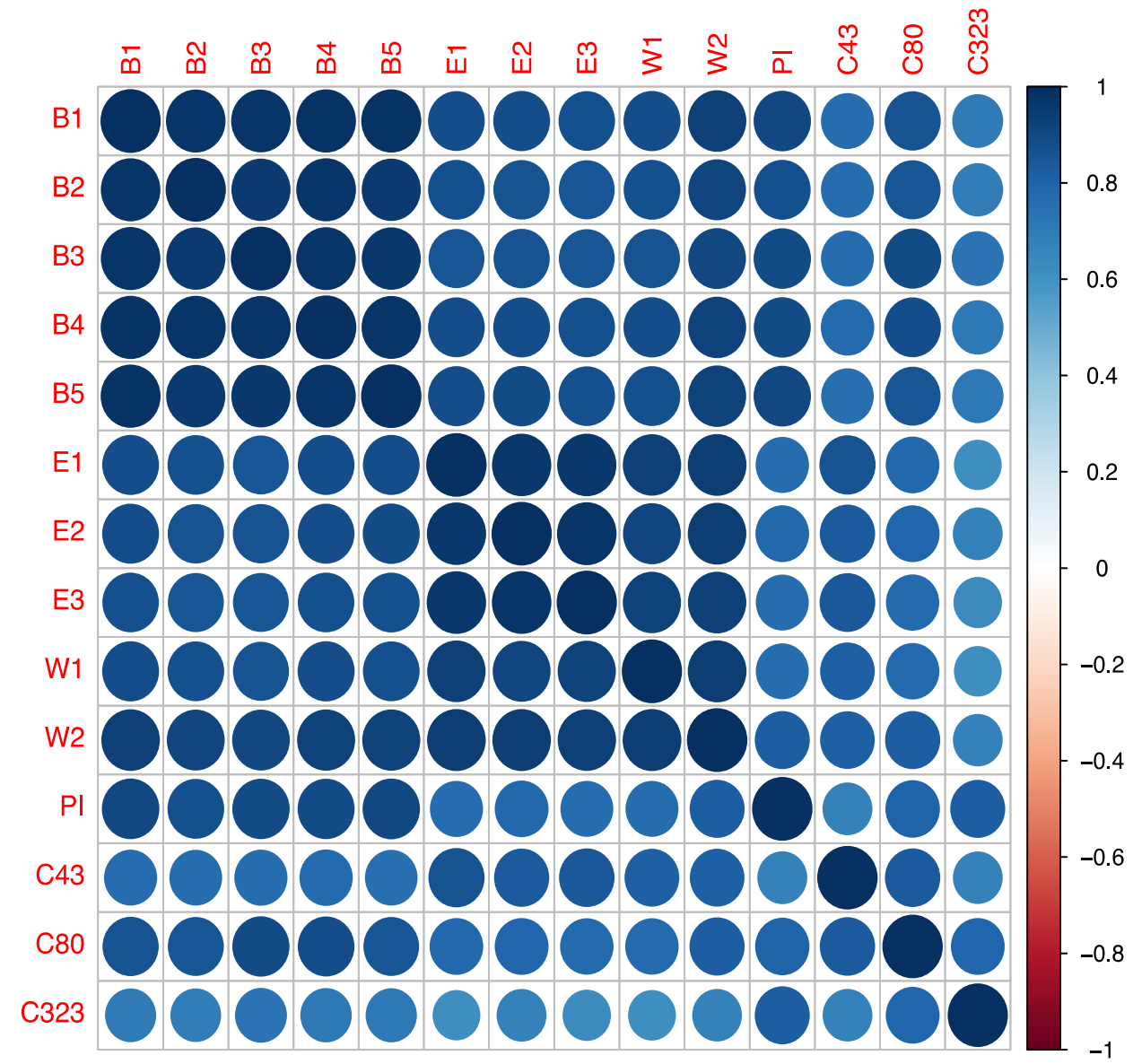

Figure 5.3: Spearman's rho correlational colored matrix for all the selected sites.

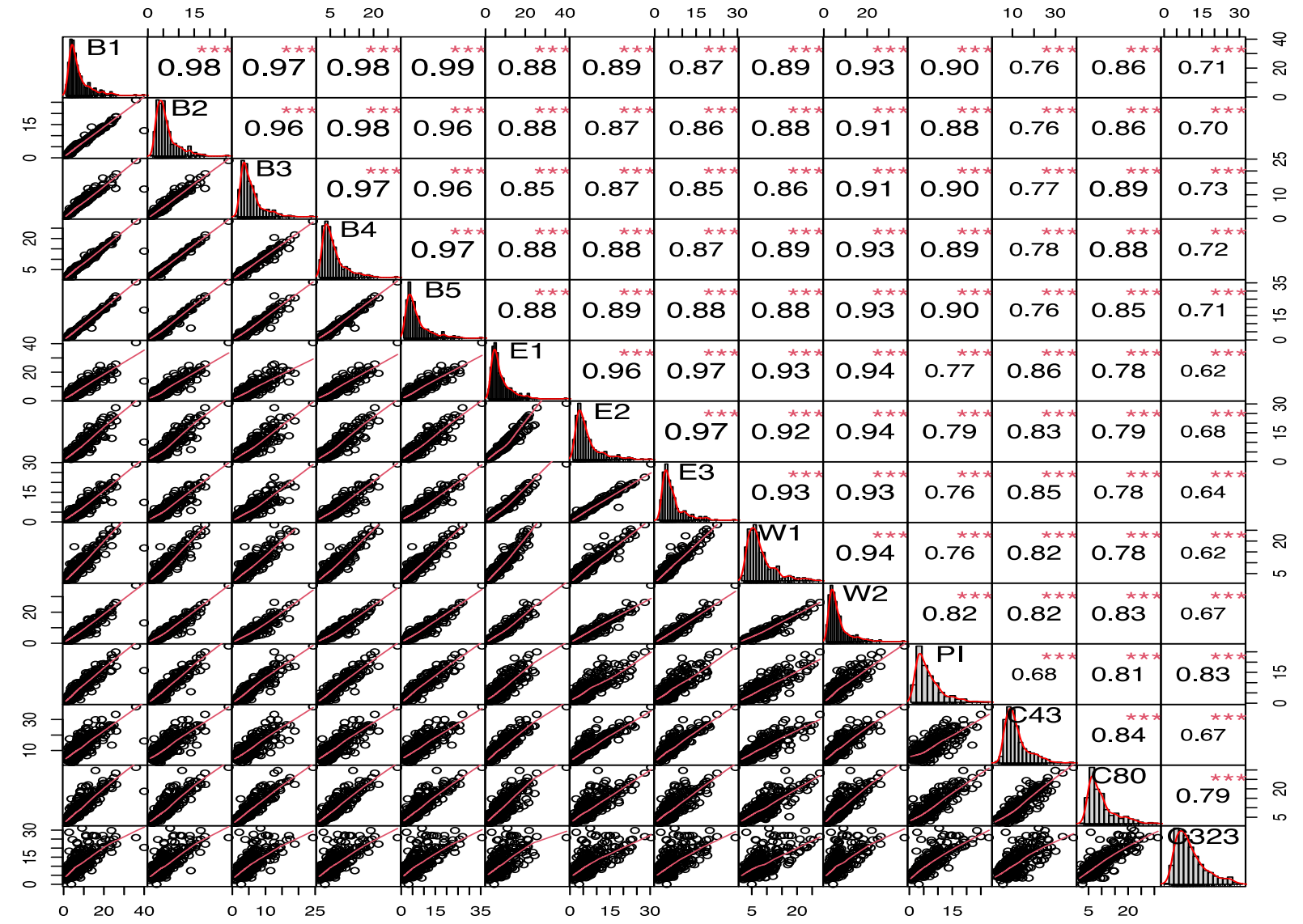

Figure 5.4: Spearman's correlation plot with histograms, regression lines, and density functions.

5.4 Surface Meteorological Conditions

Descriptive statistics of 24-hour meteorological parameters from LCSs and CAMSs are portrayed in Table 5.4 and Table 5.5 respectively. The LCS parameters provided temperature (T) and relative humidity (RH). According to the Air Quality Sensor Performance Evaluation Center AQ-SPEC summary evaluation, T and RH reported minimal effects on the LCS' precision (*TSI - BlueSky*). Therefore, a correction formula was not necessary for the resulting $PM_{2.5}$ concentrations.

Table 5.4: Summary statistics of 24-hour meteorological parameters from the LCSs.

	Site	Mean	Median	Max	Min	StDev	N
T (C)	B1	26.7	27.6	35.1	5.4	6.2	385
	B2	28.2	28.7	37.8	7.4	5.8	354
	B3	28.8	30.4	36.3	6.8	5.7	378
	B4	26.8	27.4	35.9	5.6	6.0	373
	B5	26.9	28.0	35.6	5.7	5.9	385
	E1	28.7	29.7	37.7	8.8	6.7	392
	E2	28.2	29.6	36.1	8.6	5.5	396
	E3	26.4	27.4	35.6	6.5	6.7	394
	W1	26.2	27.3	34.4	5.9	6.4	383
	W2	27.8	29.0	35.5	6.8	5.8	396
	PI	27.0	27.5	35.1	5.8	6.1	396
RH %	B1	66.4	66.2	83.8	34.2	7.4	385
	B2	62.1	62.6	80.4	30.7	7.9	354
	B3	58.8	60.0	78.4	26.7	8.5	378
	B4	65.2	65.6	84.0	31.6	8.6	373
	B5	65.2	65.9	83.4	32.9	8.2	385
	E1	52.7	53.0	69.8	21.0	8.6	392
	E2	57.2	58.8	80.9	18.8	10.0	396
	E3	63.0	63.2	83.1	28.8	9.1	394
	W1	65.9	66.4	86.9	28.3	8.9	383
	W2	59.8	61.4	83.2	19.6	10.2	396
	PI	68.3	68.7	85.2	40.0	7.8	396

StDev = standard deviation, T = temperature in (^{o}C), RH = relative humidity %.

Notably, throughout the entire study period, there were no detected abnormal T or RH readings from the sensors. The LCS PM sensor's operational temperature range is -10^{o}C to 60^{o}C

or 14ºF to 140ºF, while the operational humidity range is between 0 to 95% non-condensing (*BlueSky Air Quality Monitor*, 2020). The lowest T recorded was in site B1 at 5.4°C (41.7°F) and the highest T was in site B2 at 37.8°C (100.1°F), which is not an abnormally high T value for the RGV region. In the Lower RGV summers often do reach the 37.8°C (100.1°F) range. Overall, the LCS sites averaged T was within the PM sensor operational temperature range varying from 26.2°C < T > 28.8°C or 79.2°F < T > 83.8°F. Similarly, the RH throughout the study duration was within the PM sensor humidity operational range, with the average range between 52.7% < RH > 68.3%. The lowest percentage of RH was logged at site E2 (18.8%) while the maximum percentage was in site W1 (86.9%). Evidently, T and RH observed samples (N) are greater than the N of $PM_{2.5}$ samples because the T and RH sensors did not encounter malfunction errors like the PM sensors.

Moreover, applicable meteorological parameters from the TCEQ CAMSs in the Lower RGV region (C43, C80, C323, C1023, and C1046) are summarized in Table 5.5. All CAMSs in the Lower RGV were included for meteorological analysis, regardless of their PM status, in order to assess conditions throughout the region in the five cities (Mission, Brownsville, South Padre, Harlingen, and Edinburg). Resultant wind speed and direction from the CAMSs were concocted as wind roses in Figures 3.14 -3.18 illustrating southeast winds. Windspeed and direction are meteorological variables that may significantly affect particulate matter vertical mixing, horizontal transportation, and dispersion (Seaman, 2000; Tian et al., 2022).

Additionally, the CAMSs similarly documented an average of 23°C or 73.4°F for the entire study duration. It is noted in Table 5.4 the deployed sensors demonstrate greater variability of temperature rather than the temperature from the CAMSs in Table 5.5. Furthermore, solar radiation (SR) values were expressed in Langley's per minute to measure the total

electromagnetic radiation emitted at the sites. Only two CAMSs monitored solar radiation with daily averages of C43 (0.3) and C80 (0.3) Langley's per minute.

Table 5.5: Summary statistics of 24-hour meteorological parameters from CAMSs.

	Site	Mean	Median	Max	Min	StDev	N
RWS	C43	2.8	2.7	6.1	1.0	1.0	396
(m/s)	C80	3.0	2.8	8.3	0.1	1.4	393
	C323	3.4	3.7	6.7	1.1	1.1	396
	C1023	3.6	3.3	8.7	1.4	1.3	396
	C1046	2.7	2.4	8.2	0.8	1.3	394
RWD	C43	148.8	143.3	336.5	46.9	46.2	396
	C80	162.3	158.8	340.2	43.8	51.7	393
	C323	150.5	145.2	343.4	27.8	54.3	396
	C1023	158.2	156.0	349.6	33.6	47.8	396
	C1046	147.6	139.4	334.4	19.0	47.0	394
T	C43	23.3	24.6	31.3	4.4	-11.7	396
(°C)	C80	23.2	24.1	30.6	2.8	-12.1	396
	C323	23.5	24.5	30.9	3.3	-12.1	395
	C1023	23.2	24.3	31.1	3.1	-11.7	396
	C1046	23.4	24.6	31.3	4.1	-11.7	396
SR	C43	0.3	0.3	0.5	0.03	0.1	396
	C80	0.3	0.3	0.5	0.02	0.1	396

StDev = standard deviation, RWS = resultant wind speed in m/s, RWD = resultant wind direction in degrees compass, T = temperature in (°C), SR = solar radiation measured in Langley's per minute.

5.5 Seasonal Analyses

To capture various seasonal and temporal $PM_{2.5}$ ($\mu g/m^3$) patterns at the various locations, box and whisker plots were plotted for each season (Figure 5.5 -5.8). Season variability may outline PM concentration fluctuations from weather conditions and determine LCSs' performance levels (Chen, 2020). The color coordination in the legend is akin to Figure 5.1, in which the color categorizes the LCSs by city.

As reported by the boxplots, spring expresses higher $PM_{2.5}$ ($\mu g/m^3$) average concentrations and decreases during summer. Autumn continues to present lower PM concentrations then increases once more in winter. The temporal variation may be influenced by

the meteorological parameters associated with the Lower RGV's hurricane season (June 1st to November 30th or summer to autumn). Additionally, winter detects greater amounts of outliers than the other three seasons which may be a result of the use of heaters and fireplaces to keep warm during the cold weather (*Indoor Air Quality (IAQ),* 2022). Seasonal descriptive statistics for 24-hour $PM_{2.5}$ concentrations ($\mu g/m^3$) in the studied sites are shown in Table 5.6. Markedly, the CAMSs indicated a mean higher than the LCSs during each season. The maximum mean throughout the seasons is from sites C323 (14.17 ± 5.72 $\mu g/m^3$), C232 (12.77 ± 6.28 $\mu g/m^3$), C43 (8.94 ± 4.88 $\mu g/m^3$), and C43 (10.77 ± 5.81 $\mu g/m^3$) for spring, summer, autumn, and winter respectively.

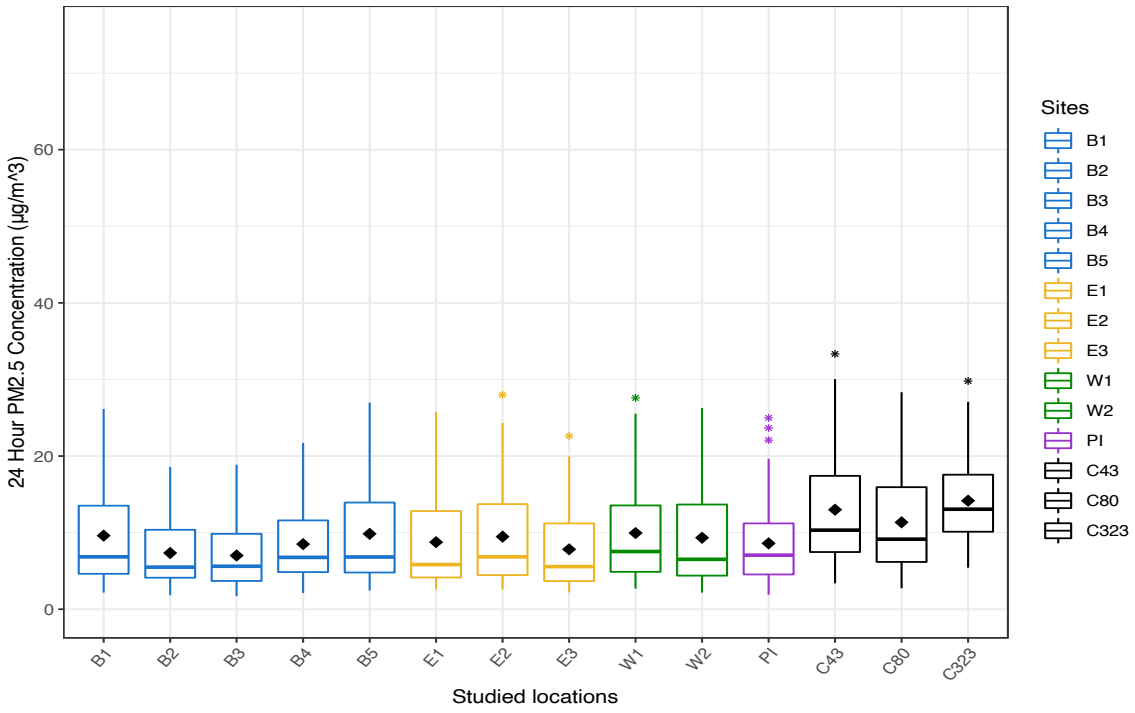

Figure 5.5: Boxplot of 24-hour $PM_{2.5}$ concentrations ($\mu g/m^3$) from the LCSs and CAMSs during spring (March-May 2021). Asterisks correspond to outliers and diamond corresponds to the mean.

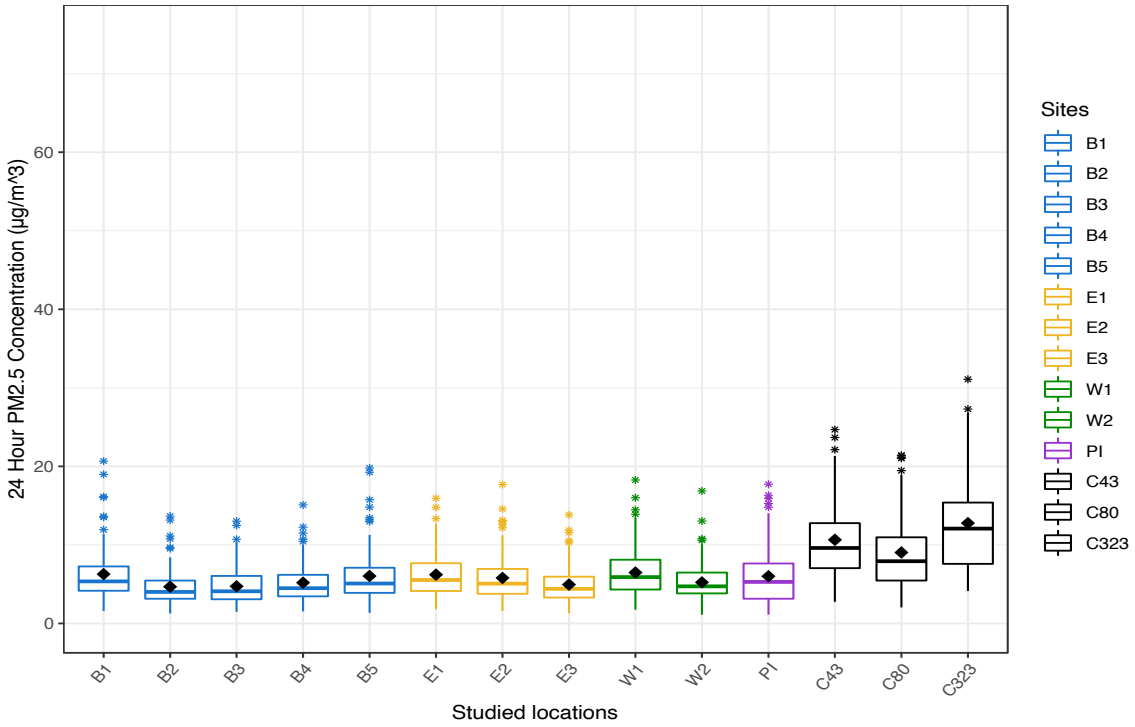

Figure 5.6: Boxplot of 24-hour $PM_{2.5}$ concentrations (µg/m^3) from the LCSs and CAMSs during summer (June-August 2021). Asterisks correspond to outliers and diamond corresponds to the mean.

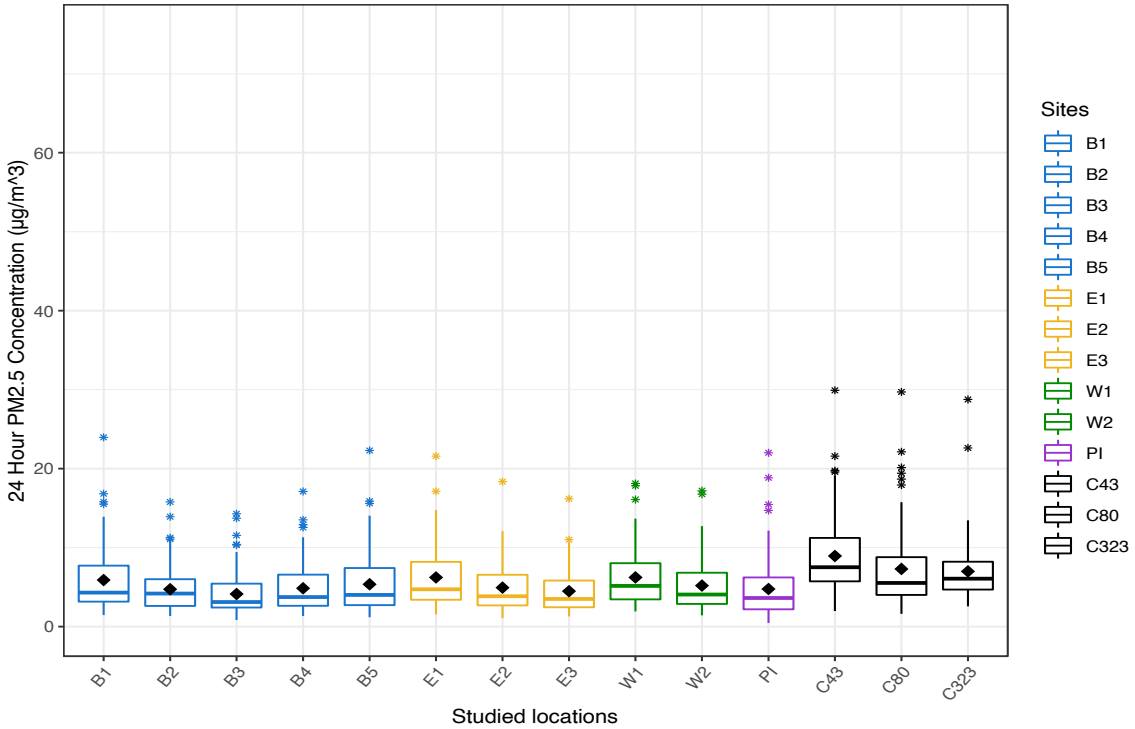

Figure 5.7: Boxplot of 24-hour $PM_{2.5}$ concentrations (µg/m^3) from the LCSs and CAMSs during autumn (September-November 2021). Asterisks correspond to outliers and diamond corresponds to the mean.

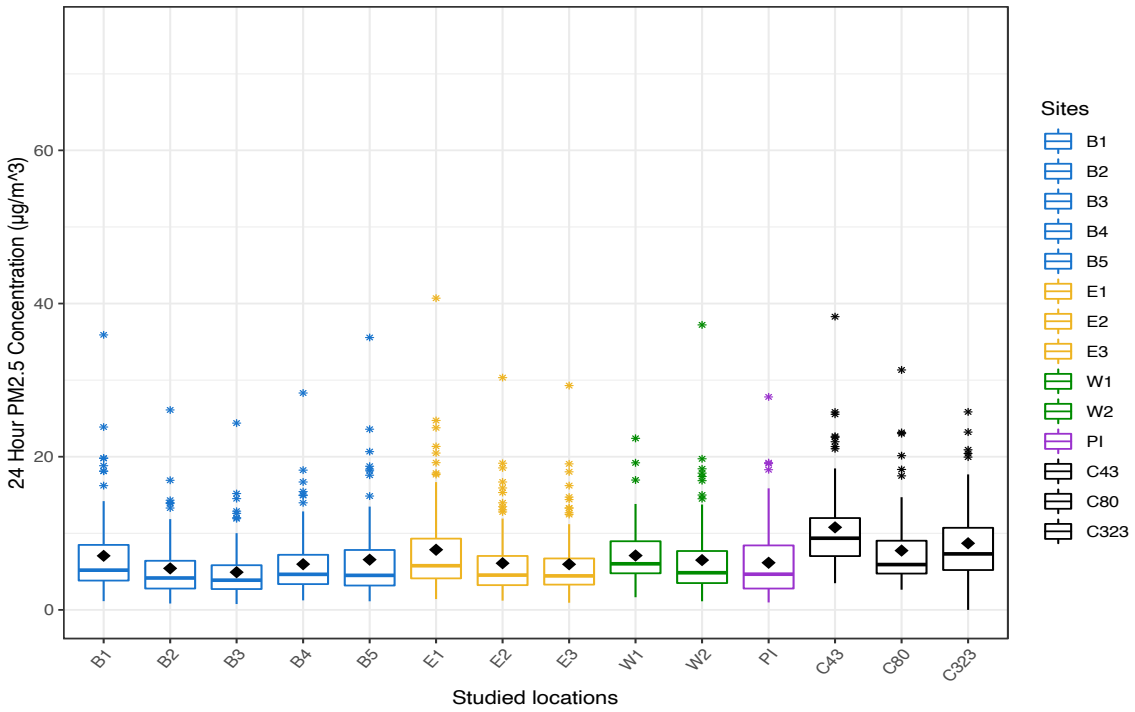

Figure 5.8: Boxplot of 24-hour $PM_{2.5}$ concentrations ($\mu g/m^3$) from the LCSs and CAMSs during winter (December 2021-February 2022). Asterisks correspond to outliers and diamond corresponds to the mean.

Table 5.6: Seasonal descriptive statistics for 24-hour $PM_{2.5}$ concentrations ($\mu g/m^3$) in the studied sites.

	Site	Mean	Median	Max	Min	StDev	N
Spring	B1	9.61	6.82	26.15	2.17	6.33	92
	B2	7.34	5.48	18.57	1.81	4.44	80
	B3	7.00	5.61	18.86	1.70	4.16	75
	B4	8.50	6.76	21.72	2.10	5.03	80
	B5	9.84	6.81	26.98	2.45	6.61	81
	E1	8.75	5.83	25.75	2.58	6.04	86
	E2	9.48	6.83	28.00	2.58	6.51	92
	E3	7.82	5.55	22.62	2.18	5.33	92
	W1	9.95	7.53	27.58	2.69	6.44	92
	W2	9.32	6.52	26.27	2.17	6.34	92
	PI	8.60	7.06	24.98	1.88	5.19	92
	C43	12.99	10.31	33.33	3.38	7.20	92
	C80	11.35	9.15	28.33	2.74	6.19	92
	C323	14.17	13.06	29.80	5.42	5.72	92
Summer	B1	6.27	5.35	20.67	1.58	3.59	92
	B2	4.67	4.02	13.67	1.27	2.49	84
	B3	4.72	4.08	13.02	1.47	2.40	92

Table 5.6 continued.

	B4	5.19	4.48	15.08	1.53	2.59	81
	B5	6.04	5.08	19.79	1.33	3.58	92
	E1	6.21	5.53	15.94	1.81	3.05	92
	E2	5.79	5.06	17.68	1.59	3.01	92
	E3	4.95	4.41	13.82	1.29	2.51	90
	W1	6.48	5.89	18.26	1.75	3.23	92
	W2	5.23	4.72	16.87	1.1	2.52	92
	PI	6	5.28	17.72	1.11	3.6	92
	C43	10.64	9.6	24.67	2.75	5.04	92
	C80	9.03	7.91	21.42	2.04	4.8	92
	C323	12.77	12.07	31.09	4.13	6.28	69
Autumn	B1	5.89	4.3	23.96	1.45	4.02	91
	B2	4.73	4.17	15.78	1.34	2.8	86
	B3	4.12	3.1	14.29	0.84	2.73	91
	B4	4.85	3.74	17.11	1.33	3.07	91
	B5	5.35	4	22.3	1.18	3.84	91
	E1	6.22	4.72	21.58	1.54	3.94	91
	E2	4.93	3.84	18.35	1.06	3.21	91
	E3	4.48	3.49	16.18	1.28	2.82	91
	W1	6.23	5.15	18.12	1.91	3.71	91
	W2	5.19	4.06	17.2	1.42	3.33	91
	PI	4.76	3.62	22	0.45	3.9	91
	C43	8.94	7.52	29.92	1.96	4.88	90
	C80	7.29	5.52	29.71	1.61	4.97	89
	C323	6.99	6.06	28.76	2.56	3.88	78
Winter	B1	7.05	5.18	35.91	1.14	5.61	90
	B2	5.42	4.16	26.1	0.82	4.09	81
	B3	4.92	3.87	24.39	0.76	3.65	90
	B4	5.95	4.64	28.32	1.24	4.32	90
	B5	6.56	4.51	35.57	1.12	5.6	90
	E1	7.85	5.76	40.7	1.41	6.28	90
	E2	6.09	4.54	30.33	1.21	4.8	90
	E3	5.95	4.44	29.29	0.93	4.59	90
	W1	7.09	6.02	22.4	1.65	3.83	77
	W2	6.49	4.84	37.21	1.11	5.32	90
	PI	6.14	4.66	27.81	0.97	4.81	90
	C43	10.77	9.35	38.29	3.48	5.81	90
	C80	7.74	5.92	31.33	2.63	4.96	88
	C323	8.69	7.31	25.85	0	5.03	82

StDev = standard deviation

Meteorological parameters from each season were assessed in Table 5.7 to read 24-hour RWS (m/s), T (°C), and solar radiation from the three CAMSs that actively log $PM_{2.5}$ (C43, C80, C323). Wind speeds at CAMS C80 fluctuated from 3.60, 2.68, and 2.35, to 3.11m/s during spring, summer, autumn, and winter respectively. Consistent with the temporal pattern exhibited with $PM_{2.5}$, averaged wind speeds decreased after spring and increased in winter. Temperature and solar radiation peaked in the summer with CAMSs reaching an average of 28 °C (83°F) and 0.36 Langley's per min (C43).

Table 5.7: Seasonal descriptive statistics of 24-hour meteorological parameters from selected CAMSs.

	Site	Parameter	Mean	Median	Max	Min	StDev	N
Spring	C43	RWS (m/s)	3.37	3.34	5.32	1.41	0.89	92
		T (°C)	23.78	24.45	29.12	14.04	3.86	92
		SR	0.30	0.31	0.47	0.04	0.11	92
	C80	RWS (m/s)	3.60	3.31	7.68	0.85	1.28	92
		T (°C)	23.28	23.66	28.29	13.62	3.53	92
		SR	0.27	0.28	0.44	0.03	0.11	92
	C323	RWS (m/s)	3.72	3.62	6.55	1.77	1.11	92
		T (°C)	22.81	23.43	28.09	13.50	3.53	92
Summer	C43	RWS (m/s)	2.81	2.76	4.70	1.10	0.79	92
		T (°C)	28.98	29.42	31.21	23.59	1.54	92
		SR	0.36	0.39	0.47	0.04	0.08	92
	C80	RWS (m/s)	2.68	2.44	6.11	0.12	1.10	92
		T (°C)	28.59	28.88	30.56	23.17	1.32	92
		SR	0.32	0.35	0.43	0.06	0.09	92
	C323	RWS (m/s)	2.97	2.89	5.03	1.72	0.66	92
		T (°C)	28.64	29.43	30.86	-17.78	5.00	92
Autumn	C43	RWS (m/s)	2.41	2.31	4.25	1.12	0.69	91
		T (°C)	24.92	25.73	31.27	12.92	4.52	91
		SR	0.28	0.28	0.40	0.04	0.08	91
	C80	RWS (m/s)	2.35	2.03	5.85	0.20	1.14	91
		T (°C)	24.87	25.43	30.45	13.30	4.09	91
		SR	0.27	0.28	0.40	0.07	0.09	91
	C323	RWS (m/s)	3.54	3.32	5.99	1.73	0.99	91
		T (°C)	26.14	26.93	30.73	16.27	3.50	91
Winter	C43	RWS (m/s)	2.60	2.46	5.43	1.02	0.99	90
		T (°C)	16.79	16.49	26.42	4.39	5.97	90
		SR	0.19	0.21	0.36	0.03	0.09	90
	C80	RWS (m/s)	3.11	3.00	6.73	0.13	1.36	87

Table 5.7 continued.

	T (°C)	17.11	17.43	25.80	2.80	5.80	90
	SR	0.19	0.20	0.38	0.02	0.09	90
C323	RWS (m/s)	3.38	3.12	6.65	1.05	1.41	90
	T (°C)	17.65	17.71	25.62	3.30	5.26	90

StDev = standard deviation, RWS = resultant wind speed in m/s, T = temperature in (°C), SR = solar radiation measured in Langley's per minute.

5.6 Hot Spot Analysis

Hot Spot Analysis (Getis-Ord Gi) was conducted to determine $PM_{2.5}$ distribution in the Lower RGV region using ArcGis. 3000 m was the average distance reported for the analysis. The z-scores were analyzed to better understand the statistical significance of $PM_{2.5}$ distribution in the appropriate counties. Figure 5.9 illustrates the hot spot output of the average $PM_{2.5}$ data from March 1st, 20221, to March 31st, 2022. Evidently, the results illustrate higher z-values in the cities of South Padre and Port Isabel (Cameron County) while Hidalgo County shows greater scores in the Mission city area.

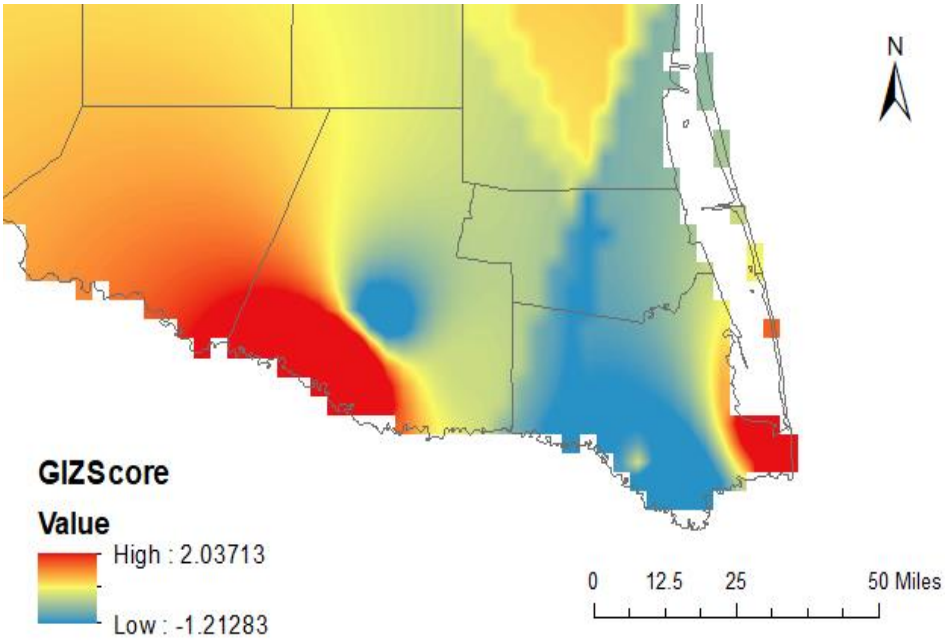

Figure 5.9: Hot spot analysis for $PM_{2.5}$ concentrations in the Lower RGV region.

Additionally, Cluster & Outlier Analysis (Anselin Local Morans I) was conducted to assess autocorrelational patterns in $PM_{2.5}$ distributions from the CAMSs and LCS sites. The Z-score results in this analysis examine the degree of spatial clustering. Figure 5.10 demonstrates the spatial clustering reporting random $PM_{2.5}$ distribution. Moran's Index is indicated as 0.41 with a z-score of 1.35 ($p< 0.18$).

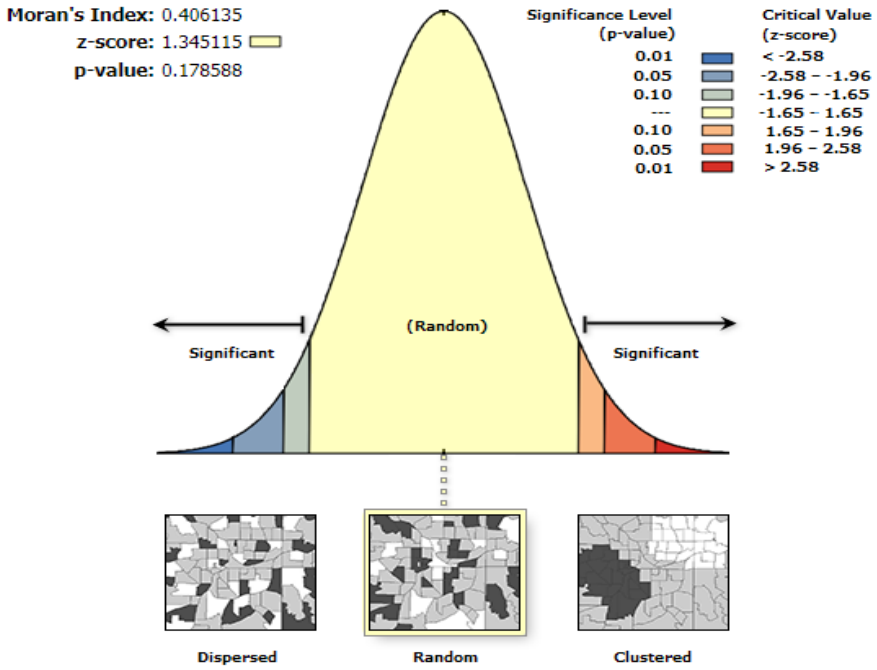

Figure 5.10: Spatial clustering report for $PM_{2.5}$ concentrations in the Lower RGV region.

Various maps were designed using hot spot analysis to accentuate the demographic and socio-economic results in the RGV region. The metrics used were from the 2018 census tract by the Centers for Disease Control and Prevention (CDC) Agency for Toxic Substance and Disease Registry (ATSDR) found at www.atsdr.cdc.gov (accessed in June 2022). The social vulnerability indexes are calculated by county. ArcGis outputs express the percent of persons below poverty, the amount per capita income (US dollars), the percent of persons aged 65 and older, and the percent of minorities in the RGV region (Figures 5.11 -5.14 respectively). These figures were examined to provide necessary interpretation for the Lower RGV region of South Texas.

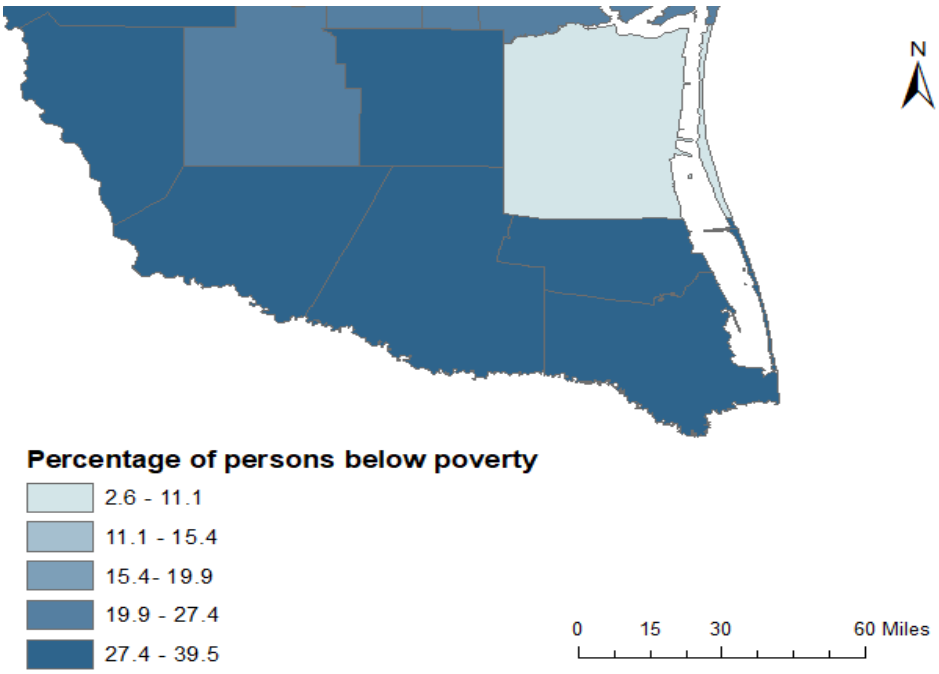

Figure 5.11: Hot spot analysis for the percentage of persons below poverty in the Lower RGV region.

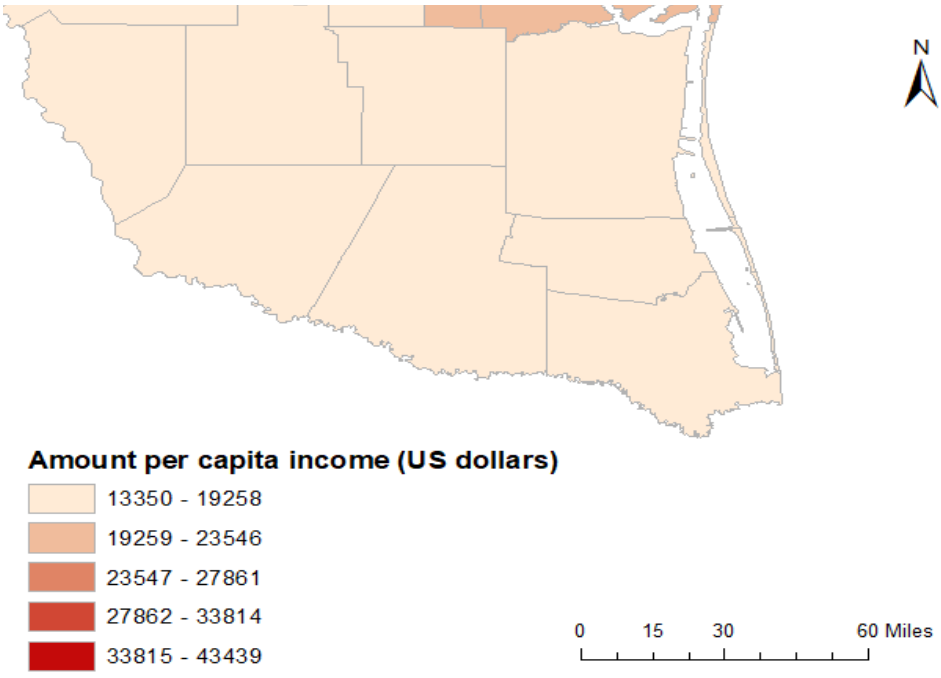

Figure 5.12: Hot spot analysis for the amount per capita income (US dollars) in the Lower RGV region.

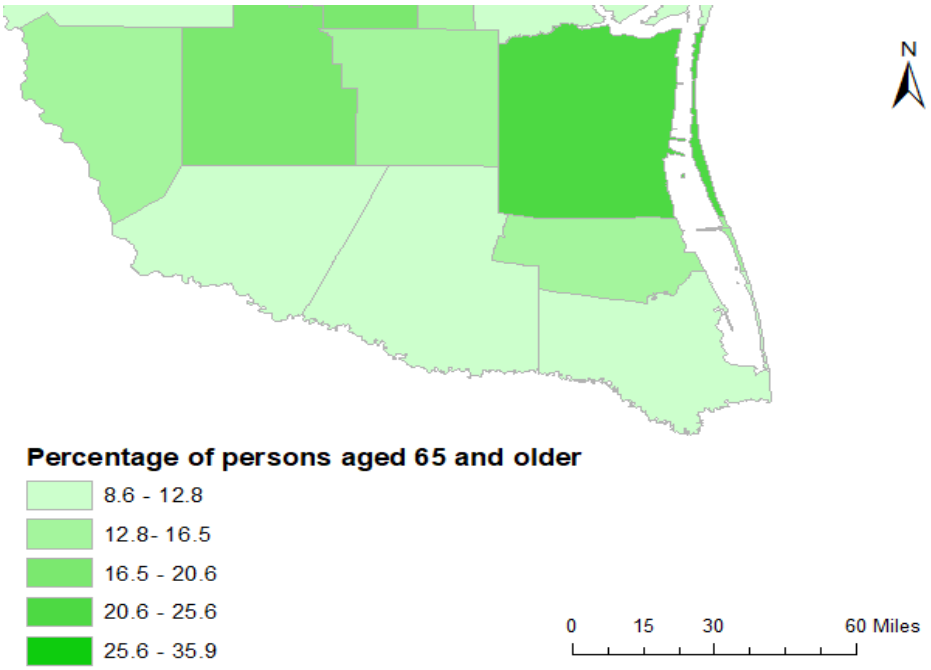

Figure 5.13: Hot spot analysis for the percentage of persons aged 65 and older in the Lower RGV region.

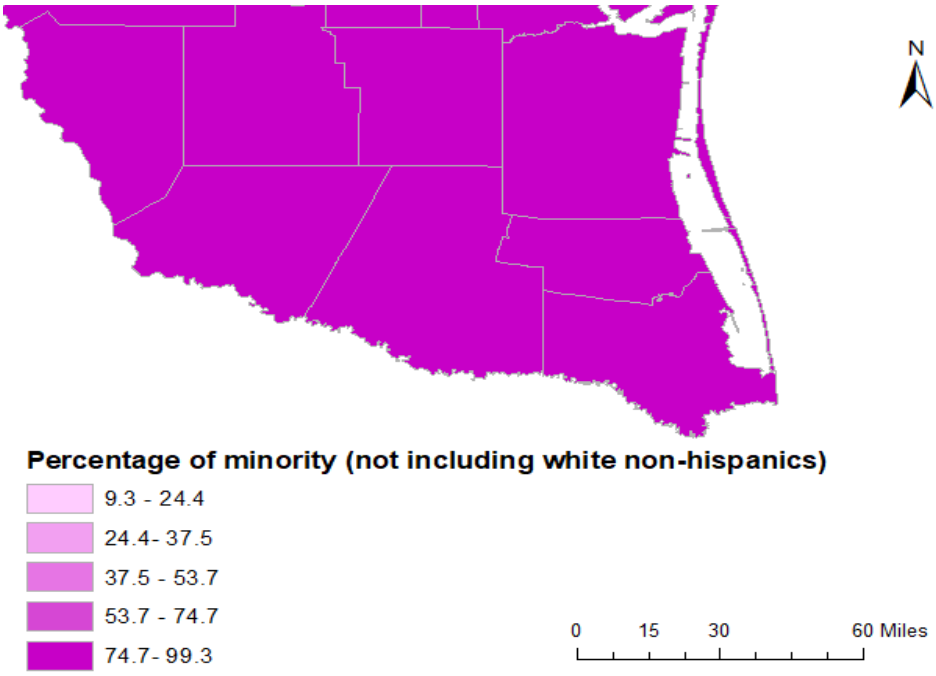

Figure 5.14: Hot spot analysis for the percentage of minorities in the Lower RGV region.

The included variables are estimated percentages of the data collected over the five years period (2014-2018) from the American Community Survey (ACS). The cities in this study were

based in the Hidalgo and Cameron counties, this is considered the lower area of the RGV. However, the entire RGV is included in the figures i.e., Starr, Hidalgo, Cameron, and Willacy counties. The RGV community's social vulnerability is exhibited by socioeconomic variables. Notably, the recorded persons living below poverty were 27% to 40% of the population in the RGV with bordering counties documenting 3% to 15%. The entire RGV region along with neighboring counties convey per capita income of less than $19,258. The household composition of persons aged 65 and older in the Lower RGV encompassed less than 13% of the population. The elderly populace is significant because they are a type of sensitive group that is more susceptible to human health issues.

The estimated total population of minorities was divided over the total population to assess the percentage of the minority population. Persons of white (non-Hispanic) ethnicity were not included in the estimate. Prominently, the demographic composition of minorities in the RGV region and adjoining counties comprised about 75% to 99% of the entire population. The resulting percentage is expected, considering the geographical proximately of the RGV with the U.S. -Mexican border. Correspondingly, Hispanics/Latinos comprise about 94% of the total population (1,402,340 persons) in the RGV region as of 2022 (*Population Data for Region: Rio Grande Valley*).

5.7 Discussion

Overall, the objective of this study was to assess $PM_{2.5}$ neighborhood-level monitoring with low-cost sensors. The results from this study characterize accurate exposure burdens in different communities of the Lower Rio Grande Valley. The $PM_{2.5}$ daily concentration averages in the cities of Brownsville, Edinburg, Weslaco, South Padre, and Port Isabel were within the designated standards from the NAAQS and WHO daily average standards. Thresholds for

harmful particulate matter levels are placed significantly for the protection of the public's health and welfare. Notably, there were short-term $PM_{2.5}$ daily values that did exceed the threshold warning of 15 μg/m³. Greater PM exposure levels in these urban areas would affect human health. The study period occurred around a year after the 2020 coronavirus mandatory lockdown in Texas. The $PM_{2.5}$ daily concentration averages could be a demonstration of people's exposure in the RGV region during and after quarantine. A study by (Chadwick et al., 2021) compared monthly $PM_{2.5}$ averaged concentrations using LCSs to show a significant reduction of 71.1% and 21.3% from 2019 to 2020, due to the quarantine measures limiting traffic use.

$PM_{2.5}$ concentrations were expected to vary spatially and temporally because of the various placements in the cities of Brownsville, Edinburg, Weslaco, and Port Isabel in the Lower Rio Grande Valley region. Spearman's rho correlational matrix analyzed moderate to strong positive relationships amongst the LCSs themselves ($r < 0.98$) and the relationship between the LCSs and CAMSs ($r < 0.89$). High spatial resolution for these selected cities was provided by the LCSs and demonstrated with $PM_{2.5}$ temporal and spatial trends. The resultant COD statistics confirmed the spatial heterogeneity between $PM_{2.5}$ concentrations from the TCEQ CAMSs (C43, C80, and C323) and LCSs. Henceforth, the significance of this study highlights CAMS central monitoring may not be a true representation of intra-urban exposures of fine particulate matter. The deployment of LCSs in intra-and-inter-urban locations provided better access to the personal exposure levels of $PM_{2.5}$.

Ambient monitoring with sample reference-grade instruments Federal Reference Methods (FRM) and Federal Equivalent Method (FEM) may fail to distinguish important pollution occurrences or spatial clustering of high pollution values i.e., hot spots (Connolly et al., 2022; Kelly et al., 2021; McLaughlin et al., 2020). Multiple studies examine traffic air pollutants

by collecting pollution data from central ambient monitoring sites to express long-term or short-term exposures (Raysoni et al., 2013; Dockery et al., 1993; Pope et al., 2002). Air quality performance with air monitoring instruments is exorbitant; therefore, studies typically use central ambient monitoring sites providing outdoor measurements (Wang, 2020; Faridi et al., 2018; Guo et al., 2017; Pun et al., 2017). These central ambient monitoring sites may not be appropriate for determining personal exposures. Studies have assessed central ambient monitoring sites for personal exposures of sensitive groups i.e., asthmatic children to determine potential exposure misclassifications (Raysoni et al., 2013, Adgate et al., 2002; Kousa et al., 2002). Henceforth, air quality LCSs are part of the ever-growing air quality studies around the world, because of their cost, accessible properties, and locally relevant data (Pang et al., 2021, deSouza et al., 2017; Morawska et al., 2018; Sun et al., 2016; Weissert et al., 2017). Objectively, this is a case study of ambient $PM_{2.5}$ monitoring in the Lower RGV region with novel LCSs. FRM/FEM samples and other collocation samples were performed pre- and post-study to calibrate the LCSs' accuracy and precision, as suggested from the literature reviewed on LCSs (Lee et al., 2019; Lu et al., 2021; Feenstra, 2020; Lung et al., 2022). The results from the literature review helped guide this study's methodology with LCSs.

The difficulties encountered in this study would be the sensitivity of the PM sensors to malfunctions and not having an immediate replacement. Therefore, to avoid similar complications, extra LCSs should be added to act as an immediate spare to the sensors that become faulty during the study.

CHAPTER VI

CONCLUSION

This novel study is one of the first of its type in the Lower Rio Grande Valley in South Texas to use low-cost sensors to monitor multiple towns and cities (Brownsville, Edinburg, Weslaco, and Port Isabel) and characterize $PM_{2.5}$ exposures at the intra-and-inter-urban level. Since this is the first of its kind, this research work will influence and aid with upcoming air quality assessments in the RGV region. Our focus in this study was solely on characterizing fine particulate matter ($PM_{2.5}$). Nevertheless, with the ever-growing market of novel low-cost sensors, diverse air pollutant species (i.e. NO_2, CO, O_3) can be incorporated into future air quality studies to determine different exposure burdens for various criteria air pollutant lands in the RGV. Building upon this study will ultimately provide vital information for the citizens residing in the RGV while adding to the steadily growing body of air quality literature in this region.

This research study will aid local policymakers in drafting guidelines for the citizenry to limit their particulate matter exposure burden to the general population in the RGV region. Given the standards already provided by NAAQS and WHO, daily averaged $PM_{2.5}$ concentrations in this study were still within the designated guidelines throughout the study period. However, short-term $PM_{2.5}$ levels throughout the study duration were still high enough to result in respiratory health issues.

Findings from this study become ever more important due to the 2020 coronavirus pandemic that primarily targeted the human respiratory system. The impact of $PM_{2.5}$ exposure

causes major acute and chronic health effects, and only increase when paired with the effects of the 2020 pandemic. Low-cost sensor technology is advancing rapidly. Together with central ambient monitoring sites, these low-cost sensors help the community to monitor both spatial and temporal pollutant patterns in real-time.

Future studies in this region focusing on other criteria air pollutants will definitely contribute to the growing body of air quality literature, especially in the U.S. -Mexico border region. Future studies should also contemplate performing similar pollutant monitoring across the international border in Mexico, once the security situation improves.

REFERENCES

Adgate, J. L., Ramachandran, G., Pratt, G. C., Waller, L. A., & Sexton, K. (2002). Spatial and temporal variability in outdoor, indoor, and personal PM2.5 exposure. *Atmospheric Environment*, *36*(20), 3255-3265. https://doi.org/https://doi.org/10.1016/S1352-2310(02)00326-6

Akland, G. G., Schwab, M., Zenick, H., & Pahl, D. (1997). An interagency partnership applied to the study of environmental health in the Lower Rio Grande Valley of Texas. *Environment International*, *23*(5), 595-609. https://doi.org/https://doi.org/10.1016/S0160-4120(97)00064-0

Al Hanai, A. H. (2019). *Methods to Investigate Fine PM in Developing Countries: Spatial Distribution and Biological Responses* (Publication Number 13900985) [Ph.D., The University of Wisconsin - Madison]. ProQuest Dissertations & Theses Global. Ann Arbor. https://proxy.openathens.net/login?entityID=https://idp.utrgv.edu/openathens&qurl=https://www.proquest.com/dissertations-theses/methods-investigate-fine-pm-developing-countries/docview/2366907903/se-2?accountid=7119

Ambient (outdoor) air pollution. (2021). World Health Organization https://www.who.int/news-room/fact-sheets/detail/ambient-(outdoor)-air-quality-and-health

Anderson, J. O., Thundiyil, J. G., & Stolbach, A. (2012). Clearing the air: a review of the effects of particulate matter air pollution on human health. *J Med Toxicol*, *8*(2), 166-175. https://doi.org/10.1007/s13181-011-0203-1

Ardon-Dryer, K., Dryer, Y., Williams, J. N., & Moghimi, N. (2020). Measurements of PM2.5 with PurpleAir under atmospheric conditions. *Atmos. Meas. Tech.*, *13*(10), 5441-5458. https://doi.org/10.5194/amt-13-5441-2020

Arvind, D. K., Mann, J., Bates, A., & Kotsev, K. (2016). *The AirSpeck Family of Static and Mobile Wireless Air Quality Monitors* 2016 Euromicro Conference on Digital System Design (DSD).

Askariyeh, M. H., Venugopal, M., Khreis, H., Birt, A., & Zietsman, J. (2020). Near-Road Traffic-Related Air Pollution: Resuspended PM2.5 from Highways and Arterials. *International Journal of Environmental Research and Public Health*, *17*(8), 2851. https://www.mdpi.com/1660-4601/17/8/2851

Atkinson, R. W., Fuller, G. W., Anderson, H. R., Harrison, R. M., & Armstrong, B. (2010). Urban Ambient Particle Metrics and Health: A Time-series Analysis. *Epidemiology*, *21*(4). https://journals.lww.com/epidem/Fulltext/2010/07000/Urban_Ambient_Particle_Metrics_and_Health__A.13.aspx

Austin, E., Novosselov, I., Seto, E., & Yost, M. G. (2015). Laboratory Evaluation of the Shinyei PPD42NS Low-Cost Particulate Matter Sensor. *PloS one*, *10*(9), 1. https://doi.org/http://dx.doi.org/10.1371/journal.pone.0137789

BlueSky Air Quality Monitor. TSI Inc. https://tsi.com/bluesky/

BlueSky Air Quality Monitor (2020). TSI Inc. https://tsi.com/getmedia/4c72a030-4585-4df4-a7c8-596aa1994734/BlueSky-Air-Quality-Monitor_A4_5002492_RevB_Web?ext=.pdf

BlueSky Air Quality Monitor Operation and Maintenance Manual (2021). TSI Inc. https://tsi.com/getmedia/a9299d7b-de37-4177-ab3b-488dfbfd2d07/BlueSky_Op_Maint_Manual_6013929?ext=.p

Borrego, C., Costa, A. M., Ginja, J., Amorim, M., Coutinho, M., Karatzas, K., Sioumis, T., Katsifarakis, N., Konstantinidis, K., De Vito, S., Esposito, E., Smith, P., André, N., Gérard, P., Francis, L. A., Castell, N., Schneider, P., Viana, M., Minguillón, M. C., Reimringer, W., Otjes, R. P., von Sicard, O., Pohle, R., Elen, B., Suriano, D., Pfister, V., Prato, M., Dipinto, S., & Penza, M. (2016). Assessment of air quality microsensors versus reference methods: The EuNetAir joint exercise. *Atmospheric Environment*, *147*, 246-263. https://doi.org/10.1016/j.atmosenv.2016.09.050

Bozlaker, A., Buzcu-Güven, B., Fraser, M. P., & Chellam, S. (2013). Insights into PM10 sources in Houston, Texas: Role of petroleum refineries in enriching lanthanoid metals during episodic emission events. *Atmospheric Environment*, *69*, 109-117. https://doi.org/https://doi.org/10.1016/j.atmosenv.2012.11.068

Bozlaker, A., Spada, N. J., Fraser, M. P., & Chellam, S. (2014). Elemental characterization of PM2.5 and PM10 emitted from light duty vehicles in the Washburn Tunnel of Houston, Texas: release of rhodium, palladium, and platinum. *Environ Sci Technol*, *48*(1), 54-62. https://doi.org/10.1021/es4031003

Brook, R. D., Franklin, B., Cascio, W., Hong, Y., Howard, G., Lipsett, M., Luepker, R., Mittleman, M., Samet, J., Smith, S. C., Jr., & Tager, I. (2004). Air pollution and cardiovascular disease: a statement for healthcare professionals from the Expert Panel on Population and Prevention Science of the American Heart Association. *Circulation*, *109*(21), 2655-2671. https://doi.org/10.1161/01.Cir.0000128587.30041.C8

Brown, J. S., Gordon, T., Price, O., & Asgharian, B. (2013). Thoracic and respirable particle definitions for human health risk assessment. *Particle and Fibre Toxicology*, *10*(1), 12. https://doi.org/10.1186/1743-8977-10-12

Brugge, D., Durant, J. L., & Rioux, C. (2007). Near-highway pollutants in motor vehicle exhaust: a review of epidemiologic evidence of cardiac and pulmonary health risks. *Environ Health*, *6*, 23. https://doi.org/10.1186/1476-069x-6-23

Brunekreef, B., & Forsberg, B. (2005). Epidemiological evidence of effects of coarse airborne particles on health. *Eur Respir J*, *26*(2), 309-318. https://doi.org/10.1183/09031936.05.00001805

Burton, R. K. (2017). *Analysis of Low-Cost Particulate Matter Shinyei Sensor for Asthma Research* (Publication Number 10615301) [M.S., University of Maryland, Baltimore County]. ProQuest Dissertations & Theses Global. Ann Arbor. https://proxy.openathens.net/login?entityID=https://idp.utrgv.edu/openathens&qurl=https://www.proquest.com/dissertations-theses/analysis-low-cost-particulate-matter-shinyei/docview/1967162457/se-2?accountid=7119

Cadelis, G., Tourres, R., & Molinie, J. (2014). Short-Term Effects of the Particulate Pollutants Contained in Saharan Dust on the Visits of Children to the Emergency Department due to Asthmatic Conditions in Guadeloupe (French Archipelago of the Caribbean). *PloS one*, *9*(3), e91136. https://doi.org/10.1371/journal.pone.0091136

Carvlin, G. N., Lugo, H., Olmedo, L., Bejarano, E., Wilkie, A., Meltzer, D., Wong, M., King, G., Northcross, A., Jerrett, M., English, P. B., Hammond, D., & Seto, E. (2017). Development and field validation of a community-engaged particulate matter air quality monitoring network in Imperial, California, USA. *Journal of the Air & Waste Management Association*, *67*(12), 1342-1352. https://doi.org/http://dx.doi.org/10.1080/10962247.2017.1369471

Casati, R., Scheer, V., Vogt, R., & Benter, T. (2007). Measurement of nucleation and soot mode particle emission from a diesel passenger car in real world and laboratory in situ dilution. *Atmospheric Environment*, *41*(10), 2125-2135. https://doi.org/https://doi.org/10.1016/j.atmosenv.2006.10.078

Castell, N., Dauge, F. R., Schneider, P., Vogt, M., Lerner, U., Fishbain, B., Broday, D., & Bartonova, A. (2017). Can commercial low-cost sensor platforms contribute to air quality monitoring and exposure estimates? *Environ Int*, *99*, 293-302. https://doi.org/10.1016/j.envint.2016.12.007

Chadwick, E., Le, K., Pei, Z., Sayahi, T., Rapp, C., Butterfield, A. E., & Kelly, K. E. (2021). Technical note: Understanding the effect of COVID-19 on particle pollution using a low-cost sensor network. *Journal of Aerosol Science*, *155*, 105766. https://doi.org/https://doi.org/10.1016/j.jaerosci.2021.105766

Chen, Y.-H. (2020). *Applying Low-Cost Air Sensors for Spatiotemporal Variability of Particulate Matter in a Local Community Adjacent to Interstate Highway* (Publication Number 28260199) [M.Sc., University of California, Los Angeles]. ProQuest Dissertations & Theses Global. Ann Arbor. https://proxy.openathens.net/login?entityID=https://idp.utrgv.edu/openathens&qurl=https:

//www.proquest.com/dissertations-theses/applying-low-cost-air-sensors-spatiotemporal/docview/2470267376/se-2?accountid=7119

Cheung, K., Daher, N., Kam, W., Shafer, M. M., Ning, Z., Schauer, J. J., & Sioutas, C. (2011). Spatial and temporal variation of chemical composition and mass closure of ambient coarse particulate matter (PM10–2.5) in the Los Angeles area. *Atmospheric Environment*, *45*(16), 2651-2662. https://doi.org/https://doi.org/10.1016/j.atmosenv.2011.02.066

Connolly, R. E., Yu, Q., Wang, Z., Chen, Y.-H., Liu, J. Z., Collier-Oxandale, A., Papapostolou, V., Polidori, A., & Zhu, Y. (2022). Long-term evaluation of a low-cost air sensor network for monitoring indoor and outdoor air quality at the community scale. *Science of The Total Environment*, *807*, 150797. https://doi.org/https://doi.org/10.1016/j.scitotenv.2021.150797

Correia, A. W., Pope, C. A., 3rd, Dockery, D. W., Wang, Y., Ezzati, M., & Dominici, F. (2013). Effect of air pollution control on life expectancy in the United States: an analysis of 545 U.S. counties for the period from 2000 to 2007. *Epidemiology*, *24*(1), 23-31. https://doi.org/10.1097/EDE.0b013e3182770237

Danner, J. (2022). *Get ready, Saharan Dust is headed for the Rio Grande Valley*. Local 23 Valley Central. https://www.valleycentral.com/news/local-news/get-ready-saharan-dust-is-headed-for-the-rio-grande-valley/

Datta, A., Saha, A., Zamora, M. L., Buehler, C., Hao, L., Xiong, F., Gentner, D. R., & Koehler, K. (2020). Statistical field calibration of a low-cost PM2.5 monitoring network in Baltimore. *Atmos Environ (1994)*, *242*. https://doi.org/10.1016/j.atmosenv.2020.117761

Dausman, T. B. C. (2017). *Low Cost Air Quality Monitors in Agriculture* (Publication Number 10262230) [M.S., The University of Iowa]. ProQuest Dissertations & Theses Global. Ann Arbor. https://proxy.openathens.net/login?entityID=https://idp.utrgv.edu/openathens&qurl=https://www.proquest.com/dissertations-theses/low-cost-air-quality-monitors-agriculture/docview/1929896237/se-2?accountid=7119

de Kok, T. M., Driece, H. A., Hogervorst, J. G., & Briedé, J. J. (2006). Toxicological assessment of ambient and traffic-related particulate matter: a review of recent studies. *Mutat Res*, *613*(2-3), 103-122. https://doi.org/10.1016/j.mrrev.2006.07.001

deSouza, P. N., Nthusi, V. K., Klopp, J., Shaw, B. E., Ho, W. O., Saffell, J., Jones, R. L., & Ratti, C. (2017). A Nairobi experiment in using low cost air quality monitors. *Clean Air Journal*, *27*, 12-12.

Dockery, D. W., Pope, C. A., Xu, X., Spengler, J. D., Ware, J. H., Fay, M. E., Ferris Jr, B. G., & Speizer, F. E. (1993). An association between air pollution and mortality in six US cities. *New England journal of medicine*, *329*(24), 1753-1759.

Draggan, S. (2011). *Indoor fine particulate matter sources*. The Encyclopedia of Earth. https://editors.eol.org/eoearth/wiki/Indoor_Fine_Particulate_Matter_Sources

Esworthy, R. (2013). Air quality: EPA'S 2013 changes to the particulate matter (PM) standard. In (pp. 157-208).

Fang, Y., Naik, V., Horowitz, L. W., & Mauzerall, D. L. (2013). Air pollution and associated human mortality: the role of air pollutant emissions, climate change and methane concentration increases from the preindustrial period to present. *Atmos. Chem. Phys.*, *13*(3), 1377-1394. https://doi.org/10.5194/acp-13-1377-2013

Faridi, S., Shamsipour, M., Krzyzanowski, M., Künzli, N., Amini, H., Azimi, F., Malkawi, M., Momeniha, F., Gholampour, A., Hassanvand, M. S., & Naddafi, K. (2018). Long-term trends and health impact of PM2.5 and O3 in Tehran, Iran, 2006–2015. *Environment International*, *114*, 37-49. https://doi.org/https://doi.org/10.1016/j.envint.2018.02.026

Feenstra, B., Papapostolou, V., Hasheminassab, S., Zhang, H., Boghossian, B. D., Cocker, D., & Polidori, A. (2019). Performance evaluation of twelve low-cost PM2.5 sensors at an ambient air monitoring site. *Atmospheric Environment*, *216*, 116946. https://doi.org/https://doi.org/10.1016/j.atmosenv.2019.116946

Feenstra, B. J. (2020). *Development of Methodologies for the Use and Application of Air Quality Sensors to Enable Community Air Monitoring* (Publication Number 27963261) [Ph.D., University of California, Riverside]. ProQuest Dissertations & Theses Global. Ann Arbor. https://proxy.openathens.net/login?entityID=https://idp.utrgv.edu/openathens&qurl=https://www.proquest.com/dissertations-theses/development-methodologies-use-application-air/docview/2438674363/se-2?accountid=7119

Gao, M., Cao, J., & Seto, E. (2015). A distributed network of low-cost continuous reading sensors to measure spatiotemporal variations of PM2.5 in Xi'an, China. *Environmental Pollution*, *199*, 56-65. https://doi.org/https://doi.org/10.1016/j.envpol.2015.01.013

Girguis, M. S., Strickland, M. J., Hu, X., Liu, Y., Bartell, S. M., & Vieira, V. M. (2016). Maternal exposure to traffic-related air pollution and birth defects in Massachusetts. *Environmental Research*, *146*, 1-9. https://doi.org/https://doi.org/10.1016/j.envres.2015.12.010

Gómez-Suárez, J., Arroyo, P., Alfonso, R., Suárez, J. I., Pinilla-Gil, E., & Lozano, J. (2022). A Novel Bike-Mounted Sensing Device with Cloud Connectivity for Dynamic Air-Quality Monitoring by Urban Cyclists. *Sensors*, *22*(3), 1272. https://www.mdpi.com/1424-8220/22/3/1272

Guaita, R., Pichiule, M., Maté, T., Linares, C., & Díaz, J. (2011). Short-term impact of particulate matter (PM(2.5)) on respiratory mortality in Madrid. *Int J Environ Health Res*, *21*(4), 260-274. https://doi.org/10.1080/09603123.2010.544033

Guo, H., Cheng, T., Gu, X., Wang, Y., Chen, H., Bao, F., Shi, S., Xu, B., Wang, W., Zuo, X., Zhang, X., & Meng, C. (2017). Assessment of PM2.5 concentrations and exposure throughout China using ground observations. *Science of The Total Environment*, *601-602*, 1024-1030. https://doi.org/https://doi.org/10.1016/j.scitotenv.2017.05.263

Gupta, P., Doraiswamy, P., Levy, R., Pikelnaya, O., Maibach, J., Feenstra, B., Polidori, A., Kiros, F., & Mills, K. C. (2018). Impact of California Fires on Local and Regional Air Quality: The Role of a Low-Cost Sensor Network and Satellite Observations. *GeoHealth*, *2*(6), 172-181. https://doi.org/http://dx.doi.org/10.1029/2018GH000136

Halonen, J. I., Lanki, T., Yli-Tuomi, T., Tiittanen, P., Kulmala, M., & Pekkanen, J. (2009). Particulate air pollution and acute cardiorespiratory hospital admissions and mortality among the elderly. *Epidemiology*, *20*(1), 143-153. https://doi.org/10.1097/EDE.0b013e31818c7237

Hartin, K. (2015). *Fine Particle (PM_{2.5}) Composition of Indoor and Outdoor Air Samples Collected in Xuanwei County, China* (Publication Number 10000202) [Master's, University of Washington]. ProQuest Dissertations & Theses Global. Ann Arbor. https://proxy.openathens.net/login?entityID=https://idp.utrgv.edu/openathens&qurl=https://www.proquest.com/dissertations-theses/fine-particle-pm-sub-2-5-composition-indoor/docview/1759139219/se-2?accountid=7119

He, J., Huang, C.-H., Yuan, N., Austin, E., Seto, E., & Novosselov, I. (2022). Network of Low-cost Air Quality Sensor for Monitoring Indoor, Outdoor, and PersonalPM2.5Exposure in Seattleduring the 2020 Wildfire Season. https://doi.org/10.48550/arxiv.2203.14140

Hidalgo County declares local state of disaster due to wildfires. (2022). KRGV Rio Grande Valley Tx. https://www.krgv.com/videos/hidalgo-county-declares-local-state-of-disaster-due-to-wildfires#:~:text=The%20Hidalgo%20County%20Commissioners%20Court%20on%20Tuesday%20voted,burned%20in%20four%20separate%20wildfires%20in%20the%20county

Huang, J., Kwan, M.-P., Cai, J., Song, W., Yu, C., Kan, Z., & Yim, S. H.-L. (2022). Field Evaluation and Calibration of Low-Cost Air Pollution Sensors for Environmental Exposure Research. *Sensors*, *22*(6), 2381. https://doi.org/10.3390/s22062381

Indoor Air Quality (IAQ). (2022). EPA United States Environmental Protection Agency https://www.epa.gov/indoor-air-quality-iaq/indoor-particulate-matter#indoor_pm

Jayaratne, R., Kuhn, T., Christensen, B., Liu, X., Zing, I., Lamont, R., Dunbabin, M., Maddox, J., Fisher, G., & Morawska, L. Using a Network of Low-Cost Particle Sensors to Assess the Impact of Ship Emissions on a Residential Community.

Jiao, W., Hagler, G., Williams, R., Sharpe, R., Brown, R., Garver, D., Judge, R., Caudill, M., Rickard, J., Davis, M., Weinstock, L., Zimmer-Dauphinee, S., & Buckley, K. (2016). Community Air Sensor Network (CAIRSENSE) project: evaluation of low-cost sensor performance in a suburban environment in the southeastern United States. *Atmos Meas Tech*, *9*(11), 5281-5292. https://doi.org/10.5194/amt-9-5281-2016

Juda-Rezler, K., Reizer, M., & Oudinet, J.-P. (2011). Determination and analysis of PM10 source apportionment during episodes of air pollution in Central Eastern European urban areas:

The case of wintertime 2006. *Atmospheric Environment - ATMOS ENVIRON*, *45*, 6557-6566. https://doi.org/10.1016/j.atmosenv.2011.08.020

Karagulian, F., Barbiere, M., Kotsev, A., Spinelle, L., Gerboles, M., Lagler, F., Redon, N., Crunaire, S., & Borowiak, A. (2019). Review of the Performance of Low-Cost Sensors for Air Quality Monitoring. *Atmosphere*, *10*(9). https://doi.org/10.3390/atmos10090506

Kelly, K. E., Whitaker, J., Petty, A., Widmer, C., Dybwad, A., Sleeth, D., Martin, R., & Butterfield, A. (2017). Ambient and laboratory evaluation of a low-cost particulate matter sensor. *Environ Pollut*, *221*, 491-500. https://doi.org/10.1016/j.envpol.2016.12.039

Kelly, K. E., Xing, W. W., Sayahi, T., Mitchell, L., Becnel, T., Gaillardon, P. E., Meyer, M., & Whitaker, R. T. (2021). Correction to Community-Based Measurements Reveal Unseen Differences during Air-Pollution Episodes. *Environ Sci Technol*, *55*(16), 11466. https://doi.org/10.1021/acs.est.1c04668

Khreis, H., Johnson, J., Jack, K., Dadashova, B., & Park, E. S. (2022). Evaluating the Performance of Low-Cost Air Quality Monitors in Dallas, Texas. *International Journal of Environmental Research and Public Health*, *19*(3), 1647. https://doi.org/10.3390/ijerph19031647

Kim, K.-H., Kabir, E., & Kabir, S. (2015). A review on the human health impact of airborne particulate matter. *Environment International*, *74*, 136-143. https://doi.org/https://doi.org/10.1016/j.envint.2014.10.005

Kioumourtzoglou, M. A., Schwartz, J. D., Weisskopf, M. G., Melly, S. J., Wang, Y., Dominici, F., & Zanobetti, A. (2016). Long-term PM2.5 Exposure and Neurological Hospital Admissions in the Northeastern United States. *Environ Health Perspect*, *124*(1), 23-29. https://doi.org/10.1289/ehp.1408973

Kousa, A., Oglesby, L., Koistinen, K., Künzli, N., & Jantunen, M. (2002). Exposure chain of urban air PM2.5—associations between ambient fixed site, residential outdoor, indoor, workplace and personal exposures in four European cities in the EXPOLIS-study. *Atmospheric Environment*, *36*(18), 3031-3039. https://doi.org/https://doi.org/10.1016/S1352-2310(02)00232-7

Krudysz, M. A., Froines, J. R., Fine, P. M., & Sioutas, C. (2008). Intra-community spatial variation of size-fractionated PM mass, OC, EC, and trace elements in the Long Beach, CA area. *Atmospheric Environment*, *42*(21), 5374-5389. https://doi.org/https://doi.org/10.1016/j.atmosenv.2008.02.060

Kulkarni, P., Chellam, S., & Fraser, M. P. (2006). Lanthanum and lanthanides in atmospheric fine particles and their apportionment to refinery and petrochemical operations in Houston, TX. *Atmospheric Environment*, *40*(3), 508-520. https://doi.org/https://doi.org/10.1016/j.atmosenv.2005.09.063

Kulkarni, P., Chellam, S., & Fraser, M. P. (2007). Tracking petroleum refinery emission events using lanthanum and lanthanides as elemental markers for PM2.5. *Environ Sci Technol*, *41*(19), 6748-6754. https://doi.org/10.1021/es062888i

Lee, C.-H., Wang, Y.-B., & Yu, H.-L. (2019). An efficient spatiotemporal data calibration approach for the low-cost PM2.5 sensing network: A case study in Taiwan. *Environment International*, *130*, 104838. https://doi.org/https://doi.org/10.1016/j.envint.2019.05.032

Levy Zamora, M., Xiong, F., Gentner, D., Kerkez, B., Kohrman-Glaser, J., & Koehler, K. (2019). Field and Laboratory Evaluations of the Low-Cost Plantower Particulate Matter Sensor. *Environ Sci Technol*, *53*(2), 838-849. https://doi.org/10.1021/acs.est.8b05174

Lewis, A., & Edwards, P. (2016). Validate personal air-pollution sensors. *Nature*, *535*(7610), 29-31. https://doi.org/10.1038/535029a

Liu, X., Jayaratne, R., Thai, P., Kuhn, T., Zing, I., Christensen, B., Lamont, R., Dunbabin, M., Zhu, S., Gao, J., Wainwright, D., Neale, D., Kan, R., Kirkwood, J., & Morawska, L. (2020). Low-cost sensors as an alternative for long-term air quality monitoring. *Environmental Research*, *185*, 109438. https://doi.org/https://doi.org/10.1016/j.envres.2020.109438

Lu, Y., Giuliano, G., & Habre, R. (2021). Estimating hourly PM2.5 concentrations at the neighborhood scale using a low-cost air sensor network: A Los Angeles case study. *Environmental Research*, *195*, 110653. https://doi.org/https://doi.org/10.1016/j.envres.2020.110653

Lung, S.-C. C., Thi Hien, T., Cambaliza, M. O. L., Hlaing, O. M. T., Oanh, N. T. K., Latif, M. T., Lestari, P., Salam, A., Lee, S.-Y., Wang, W.-C. V., Tsou, M.-C. M., Cong-Thanh, T., Cruz, M. T., Tantrakarnapa, K., Othman, M., Roy, S., Dang, T. N., & Agustian, D. (2022). Research Priorities of Applying Low-Cost PM2.5 Sensors in Southeast Asian Countries. *International Journal of Environmental Research and Public Health*, *19*(3), 1522. https://www.mdpi.com/1660-4601/19/3/1522

Madureira, J., Paciência, I., & Fernandes Ede, O. (2012). Levels and indoor-outdoor relationships of size-specific particulate matter in naturally ventilated Portuguese schools. *J Toxicol Environ Health A*, *75*(22-23), 1423-1436. https://doi.org/10.1080/15287394.2012.721177

Magi, B. I., Cupini, C., Francis, J., Green, M., & Hauser, C. (2019). Evaluation of PM2.5 measured in an urban setting using a low-cost optical particle counter and a Federal Equivalent Method Beta Attenuation Monitor. *Aerosol Science and Technology*, *54*(2), 147-159. https://doi.org/10.1080/02786826.2019.1619915

Malings, C., Tanzer, R., Hauryliuk, A., Saha, P. K., Robinson, A. L., Presto, A. A., & Subramanian, R. (2019). Fine particle mass monitoring with low-cost sensors: Corrections and long-term performance evaluation. *Aerosol Science and Technology*, *54*(2), 160-174. https://doi.org/10.1080/02786826.2019.1623863

Marto, J. P. (2018). *Field Evaluation of Portable Air Quality Monitors and Evaluation of Short-lived Plume Events of Atmospheric Pollutants* (Publication Number 10933462) [M.S., State University of New York at Albany]. ProQuest Dissertations & Theses Global. Ann Arbor. https://proxy.openathens.net/login?entityID=https://idp.utrgv.edu/openathens&qurl=https://www.proquest.com/dissertations-theses/field-evaluation-portable-air-quality-monitors/docview/2112855666/se-2?accountid=7119

McLaughlin, T., Kearny, L., & Sanicola, L. (2020). *Special report: U.S. air monitors routinely miss pollution—even refinery explosions*. https://www.reuters.com/article/usa-pollution-airmonitors-specialreport-idUSKBN28B4RT

Measure and Record your Air Quality Data TSI Inc. https://tsi.com/focus/bluesky-landing-page/measurements/

Meister, K., Johansson, C., & Forsberg, B. (2012). Estimated short-term effects of coarse particles on daily mortality in Stockholm, Sweden. *Environ Health Perspect*, *120*(3), 431-436. https://doi.org/10.1289/ehp.1103995

Mendez, E., Rodriguez, J., Luna, A., & Raysoni, A. U. (2022). Comparative Assessment of Pollutant Concentrations and Meteorological Parameters from TCEQ CAMS Sites at Houston and Rio Grande Valley Regions of Texas, USA in 2016. *Open Journal of Air Pollution*, *11*(01), 13-27. https://doi.org/10.4236/ojap.2022.111002

Misra, C., Geller, M., Shah, P., & Solomon, P. (2001). Development and evaluation of a continuous coarse (PM10-PM2.5) particle monitor. *Journal of the Air & Waste Management Association (1995)*, *51*, 1309-1317.

Molaie, S., & Lino, P. (2021). Review of the Newly Developed, Mobile Optical Sensors for Real-Time Measurement of the Atmospheric Particulate Matter Concentration. *Micromachines (Basel)*, *12*(4). https://doi.org/10.3390/mi12040416

Morawska, L., Thai, P. K., Liu, X., Asumadu-Sakyi, A., Ayoko, G., Bartonova, A., Bedini, A., Chai, F., Christensen, B., Dunbabin, M., Gao, J., Hagler, G. S. W., Jayaratne, R., Kumar, P., Lau, A. K. H., Louie, P. K. K., Mazaheri, M., Ning, Z., Motta, N., Mullins, B., Rahman, M. M., Ristovski, Z., Shafiei, M., Tjondronegoro, D., Westerdahl, D., & Williams, R. (2018). Applications of low-cost sensing technologies for air quality monitoring and exposure assessment: How far have they gone? *Environment International*, *116*, 286-299. https://doi.org/https://doi.org/10.1016/j.envint.2018.04.018

Mukherjee, A., Stanton, L. G., Graham, A. R., & Roberts, P. T. (2017). Assessing the Utility of Low-Cost Particulate Matter Sensors over a 12-Week Period in the Cuyama Valley of California. *Sensors (Basel)*, *17*(8). https://doi.org/10.3390/s17081805

Munir, S., Mayfield, M., Coca, D., Jubb, S. A., & Osammor, O. (2019). Analysing the performance of low-cost air quality sensors, their drivers, relative benefits and calibration in cities-a case study in Sheffield. *Environmental monitoring and assessment*, *191*(2), 94. https://doi.org/http://dx.doi.org/10.1007/s10661-019-7231-8

Mykhaylova, N. (2018). *Low-cost Sensor Array Devices as a Method for Reliable Assessment of Exposure to Traffic-related Air Pollution* (Publication Number 10973729) [Ph.D., University of Toronto (Canada)]. ProQuest Dissertations & Theses Global; SciTech Premium Collection. Ann Arbor. https://proxy.openathens.net/login?entityID=https://idp.utrgv.edu/openathens&qurl=https://www.proquest.com/dissertations-theses/low-cost-sensor-array-devices-as-method-reliable/docview/2149673888/se-2?accountid=7119

North American Free Trade Agreement (NAFTA). International Trade Administration https://www.trade.gov/north-american-free-trade-agreement-nafta

Oluwadairo, T., Whitehead, L., Symanski, E., Bauer, C., Carson, A., & Han, I. (2022). Effects of aerosol particle size on the measurement of airborne PM2.5 with a low-cost particulate matter sensor (LCPMS) in a laboratory chamber. *Environmental monitoring and assessment*, *194*(2). https://doi.org/10.1007/s10661-021-09715-6

Organization, W. H. (2013). *Health effects of particulate matter: policy implications for countries in eastern Europe, Caucasus and central Asia. World Health Organization. Regional Office for Europe*. Regional Office for Europe. https://apps.who.int/iris/handle/10665/344854

Organization, W. H. (2018). Global Health Estimates 2016: Deaths by Cause, Age, Sex, by Country and by Region, 2000-2016.

Orlando, P. J. (2019). *Modeling Spatiotemporal Patterns of PM 2.5 at the Sub-Neighborhood Scale Using Low-Cost Sensor Networks* (Publication Number 22589680) [M.S., Portland State University]. ProQuest Dissertations & Theses Global. Ann Arbor. https://proxy.openathens.net/login?entityID=https://idp.utrgv.edu/openathens&qurl=https://www.proquest.com/dissertations-theses/modeling-spatiotemporal-patterns-pm-2-5-at-sub/docview/2376751758/se-2?accountid=7119

Outdoor burning (2022). Hidalgo County Texas. https://www.hidalgocounty.us/328/Burn-PermitInformation?fbclid=IwAR1yLRCF8AvAwahdhVibY3J98gPKpsmUZZpb_l85x34Z2EG3IuPqQ_x4iec

Pang, X., Chen, L., Shi, K., Wu, F., Chen, J., Fang, S., Wang, J., & Xu, M. (2021). A lightweight low-cost and multipollutant sensor package for aerial observations of air pollutants in atmospheric boundary layer. *Science of The Total Environment*, *764*, 142828. https://doi.org/https://doi.org/10.1016/j.scitotenv.2020.142828

Pang, X., Shaw, M. D., Gillot, S., & Lewis, A. C. (2018). The impacts of water vapour and co-pollutants on the performance of electrochemical gas sensors used for air quality monitoring. *Sensors and Actuators B: Chemical*, *266*, 674-684. https://doi.org/https://doi.org/10.1016/j.snb.2018.03.144

Particulate Matter (PM) Pollution. (2021). EPA United States Environmental Protection Agency. https://www.epa.gov/pm-pollution/particulate-matter-pm-basics

Pawar, H., & Sinha, B. (2022). Residential heating emissions (can) exceed paddy-residue burning emissions in rural northwest India. *Atmospheric Environment*, *269*, 118846. https://doi.org/https://doi.org/10.1016/j.atmosenv.2021.118846

Peach, J., & Williams, J. (2004). Population Projections for the US Mexican Border Region. In: San Diego, CA: San Diego State University Press.

Perez, L., Tobías, A., Querol, X., Pey, J., Alastuey, A., Díaz, J., & Sunyer, J. (2012). Saharan dust, particulate matter and cause-specific mortality: a case-crossover study in Barcelona (Spain). *Environ Int*, *48*, 150-155. https://doi.org/10.1016/j.envint.2012.07.001

Pikridas, M., Bezantakos, S., Močnik, G., Keleshis, C., Brechtel, F., Stavroulas, I., Demetriades, G., Antoniou, P., Vouterakos, P., Argyrides, M., Liakakou, E., Drinovec, L., Marinou, E., Amiridis, V., Vrekoussis, M., Mihalopoulos, N., & Sciare, J. (2019). On-flight intercomparison of three miniature aerosol absorption sensors using unmanned aerial systems (UASs). *Atmos. Meas. Tech.*, *12*(12), 6425-6447. https://doi.org/10.5194/amt-12-6425-2019

Pinto, J. P., Lefohn, A. S., & Shadwick, D. S. (2004). Spatial variability of PM2.5 in urban areas in the United States. *Journal of the Air & Waste Management Association (1995)*, *54*(4), 440-449. https://doi.org/10.1080/10473289.2004.10470919

Pope, C. A., 3rd, Burnett, R. T., Thun, M. J., Calle, E. E., Krewski, D., Ito, K., & Thurston, G. D. (2002). Lung cancer, cardiopulmonary mortality, and long-term exposure to fine particulate air pollution. *Jama*, *287*(9), 1132-1141. https://doi.org/10.1001/jama.287.9.1132

Population Data for Region: Rio Grande Valley. RGV Health Connect. https://www.rgvhealthconnect.org/demographicdata?id=281259&sectionId=935

Protection, E. U. S. E. (2001). *EPA Requirements for Quality Assurance Project Plans: EPA/240/B-01/003*. U.S. Environmental Protection Agency.

Protection, E. U. S. E. (2022). *NAAQS Table*. EPA United States Environmental Protection. https://www.epa.gov/criteria-air-pollutants/naaqs-table

Pun, V. C., Kazemiparkouhi, F., Manjourides, J., & Suh, H. H. (2017). Long-Term PM2.5 Exposure and Respiratory, Cancer, and Cardiovascular Mortality in Older US Adults. *Am J Epidemiol*, *186*(8), 961-969. https://doi.org/10.1093/aje/kwx166

QuickFacts Hidalgo County, Texas; Cameron County, Texas. United States Census Bureau. https://www.census.gov/quickfacts/fact/table/hidalgocountytexas,cameroncountytexas/IPE120220#IPE120220

Raysoni, A. U. (2011). *Assessment of Intra-Urban Traffic-Related Air Pollution on Asthmatic Children's Exposure at Schools in the Paso del Norte Region* (Publication Number 2566) Open Access Theses & Dissertations.

Raysoni, A. U. (2018). A Comparative Assessment of Food Deserts Using Geographic Information Systems (GIS) in El Paso County, TX and Loudoun County, VA.

Raysoni, A. U., Mendez, E., Luna, A., & Collins, J. (2022). Characterization of Particulate Matter Species in an Area Impacted by Aggregate and Limestone Mining North of San Antonio, TX, USA. *Sustainability*, *14*(7), 4288. https://www.mdpi.com/2071-1050/14/7/4288

Raysoni, A. U., Sarnat, J. A., Sarnat, S. E., Garcia, J. H., Holguin, F., Luèvano, S. F., & Li, W.-W. (2011). Binational school-based monitoring of traffic-related air pollutants in El Paso, Texas (USA) and Ciudad Juárez, Chihuahua (México). *Environmental Pollution*, *159*(10), 2476-2486. https://doi.org/https://doi.org/10.1016/j.envpol.2011.06.024

Raysoni, A. U., Stock, T. H., Sarnat, J. A., Montoya Sosa, T., Ebelt Sarnat, S., Holguin, F., Greenwald, R., Johnson, B., & Li, W.-W. (2013). Characterization of traffic-related air pollutant metrics at four schools in El Paso, Texas, USA: Implications for exposure assessment and siting schools in urban areas. *Atmospheric Environment*, *80*, 140-151. https://doi.org/https://doi.org/10.1016/j.atmosenv.2013.07.056

Rio Grande Valley, Texas Travel Guide. Go-Texas. https://www.go-texas.com/Rio-Grande-Valley/

Rowangould, G. M. (2013). A census of the US near-roadway population: Public health and environmental justice considerations. *Transportation Research Part D: Transport and Environment*, *25*, 59-67. https://doi.org/https://doi.org/10.1016/j.trd.2013.08.003

Rüdiger, J., Tirpitz, J. L., de Moor, J. M., Bobrowski, N., Gutmann, A., Liuzzo, M., Ibarra, M., & Hoffmann, T. (2018). Implementation of electrochemical, optical and denuder-based sensors and sampling techniques on UAV for volcanic gas measurements: examples from Masaya, Turrialba and Stromboli volcanoes. *Atmos. Meas. Tech.*, *11*(4), 2441-2457. https://doi.org/10.5194/amt-11-2441-2018

Samoli, E., Peng, R., Ramsay, T., Pipikou, M., Touloumi, G., Dominici, F., Burnett, R., Cohen, A., Krewski, D., Samet, J., & Katsouyanni, K. (2008). Acute effects of ambient particulate matter on mortality in Europe and North America: results from the APHENA study. *Environ Health Perspect*, *116*(11), 1480-1486. https://doi.org/10.1289/ehp.11345

Sayahi, T., Butterfield, A., & Kelly, K. E. (2019). Long-term field evaluation of the Plantower PMS low-cost particulate matter sensors. *Environ Pollut*, *245*, 932-940. https://doi.org/10.1016/j.envpol.2018.11.065

Seaman, N. L. (2000). Meteorological modeling for air-quality assessments. *Atmospheric Environment*, *34*(12), 2231-2259. https://doi.org/https://doi.org/10.1016/S1352-2310(99)00466-5

Spivey, S., Blake, K., & Goluszka, A. (2022). *Saharan dust returns to Texas Sunday*. KSTAT. https://www.valleycentral.com/news/local-news/get-ready-saharan-dust-is-headed-for-the-rio-grande-valley/

Srimuruganandam, B., & Shiva Nagendra, S. M. (2012). Source characterization of PM10 and PM2.5 mass using a chemical mass balance model at urban roadside. *Sci Total Environ*, *433*, 8-19. https://doi.org/10.1016/j.scitotenv.2012.05.082

Stavroulas, I., Grivas, G., Michalopoulos, P., Liakakou, E., Bougiatioti, A., Kalkavouras, P., Fameli, K. M., Hatzianastassiou, N., Mihalopoulos, N., & Gerasopoulos, E. (2020). Field Evaluation of Low-Cost PM Sensors (Purple Air PA-II) Under Variable Urban Air Quality Conditions, in Greece. *Atmosphere*, *11*(9), 926. https://doi.org/http://dx.doi.org/10.3390/atmos11090926

Steinle, S., Reis, S., Sabel, C. E., Semple, S., Twigg, M. M., Braban, C. F., Leeson, S. R., Heal, M. R., Harrison, D., Lin, C., & Wu, H. (2015). Personal exposure monitoring of PM2.5 in indoor and outdoor microenvironments. *Sci Total Environ*, *508*, 383-394. https://doi.org/10.1016/j.scitotenv.2014.12.003

Sun, L., Wong, K. C., Wei, P., Ye, S., Huang, H., Yang, F., Westerdahl, D., Louie, P. K. K., Luk, C. W. Y., & Ning, Z. (2016). Development and Application of a Next Generation Air Sensor Network for the Hong Kong Marathon 2015 Air Quality Monitoring. *Sensors*, *16*(2), 211. https://www.mdpi.com/1424-8220/16/2/211

The Official South Texas Hurricane Guide 2021 (2021). Nattional Weather Service https://www.weather.gov/media/crp/2021_HG_English_Final.pdf

Tian, Y., deSouza, P., Mora, S., Yao, X., Duarte, F., Norford, L. K., Lin, H., & Ratti, C. (2022). Evaluating the Meteorological Effects on the Urban Form–Air Quality Relationship Using Mobile Monitoring. *Environmental Science & Technology*, *56*(11), 7328-7336. https://doi.org/10.1021/acs.est.1c04854

TSI - BlueSky. South Coast AQMD. http://www.aqmd.gov/aq-spec/sensordetail/tsi---bluesky

Tsou, M.-C. M., Lung, S.-C. C., Shen, Y.-S., Liu, C.-H., Hsieh, Y.-H., Chen, N., & Hwang, J.-S. (2021). A community-based study on associations between PM2.5 and PM1 exposure and heart rate variability using wearable low-cost sensing devices. *Environmental Pollution*, *277*, 116761. https://doi.org/https://doi.org/10.1016/j.envpol.2021.116761

U.S.-Mexico border buffer polygon (la paz 1983), u.s. and mexico, 2019, u.s. environmental protection agency region 6 (2019). EPA United States Environmental Protection Agency https://edg.epa.gov/metadata/catalog/search/resource/details.page?uuid=%7B5C5B02B5-566C-4656-A078-87176BA02F25%7D&xsl=metadata_to_html_full

U.S.-Mexico Border Program. (2022). EPA United States Environmental Protection Agency. https://www.epa.gov/usmexicoborder/what-border-2025

Vallamsundar, S., Askariyeh, M. H., Zietsman, J., Ramani, T. L., Johnson, N. M., Pulczinski, J., & Koehler, K. A. (2016). Maternal Exposure to Traffic-Related Air Pollution Across Different Microenvironments. *Journal of transport and health*, *3*.

Wallace, L., Bi, J., Ott, W. R., Sarnat, J., & Liu, Y. (2021). Calibration of low-cost PurpleAir outdoor monitors using an improved method of calculating PM. *Atmospheric Environment*, *256*. https://doi.org/10.1016/j.atmosenv.2021.118432

Wang, Z. (2020). *Long-Term Evaluation of Low-Cost Air Sensors in Monitoring Indoor Air Quality at a California Community* (Publication Number 28262574) [M.S., University of California, Los Angeles]. ProQuest Dissertations & Theses Global. Ann Arbor. https://proxy.openathens.net/login?entityID=https://idp.utrgv.edu/openathens&qurl=https://www.proquest.com/dissertations-theses/long-term-evaluation-low-cost-air-sensors/docview/2476161066/se-2?accountid=7119

Weinstock, L., Watkins, N., Wayland, R., & Baldauf, R. (2013). EPA's Emerging Near-Road Ambient Monitoring Network: A Progress Report. *EM Magazine*.

Weissert, L. F., Salmond, J. A., Miskell, G., Alavi-Shoshtari, M., Grange, S. K., Henshaw, G. S., & Williams, D. E. (2017). Use of a dense monitoring network of low-cost instruments to observe local changes in the diurnal ozone cycles as marine air passes over a geographically isolated urban centre. *Science of The Total Environment*, *575*, 67-78. https://doi.org/https://doi.org/10.1016/j.scitotenv.2016.09.229

Wells, H. (2020). Assessing Low-Cost Purple Air Particulate Matter Sensors.

Wendt, E. A., Quinn, C. W., Miller-Lionberg, D. D., Tryner, J., L'Orange, C., Ford, B., Yalin, A. P., Pierce, J. R., Jathar, S., & Volckens, J. (2019). A low-cost monitor for simultaneous measurement of fine particulate matter and aerosol optical depth – Part 1: Specifications and testing. *Atmospheric Measurement Techniques*, *12*(10), 5431-5441. https://doi.org/http://dx.doi.org/10.5194/amt-12-5431-2019

Williams, R., & Duvall, R. (2018). Spatial and Temporal Trends of Air Pollutants in the South Coast Basin Using Low Cost Sensors. *U.S. Environmental Protection Agency*.

Williamson, K., Das, S., Ferro, A. R., & Chellam, S. (2021). Elemental composition of indoor and outdoor coarse particulate matter at an inner-city high school. *Atmospheric Environment*, *261*, 118559. https://doi.org/https://doi.org/10.1016/j.atmosenv.2021.118559

Wu, T.-G., Chen, Y.-D., Chen, B.-H., Harada, K. H., Lee, K., Deng, F., Rood, M. J., Chen, C.-C., Tran, C.-T., Chien, K.-L., Wen, T.-H., & Wu, C.-F. (2022). Identifying low-PM2.5 exposure commuting routes for cyclists through modeling with the random forest algorithm based on low-cost sensor measurements in three Asian cities. *Environmental Pollution*, *294*, 118597. https://doi.org/https://doi.org/10.1016/j.envpol.2021.118597

Zamora, M. L., Rice, J., & Koehler, K. (2020). One Year Evaluation of Three Low-Cost PM(2.5) Monitors. *Atmos Environ (1994)*, *235*. https://doi.org/10.1016/j.atmosenv.2020.117615

Zervaki, O. (2018). *Calibration and Evaluation of Low-cost Optical Dust Sensors and Monitors* (Publication Number 13840238) [M.S., University of Cincinnati]. ProQuest Dissertations & Theses Global. Ann Arbor.

https://proxy.openathens.net/login?entityID=https://idp.utrgv.edu/openathens&qurl=https://www.proquest.com/dissertations-theses/calibration-evaluation-low-cost-optical-dust/docview/2194847053/se-2?accountid=7119

Zhang, F. (2019). *Monitoring Indoor Air Quality Using Low-cost Sensors at a Community Scale* (Publication Number 13899896) [M.S., University of California, Los Angeles]. ProQuest Dissertations & Theses Global. Ann Arbor. https://proxy.openathens.net/login?entityID=https://idp.utrgv.edu/openathens&qurl=https://www.proquest.com/dissertations-theses/monitoring-indoor-air-quality-using-low-cost/docview/2276837760/se-2?accountid=7119

Zheng, T., Bergin, M. H., Johnson, K. K., Tripathi, S. N., Shirodkar, S., Landis, M. S., Sutaria, R., & Carlson, D. E. (2018). Field evaluation of low-cost particulate matter sensors in high- and low-concentration environments. *Atmospheric Measurement Techniques*, *11*(8), 4823-4846. https://doi.org/http://dx.doi.org/10.5194/amt-11-4823-2018

BIOGRAPHICAL SKETCH

Esmeralda Mendez graduated with her diploma and AS in Biology in spring 2018 from Weslaco High School and South Texas College. She holds a bachelor's degree in Biology with a concentration of Biological Sciences from the University of Texas Rio Grande Valley College of Science in Edinburg TX. Her BS was completed in the spring of 2020. During her undergraduate years, she interned at the Texas A&M AgriLife Research Extension in Weslaco, TX as a student lab assistant. Her research objectives were focused on citrus farming and developing a resistance to or tolerance against Citrus Huanglongbing (HLB), most known as the citrus greening disease.

Esmeralda proceeded to continue her education towards an MS in Agricultural, Environmental, and Sustainability Sciences from the University of Texas Rio Grande Valley School of Earth, Marine, and Sustainability Sciences in Brownsville TX. She completed her MS in the August 2022. During her graduate studies, she worked in Dr. Amit U. Raysoni's lab in the specialization of air quality research.

She can be contacted at Esmeralda0614@gmail.com.